FINAL REPORT WY-18/04F

EVALUATING THE RISK OF ALKALI-SILICA REACTION IN WYOMING: CONTINUED EVALUATION OF FIELD SPECIMENS AND PROPOSED MITIGATION STRATEGIES

By:
Department of Civil and Architectural Engineering
University of Wyoming
1000 East University Avenue, Dept. 3295
Laramie, WY 82071

January, 2018

Notice

This document is disseminated under the sponsorship of the Wyoming Department of Transportation (WYDOT) in the interest of information exchange. WYDOT assumes no liability for the use of the information contained in this document.

WYDOT does not endorse products or manufacturers. Trademarks or manufacturers' names appear in this report only because they are considered essential to the objective of the document.

Quality Assurance Statement

WYDOT provides high-quality information to serve Government, industry, and the public in a manner that promotes public understanding. Standards and policies are used to ensure and maximize the quality, objectivity, utility, and integrity of its information. WYDOT periodically reviews quality issues and adjusts its programs and processes to ensure continuous quality improvement.

Further, if the report contains either confidential information or, if any information in the report is subject to copyright, patent, or trademark requirements, the report must contain additional disclaimers that may be obtained through the Research Center.

Creative Commons

Copyright

No copyrighted material, except that which falls under the “fair use” clause, may be incorporated into a report without permission from the copyright owner, if the copyright owner requires such. Prior use of the material in a WYDOT or governmental publication does not necessarily constitute permission to use it in a later publication.

• Courtesy — Acknowledgment or credit will be given by footnote, bibliographic reference, or a statement in the text for use of material contributed or assistance provided, even when a copyright notice is not applicable.

• Caveat for Unpublished Work —Some material may be protected under common law or equity even though no copyright notice is displayed on the material. Credit will be given and permission will be obtained as appropriate.

• Proprietary Information — To avoid restrictions on the availability of reports, proprietary information will not be included in reports, unless it is critical to the understanding of a report and prior approval is received from WYDOT. Reports containing such proprietary information will contain a statement on the Technical Report Documentation Page restricting availability of the report

TECHNICAL REPORT DOCUMENTATION PAGE

1. Report No. WY-18/04F	**2. Government Accession No.**	**3. Recipient's Catalog No.**
4. Title and Subtitle Evaluating the Effectiveness of Fly Ashes to Mitigate ASR and Using Recycled Concrete Aggregate in New Construction		**5. Report Date** January 2018
		6. Performing Organization Code:
7. Author(s) Bryce Fiore (0000-0002-7446-3644), Md Tarik Hossain (0000-0002-4514-5620), Margaret Kimble (0000-0002-1735-7714), Fayez AlMutawa (0000-0002-2164-0416) , Jennifer Eisenhauer Tanner (0000-0002-8279-6289)		**8. Performing Organization Report No.**
9. Performing Organization Name and Address University of Wyoming Department of Civil and Architectural Engineering University of Wyoming, Dept 3295 Laramie, WY 82071-3295		**10. Work Unit No.**
		11. Contract or Grant No. RS02215
12. Sponsoring Agency Name and Address Wyoming Department of Transportation 5300 Bishop Blvd Cheyenne, WY 82009-3340 WYDOT Research Center (307)777-4182		**13. Type of Report and Period** Final Report
		14. Sponsoring Agency Code WYDOT
15. Supplementary Notes WYDOT Project Manager: Bob Rothwell, Assistant State Materials Engineer		

16. Abstract

Abstract: A comprehensive study was performed to evaluate mitigation options to reduce premature expansion due to alkali-silica reaction (ASR) for selected Wyoming aggregates. State-of-the-art and standardized test methods were performed and results were used to compare expansion levels. Four different fly-ash sources were tested. All of the sources mitigated the moderately reactive aggregates; the most highly expansive aggregate was mitigated by two out of the four fly ash sources.

An exploratory test, the Autoclave Concrete Prism Test (ACPT) was evaluated by comparing results with the University of Wyoming and the University of Alabama. Test data shows agreement between two independent laboratories.

17. Key Words Wyoming, Alkali silica reaction, expansion, aggregate, concrete, durability	**18. Distribution Statement** This document is available through the National Transportation Library and the Wyoming State Library.

19. Security Classif. (of this report) Unclassified	**20. Security Classif. (of this page)** Unclassified	**21. No. of Pages** 92	**22. Price**

Form DOT F 1700.7 (8-72) Reproduction of completed page authorized.

SI* (MODERN METRIC) CONVERSION FACTORS

APPROXIMATE CONVERSIONS TO SI UNITS

Symbol	When You Know	Multiply By	To Find	Symbol
		LENGTH		
in	inches	25.4	millimeters	mm
ft	feet	0.305	meters	m
yd	yards	0.914	meters	m
mi	miles	1.61	kilometers	km
		AREA		
in^2	square inches	645.2	square millimeters	mm^2
ft^2	square feet	0.093	square meters	m^2
yd^2	square yard	0.836	square meters	m^2
ac	acres	0.405	hectares	ha
mi^2	square miles	2.59	square kilometers	km^2
		VOLUME		
fl oz	fluid ounces	29.57	milliliters	mL
gal	gallons	3.785	liters	L
ft^3	cubic feet	0.028	cubic meters	m^3
yd^3	cubic yards	0.765	cubic meters	m^3
	NOTE: volumes greater than 1000 L shall be shown in m^3			
		MASS		
oz	ounces	28.35	grams	g
lb	pounds	0.454	kilograms	kg
T	short tons (2000 lb)	0.907	megagrams (or "metric ton")	Mg (or "t")
		TEMPERATURE (exact degrees)		
^oF	Fahrenheit	5 (F-32)/9 or (F-32)/1.8	Celsius	^oC
		ILLUMINATION		
fc	foot-candles	10.76	lux	lx
fl	foot-Lamberts	3.426	$candela/m^2$	cd/m^2
		FORCE and PRESSURE or STRESS		
lbf	poundforce	4.45	newtons	N
lbf/in^2	poundforce per square inch	6.89	kilopascals	kPa

APPROXIMATE CONVERSIONS FROM SI UNITS

Symbol	When You Know	Multiply By	To Find	Symbol
		LENGTH		
mm	millimeters	0.039	inches	in
m	meters	3.28	feet	ft
m	meters	1.09	yards	yd
km	kilometers	0.621	miles	mi
		AREA		
mm^2	square millimeters	0.0016	square inches	in^2
m^2	square meters	10.764	square feet	ft^2
m^2	square meters	1.195	square yards	yd^2
ha	hectares	2.47	acres	ac
km^2	square kilometers	0.386	square miles	mi^2
		VOLUME		
mL	milliliters	0.034	fluid ounces	fl oz
L	liters	0.264	gallons	gal
m^3	cubic meters	35.314	cubic feet	ft^3
m^3	cubic meters	1.307	cubic yards	yd^3
		MASS		
g	grams	0.035	ounces	oz
kg	kilograms	2.202	pounds	lb
Mg (or "t")	megagrams (or "metric ton")	1.103	short tons (2000 lb)	T
		TEMPERATURE (exact degrees)		
^oC	Celsius	1.8C+32	Fahrenheit	^oF
		ILLUMINATION		
lx	lux	0.0929	foot-candles	fc
cd/m^2	$candela/m^2$	0.2919	foot-Lamberts	fl
		FORCE and PRESSURE or STRESS		
N	newtons	0.225	poundforce	lbf
kPa	kilopascals	0.145	poundforce per square inch	lbf/in^2

TABLE OF CONTENT

LIST OF TABLE

LIST OF FIGURES

EXECUTIVE SUMMARY

ASR is a global concrete durability problem with a complexity that continues to challenge Wyoming. Currently the Wyoming Department of Transportation (WYDOT) evaluates ASR potential in aggregates using the Accelerated Mortar Bar Test (AMBT) before using them in new concrete. Although, this test is appealing because of its relatively short duration (16 days), the curing environment is harsh and the test produces both false positives and negatives. Researchers classified each aggregate on the basis of both standardized and state-of-the art methods including: the Concrete Prism Test (CPT); the Accelerated Mortar Bar Test (AMBT); the Autoclaved Concrete Prism Test (ACPT); petrography; and real-time field exposure. Despite the one-year time frame to complete CPTs of aggregates, researchers consider this the most reliable accelerated test method because it correlates best with field performance.

A large scale, outdoor exposure, real-time field site was developed at the Civil and Architectural Engineering Research Facility at the University of Wyoming. A total of 28 blocks measuring 380 x 380 x 660 mm (15 x 15 x 26 in.) specimens were built in order to measure expansions over a period of 10 years. Results from the first nine years of exposure are presented in this report.

Although an effective mitigation technique exists in the form of adding effective fly ashes to concrete mix designs, not all fly ashes mitigate ASR in an equal manner. A preliminary study showed that moderate to highly reactive aggregates can be mitigated by replacing 25 percent of the cement using a locally sourced fly ash. However, recent changes in regulations and availability indicate a need to evaluate different fly ashes. This work evaluates concrete prism testing with another four fly ashes. All four fly-ashes mitigated the aggregates, with the exception of one highly-reactive source. This particular source was mitigated by two of the four fly ashes. Although a simple, expeditious way to identify reactive aggregate, cement, and an appropriate mitigation measure does not exist; previous work showed promise of a week-long autoclave test to evaluate fine aggregates. In this report, data from a combined study is presented. This proposed test has the potential to replace the year-long concrete prism test.

1 INTRODUCTION

ASR is a phenomenon that occurs when constituents, in particular aggregates, react with the alkalis in the concrete pore solution. The result is the formation of an expansive gel within the concrete matrix, which leads to cracking and diminished durability over the life of the structure. Unfortunately, the process is slow, which makes detection and prevention difficult. Currently, there is no single test to expediently evaluate the ASR potential of a cement/aggregate combination with a high degree of accuracy and precision.

The Wyoming Department of Transportation (WYDOT) has traditionally handled the problem by replacing 20-25 percent of cement with a suitable fly ash. The mitigated ASR potential of the mix is confirmed after testing. The changes in coal sources and burning methods may unexpectedly impact the mitigation capabilities of any fly ash. To effectively mitigate the effects of ASR, experimental identification of several fly ash sources is imperative; identification with mathematical models is ideal to narrow the wide range of available material. While time and reliability are the most important testing factors, experimental work will never be eliminated. Therefore, establishing quicker and more effective test methods is crucial.

1.1 Introduction to the Wyoming Department of Transportation (WYDOT) Project

WYDOT has evaluated eight aggregate sources. After extensive testing, the UW research team provided a graphical classification illustrated in Figure 1 with results tabulated in Table 1. Reactivity is indicated by the size and color of the stars. For example, non-reactive, moderately reactive and highly reactive pits are identified with a green, yellow and red star respectively.

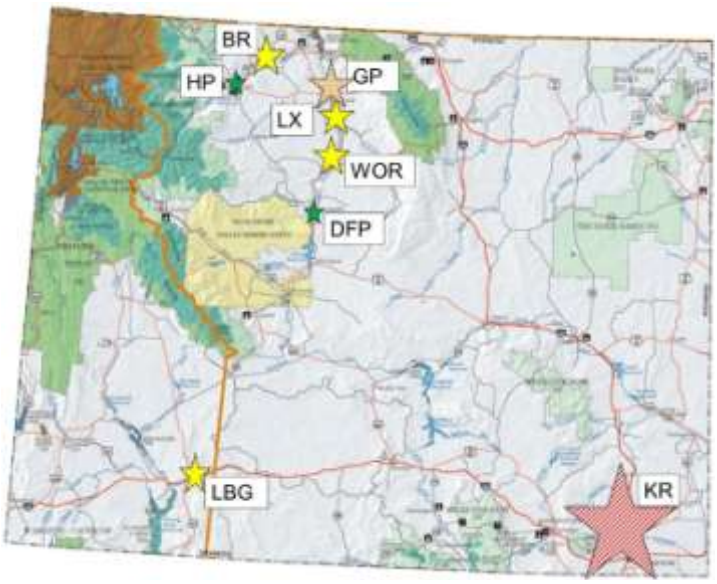

Source: UW Tanner research group.

Figure 1. Wyoming map showing the location of each aggregate source.

Table 1. Aggregate abbreviations and locations.

Aggregate Name	Abbreviation	WY Location	Classification
Black Rock	BR	Powell	MR
Devries Farm	DFP	Thermopolis	NR
Goton	GP	Greybull	MR/HR
Harris	HP	Cody	NR
Knife River	KR	Cheyenne	HR
Labarge	LBG	Worland	MR
Lamax	LX	Basin	MR
Worland	WOR	Worland	MR

*NR=non-reactive, MR=moderately reactive, HR=highly reactive.

Source: UW Tanner research group.

This research builds on work by Fertig (2010) and Kimble (2015). The testing methods included the commonly used Accelerated Mortar Bar Test (AMBT) and Concrete Prism Test (CPT). Less commonly used tests include large-scale field site specimens. Additional experimental work was conducted using an ultra-rapid Autoclaved Concrete Prism Test (ACPT).

The second portion of this research is the evaluation of ASR mitigation through the replacement of cement with low calcium oxide (CaO) fly ash. As appropriate fly ash sources and other mitigating agents become harder to acquire or more expensive, it has become even more important to correctly identify an aggregate's ASR potential. Adding mitigating agents when they are not needed adds considerable cost to a construction project and uses valuable resources that could mitigate more reactive aggregates. Reactive or potentially reactive aggregates were further tested with a 25 percent fly ash replacement using the Mitigated Concrete Prism (MCPT) and Mitigated Accelerated Mortar Bar (MAMBT) tests.

1.2 Report Overview

This document is organized as follows:

Section 1 introduces the project.
Section 2 presents project scope and objectives.
Section 3 reviews the literature concerning ASR including a brief history, mechanism and mitigation of ASR and a description of the procedures, advantages, and shortcomings of the test methods that were most applicable to this research.
Section 4 details material characteristics of coarse and fine aggregates; cement, fly ash and additional materials used in this project.
Section 5 describes the test methods and equipment used in this work.
Section 6 demonstrates the results of the experiments on outdoor exposure blocks, mitigated concrete prism tests and the autoclaved method. The chemical models used to predict fly ash dosages are presented and a comparison of the predictions to the results of the experiment is given.
Section 7 presents conclusions from the work presented in Section 6 and suggestions for future work.

2 PROJECT SCOPE AND OBJECTIVES

Previous work at the University of Wyoming (UW) has investigated the efficacy of one fly ash source, which proved effective; classified the ASR potential and mineralogical composition of eight different aggregate sources across Wyoming; preliminarily evaluated the effect RCA has on ASR in new concrete and performed a pilot study on an autoclaved test method (Fertig, 2010; Hacker, 2014; Jones, 2011; Kimble, 2015). This project is broken down into two sections to expand on this cumulative understanding of ASR. These primary investigations are listed below, along with their respective objectives:

a) Standard aggregate assessment and classification (Sections 6.1 through 6.3 and Chapter 7**):**

The overall objective is to utilize standardized testing methods to evaluate ASR potential in two areas:

- **Unmitigated** – This portion of the project is intended to create a baseline for the Autoclaved Concrete Prism Test (ACPT) (Giannini and Folliard, 2013) and to deepen our understanding of the ASR potential of the Wyoming aggregates by analyzing either the reactive coarse or reactive fine aggregate separately in the Concrete Prism Test (CPT) (ASTM C1293, 2014).
- **Mitigated –** Experimental work was performed to establish which of the four tested fly ashes are the most effective based on the CPT. A secondary objective is to corroborate existing fly ash dosage predicting models with experimental data

b) **Supplementary experimental procedures** (**Section 6.4 through 6.5 and Chapter** 7**):**

The overall objective is to either bring new methods one step closer to standardization, or enhance our understanding of ASR behavior.

- **ACPT –** The main goal of the continued ACPT work is to determine if the test improvements reduce the variability observed in a previous inter-laboratory study. Additionally, this work aims to verify the preliminary classification limit of the ACPT when compared to the already standardized CPT limit.
- **Outdoor Exposure Blocks (OEB)** – A topic of interest is the impact freeze thaw has on OEBs. In an effort of quantify this, more frequent measurements were taken during the winter months to detect this effect.

3 BACKGROUND AND LITERATURE REVIEW

3.1 A History of ASR

Alkali Silica Reaction (ASR) is a chemical process that damages the structural integrity of concrete over time and has been a topic of investigation since its discovery by Stanton in the 1940s (Stanton, T. E., 1940). The literature on ASR from the 1940s to early 2000s have been summarized extensively and only a brief outline is provided here (ACI Committee 211, 2008; Thomas et al., 2006b).

Stanton's pioneering work thoroughly laid the foundation for the main topics of investigation today: What is ASR, the mechanisms behind the process, detection of ASR potential in aggregate and mitigation? He discovered that ASR occurs between cements of high alkali content and certain minerals within the aggregate to produce a gel-like product (Stanton, T. E., 1940; Stanton, 1950). Subsequently, he developed the mortar bar test method for detecting ASR potential in an aggregate and documented the pessimum effect of particle size and expansive behavior (Stanton, T. E., 1940). The mitigating behavior of pozzolans was also a direct conclusion from his work (Stanton, 1950).

3.2 ASR Mechanism

While ASR has been investigated quite extensively, the physiochemical reactions are still poorly understood. This knowledge gap may lead to misdiagnosing the reactivity of the aggregate or improper mitigation techniques for structures. The available literature on the topic has been extensively summarized in published work (Lindgard et al., 2011; Rajabipour et al., 2015). An overview of the ASR process is as follows (Rajabipour et al., 2015):

1. Dissolution of silica through attack of hydroxyl ions.
2. Gelation of the silica.
3. Swelling of the gel.

The requirements for ASR to occur are as follows: (Berube et al., 2002; Mukhopadhyay, 2013)

1. Presence of reactive siliceous aggregate.
2. Sufficient pH and alkalis.
3. Sufficient moisture.

Alkali hydroxides in the concrete pore solution react with free silica in the aggregate, producing an alkali-silica gel product. This gel readily absorbs water and expands; this can lead to cracking and premature deterioration in concrete. The cyclic nature of the problem is illustrated in Figure 2.

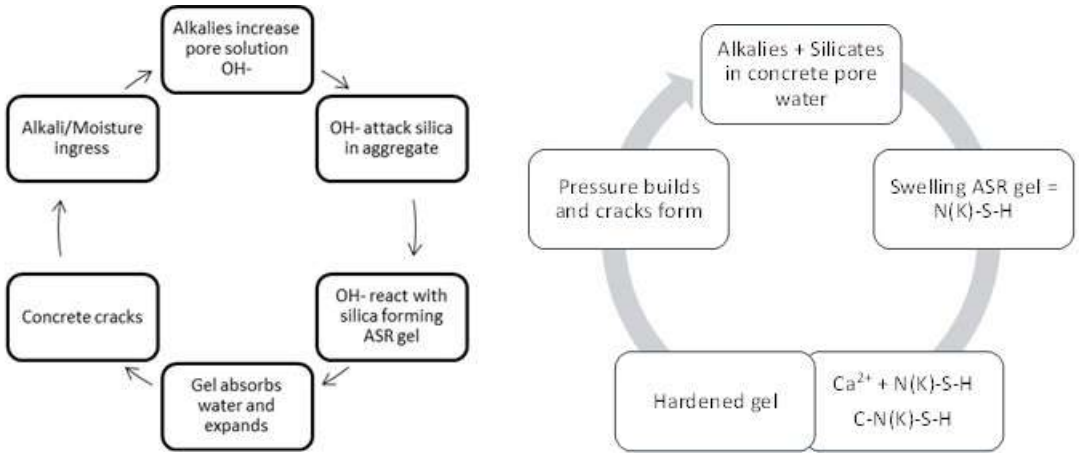

Source: UW Tanner research group.

Figure 2. Cyclic nature of ASR in concrete. Chemical breakdown of types of gel.

Before the process can be explained, the main reaction in Portland cement concrete that occurs needs to be addressed. During hydration of Portland cement, the cement reacts with the water to produce Calcium Silicate Hydrate (CSH) and Calcium Hydroxide (CH) also called portlandite. CSH provides the strength, while CH are weak links in the hardened cement.

ASR occurs as a reaction between the silica in the aggregate and the alkalis provided by cement reaction. The amount of alkalis that are considered to contribute to the process is defined by Stanton as Na_2O_{eq} (percent Na_2O + 0.658·times percent K_2O). Due to the high pH caused by hydroxyl (OH^-) ions, the concrete pore solution dissolves the reactive silica, which then behaves as a hygroscopic gel. While silica will dissolve in water with pH levels less than 11, the attack on the silica is exacerbated with higher alkalinity (Rajabipour et al., 2015). The most susceptible type of silica that is attacked is poorly crystallized silica. Well crystallized silica are less susceptible and are typically attacked on the surface, which allows for a fluid phase that prevents gelling (Glasser and Kataoka, 1981). At higher alkali concentrations however, even these stable forms are susceptible to the attack that occurs in poorly crystallized silica (Gao et al., 2013). The poorly crystallized silica allows the hydroxyl ions to attack the interior and ruptures the Si – O – Si bonds, loosening the network. Subsequently, the dissolved structure gels will take on water and swell (Glasser and Kataoka, 1981; Rajabipour et al., 2015).

The total amount of silica that can be dissolved by this process can be understood using thermodynamics to arrive at the solubility curve shown in Figure 3. While this figure is shown with a constant temperature, larger temperatures increase the solubility of amorphous silica. The figure shows that the amount of silica that can be sustained in solution causing ASR damage increases with increasing alkalinity. In fact, the pH of the pore solution has to be greater than 13.2 in order for ASR to occur (Tang and Fen, 1980). However at high pH, the aqueous silica is negatively charged and actually prevents gelation (Rajabipour et al., 2015). This never occurs in portland cement concrete due to the presence of Ca^{2+} and the ability to form poly-metal silicates (Rajabipour et al., 2015).

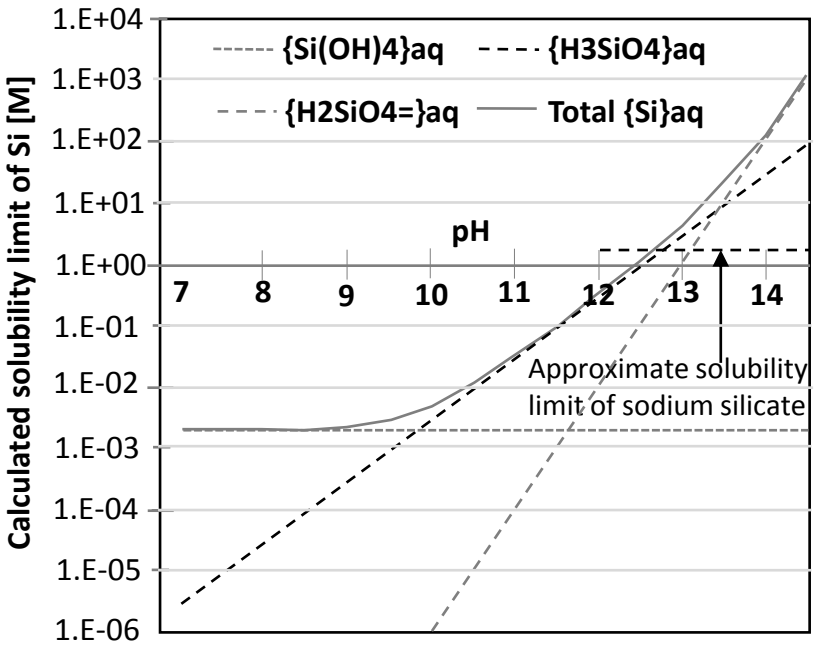

Source: Rajabipour et al. 2015.

Figure 3. Chart. Solubility limit of amorphous SiO_2 as a function of pH with T= 25^0C.

Gel swelling is in part due to "the gel being porous with a high surface area that contains many hydrophilic groups … this results in osmosis, adsorption of water and swelling of the gel". Additionally, "the swelling may be due to differential kinetics of fast inward diffusion of deleterious ions into the reactive sites and slow outward diffusion of silica ions from these sites" (Rajabipour et al., 2015).

3.3 Mitigation of the Alkali-Silica Reaction

After Stanton's pioneering work , case studies on ASR and pozzolanic mitigation ensued by several government and private organizations (Alderman et al., 1947; Meissner, 1941). An attempt at understanding the mechanism behind ASR was investigated (Diamond, 1976; Powers and Steinour, 1955). However, an infallible understanding was not achieved, and is still investigated today (Rajabipour et al., 2015). By the early 1950s, it was confirmed that a range of admixtures beyond pozzolans, including lithium hindered the reaction (Buck et al., 1953; Cox et al., 1950; Hanna, 1947; McCoy and Caldwell, 1951; Stanton, 1950). These conclusions are corroborated by field performance where fly ash was used to prevent this phenomenon (Blackwell and K., 1992; Rogers and Lane, 2000). The following conclusions from 1950 to 2000 are replicated here (Thomas et al., 2006b):

- Most, if not all, supplementary cementing materials (SCM's) can be used to prevent damaging reaction due to ASR provided they are used in sufficient quantity. The quantity required is primarily a function of (i) the composition of the SCM (particularly its CaO, SiO_2 and Na_2O_{eq} content), (ii) the nature and the level of reactivity of the aggregate (different aggregates require different levels of SCM), and (iii) the alkali content provided by the portland cement (and other sources such as aggregates and chemical admixtures).

- Lithium can be used to suppress expansion with most, if not all, reactive aggregates provided the lithium-to-alkali ratio, Li/(Na+K), is sufficient. The ratio required is primarily a function of (i) the form of lithium used and (ii) the nature of the reactive aggregate.
- "Restricting the alkali contribution from the portland cement component of the concrete can be effective in controlling ASR expansion. The maximum alkali content that can be tolerated in the concrete without causing damaging expansion is a function of the reactive aggregate type. Consideration must be given to the availability from other sources both within (e.g. aggregates) and external to (e.g. deicing salts) the concrete.

Today, ASR is understood as a "deleterious reaction in which metastable silicates contained in many natural aggregates dissolve in highly alkaline pore solution of concrete and further coagulate to form a colloidal alkali-lime-silica gel" (Diamond, 1976; Poole, 1992; Shafaatian et al., 2013).

3.3.1 Fly Ash and ASR Mitigation

Fly ash is a finely divided residue resulting from the combustion of powdered coal. Because of its physical characteristics and its pozzolanic properties, it imparts several beneficial properties to concrete. Based on its composition, fly ash is classified as Class F and Class C by ASTM C 618. Class F fly ash is usually derived from the combustion of anthracite or bituminous coal and generally contains less than 5 percent CaO by mass. Class C fly ash is usually derived from the combustion of lignite or subbituminous coal. Class C ashes typically contain 10-to-40 percent CaO by mass. As explained below, Class F ashes are generally more effective in mitigating ASR than Class C ashes. Some of the alkalies in fly ash are encapsulated in the glassy particles and are released as the fly ash reacts in concrete.

The role of fly ash alkalies and their net contribution to the alkalinity of the pore solution in concrete have been widely debated (Nixon and Page, 1987; Hobbs, 1989; and Thomas, 1995). The Canadian Standards Association (CSA) recommends that fly ash used for reducing the risk of deleterious expansion due to ASR should have a total alkali content less than 4.5 percent Na_2Oe, and a maximum water-soluble alkali content of 0.5 percent Na_2Oe (appendix of CSA A23.1). ASTM C 618 recommends an optional requirement that the maximum available alkali content of fly ash used to reduce ASR expansion be limited to 1.5 percent, by mass.

Class F fly ashes are generally efficient in controlling expansions related to ASR when used as a replacement for a portion of cement (Dunstan, 1981; Farbiarz et al., 1986; Robert, 1986; Lee, 1989). Normal proportions of Class F fly ash vary from 15 to 30 percent, by mass, of the cementitious material (Malhotra and Fournier, 1995). The effective replacement amount of Class F ash for portland cement should be determined by testing, as it will vary significantly based on the physical and chemical characteristics of the fly ash.

It has been suggested that a minimum of 15 percent class F fly ash, 30 percent class C ash, 25 percent slag, 5 percent silica fume cement replacement or lithium admixtures will be effective to mitigating ASR problems (Farny and Kerkhoff, 2007). This is generally a guideline for experimental testing with new materials. Each of these suggestions are founded upon the second fundamental reaction that takes place in concrete hydration when pozzolans are used.

This second base reaction is called pozzolanic reaction. This is where pozzolans (fly ash, slag, silica fume) consume CH and other hydroxides (OH) to precipitate CSH. Therefore, overtime, pozzolans improve the strength, permeability and durability of concrete. A number of investigators have studied the mitigating properties in fly ash. Shafaatian et al. (2013) provides a thorough synthesis of the literature available on these mechanisms and outlines several processes:

- *Alkali dilution:* If cement were replaced by a completely inert material, the amount of ASR would be reduced due to the overall reduction in the concentration of alkalis. It has been determined that fly ash mitigates beyond simply diluting alkalis.
- *Alkali binding:* This is a secondary reaction in concrete where fly ash produces CSH by removing alkalis and hydroxyl ions from the pore solution. The additional reduction in these chemicals from the pore solution reduces the ASR capacity of the mix. Additionally, the CSH from the pozzolanic reaction has a lower C/S ratio which indicates a higher alkali binding capacity than the CSH from cement hydration. It is possible that the increased acidity of silanol groups (Si-OH) or negative surface charges on low C/S CSH causes the increased binding effect.
- *Mass transport reduction:* The pozzolanic reaction additionally reduces the permeability of the concrete which not only prevents external alkalis from penetrating the concrete, but also reduces the ability for gel generation and swelling (Detwiler, 2002). This reduces the mass transport and ion diffusivity properties of the concrete.
- *Improving strength:* Over time fly ash increases the strength of the concrete. More specifically, as the tensile strength improves, its ability to resist internal tensile stresses are also increased. This effect happens over a slow reaction, and it is unclear when this effect has improved the concrete's ability to resist ASR in early ages.
- *Altering ASR gel:* Fly ash modifies the ASR gel composition and may reduce the swelling capacity. Part of this reduced capacity is due to low CaO/Na_2O_{eq} gel being able to diffuse into the surrounding cement paste without causing damage. Additionally, gels produced in a less basic environment have a fibrous structure also limiting the swelling capacity.
- *Consumption of portlandite (CH):* Portlandite has been suggested to be a necessary component to the reaction, and is reduced due to pozzolanic action. Additionally, portlandite contributes to the overall pH of the pore solution, which can help maintain the solution's alkalinity even when free hydroxyl ions are consumed.
- *Supplying soluble alumina:* Alumina has been observed to increase the effectiveness of SCMs to resist ASR. This happens by contributing to the pozzolanic reaction to form CASH (alumina modified CSH) which has more alkali binding capacity. Additionally, the rate of the dissolution of silica is reduced with CASH. Unfortunately, this type of pozzolanic reaction does not reduce the alkalinity of the pore solutions.

An additional mechanism was observed where the dissolution rate of silica is reduced even without a pH reduction.

3.4 ASR Problem in Wyoming

Alkali silica reaction (ASR) is a significant problem in Cheyenne and other towns because of the presence of reactive aggregates. Although an effective mitigation technique exists in the form of adding effective fly ashes to concrete mix designs, not all fly ashes mitigate ASR in an equal

manner. WYDOT's only means of evaluating fly ash as a mitigating agent is utilizing ASTM C1567 along with the history of the fly ash and the aggregates. Currently WYDOT ships fly ash from Texas to use as a mitigating agent. Finding locally available sources will improve sustainability and use a waste product in construction of new concrete.

Examples of ASR expansions are prevalent around the state as shown in Figure 4 and Figure 5. Sections of the highway with large pop-outs are inherently unsafe and should be fixed using simple and cost-effective measures.

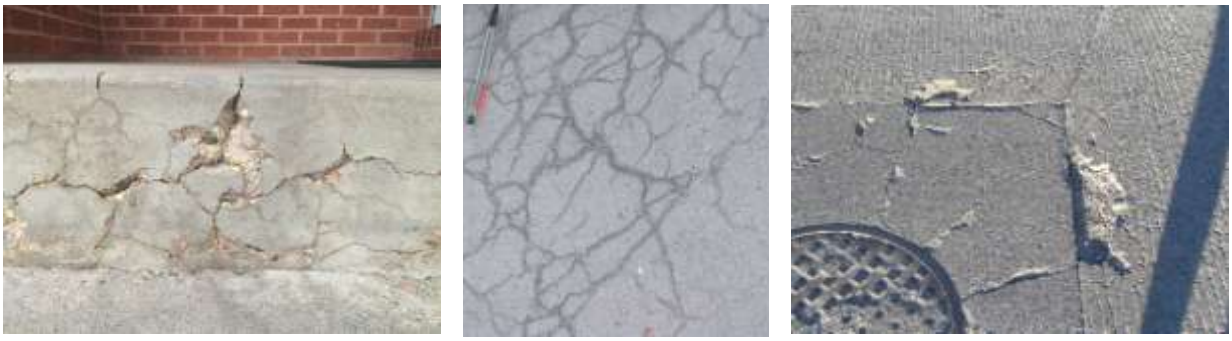

a) b) c)

Source: UW Tanner research group.

Figure 4. Examples of damage due to ASR in Wyoming a) concrete steps in Cheyenne, b) Federal Street in Riverton, and c) Federal and Pershing in Riverton.

a) b) c)

Source: UW Tanner research group.

Figure 5. ASR damage on Interstate 80, east of Cheyenne a) general ASR map cracking, b) pop-outs combined with map cracking, and c) concrete failure between dowel bars retrofits is attributed to ASR.

3.5 Test Methods

There are seven standardized test methods that have been adopted by the American Society for Testing and Materials (ASTM) to detect a particular aggregate's ASR potential in concrete. The available test methods, including many experimental methods, have been critically reviewed and discussed by many researchers. (ACI Committee 211, 2008; Farny and Kerkhoff, 2007; Lu et al., 2004; Thomas et al., 2006b; Touma et al., 2001).
The six ASTMs are listed here:

- Mortar-Bar Method ASTM C 227.
- Chemical Method ASTM C 289.
- Petrographic Examination ASTM C 295.
- Accelerated Mortar-Bar Test (AMBT) ASTM C 1260.
- Concrete Prism Test (CPT) ASTM C 1293.
- Accelerated Mortar-Bar Test w/fly ash (MAMBT) ASTM C 1567.

Additionally, there are several less common established tests (ACI Committee 211, 2008):

- Potential Volume Change of Cement-Aggregate Combinations (ASTM C 342).
- U.S. Army Corps of Engineers modified mortar bar test.
- Concrete cube test.
- Nordtest accelerated alkali-silica reactivity test.
- Gel pat test.

Finally, there are several experimental procedures that are being used by researchers to explore an aggregate's ASR potential:

- Field blocks.
- Microbars.
- Autoclave testing.
- CAMBT.

Supplementary Cementitious Materials (SCMs) have their own tests and research correlating the results and how they affect ASR behavior (Malvar and Lenke, 2006).

- ASTM C 311 and C 441 tests the effectiveness of a pozzolan or slag in reducing ASR expansions (ASTM C311, 2013; ASTM C441, 2011).
- ASTM C 618 classifies the type of fly ash based on the chemical composition results from ASTM C 311 and C 441 (ASTM C311, 2013; ASTM C441, 2011; ASTM C618, 2015).

While this is not a comprehensive list, each test is in search of the ideal test method as outlined here (Grattan-Bellew, 1997; Thomas et al., 2006b):

- The test should be reliable in terms of predicting how the combination of materials will behave under field conditions.
- The test should use the reactive aggregate (or the combination of aggregates) under consideration rather than a standard reactive aggregate (such as Pyrex glass).
- The test should not involve excessive processing of the aggregate (such as crushing a coarse aggregate to allow it to be tested in mortar).
- The test should be capable of evaluating the contribution of the cement alkalis rather than requiring an increase in the level of alkali.
- The test should be rapid, providing results in weeks or months rather than years.
- The test should be capable of assessing all types of SCM, lithium compounds and their combinations (with cements of different alkali level).

Each test has its own drawbacks, and there remains to be found a single test method that incorporates all the ideal attributes. Depending on the aggregate composition, some test methods will be better at assessing ASR reactivity than others, making it necessary to implement more than one (Berube, 1993; Hooton and Rogers, 1993). Table 2 compares several of the standardized tests against the ideal test (Thomas et al., 2006a). A check mark indicates that the test method meets the criterion, while an "x" indicates that the test method is unable to meet that criterion. Furthermore, the question mark illustrates that that criterion is unknown for the indicated test method and requires further research.

Table 2. Comparison of test methods with the "Ideal Test".

Test	Reliable	Job Agg.	Unprocessed Aggregate	Job Cement	All SCM's	Lithium Compounds	Rapid
Ideal Test	✓	✓	✓	✓	✓	✓	✓
Field performance	✓	✓	✓	✓	✓	✓	✗
CPT (ASTM C1293)	✓	✓	✓	✗	✓	✓	✗
Accelerated prism	?	✓	✓	✗	✓	✓	✓
AMBT (ASTM C1260)	?	✓	✗	✗	✗	✗	✓
Mortar Bar (ASTM C 227)	✗	✓	✗	✗	?	?	?
Pyrex mortar bar (C 441)	✗	✗	✗	?	✓	✓	✓

Source: Reproduced[1] from Thomas et al., 2006.

3.5.1 Discussion of test methods

The most common test methods are described in the following sections. The discussion emphasizes the merits and disadvantages of each test and provides a global picture of the development of ASR test methods and ASR testing today.

3.5.1.1 Petrographic Examination ASTM C 295

It is recommended that a petrographic examination be the first step in any study to evaluate the reactivity of an aggregate due to ASR (Berube, 1993). A well-experienced petrographer can "accept or even reject an aggregate under study, or at least determine the most appropriate tests to run" (Berube, 1993). Despite this advantage, it is only useful for identifying reactive minerals, but is not able to quantitatively describe how the aggregate will behave in concrete (ACI Committee 211, 2008; Farny and Kerkhoff, 2007). Due to the nature of this method, it can only test small samples in electron microscopes using techniques such as X-ray diffraction and

[1] Reprinted from Cement and Concrete Research, Volume 36, Issue 10, Michael Thomas, Benoit Fournier, Kevin Folliard, Jason Ideker, Medhat Shehata, "Test methods for evaluating preventative measures for controlling expansion due to alkali-silica reaction in concrete", pp. 11842-1856., Copyright (2006), with permission from Elsevier

infrared spectroscopy Therefore, the sample must be assumed representative of the aggregate or structure (Farny and Kerkhoff, 2007). Lastly, petrography can be used to confirm the presence and degree of ASR in hardened concrete.

3.5.1.2 Chemical Method ASTM C 289

Due to newer more reliable tests, this method is also somewhat historical. The test is fairly reliable in detecting ASR potential for highly reactive aggregates (Farny and Kerkhoff, 2007). Because carbonates interfere with this test, deleterious aggregates may be accepted (Berube, 1993; Farny and Kerkhoff, 2007), this method was withdrawn in 2016 by ASTM.

3.5.1.3 Mortar-Bar Method (ASTM C 227)

This method was first published in 1950 and is mostly a historical test. (Thomas et al., 2006b). It is not recommended to evaluate ASR due to its many shortcomings (Berube, 1993; Farny and Kerkhoff, 2007; Thomas et al., 2006b). Main problems include: sensitivity to storage conditions; variations in water to cement ratio and alkali content of the cement; and failure to distinguish between slowly reactive aggregates and innocuous ones. (ACI Committee 211, 2008; Berube, 1993; Farny and Kerkhoff, 2007; Stark et al., 1993). While this test allows for cement-fine-aggregate testing, it has been well documented to incorrectly identify the ASR potential of an aggregate (Thomas et al., 2006b). However, the test is still "considered an accurate indicator of a highly-reactive siliceous aggregate's potential for deleterious reactivity with alkalis in concrete" (ACI Committee 211, 2008).

3.5.1.4 Accelerated Mortar-Bar Test ASTM C 1260

This test method was developed by Oberholster and Davies (1986) and adopted by ASTM in 1994. It was created to improve upon the shortcomings described in the mortar bar and chemical method (Farny and Kerkhoff, 2007), The main criticism of this test is the harsh environment that the specimens are subjected to that may lead to an overestimation of an aggregates reactivity (ACI Committee 211, 2008; Farny and Kerkhoff, 2007; Fournier and Berube, 2000; Ideker et al., 2012). Another large caveat with this method is that it only utilizes the fine aggregate sizes. This means that any coarse aggregate being tested has to be crushed to the correct size which may lead to inaccurate conclusions (Ideker et al., 2012; Rajabipour et al., 2015). Additionally, there are some mineral compositions that may result in false negatives (Hooton and Rogers, 1993). Conflicts between AMBT and CPT classifications have been repeatedly documented (Ideker et al., 2012; Lu et al., 2004; Thomas et al., 2006b). Work done in Wyoming also corroborates these findings (Jones, 2011). Despite these shortcomings, this test is one of the most commonly performed in North America due to its relatively good correlation with field performance and the short time duration (16 days). However, it is highly recommended that it be used to screen an aggregate for acceptance, not rejection, of an aggregate, and that the test results should be confirmed with the CPT (Berube, 1993; Thomas et al., 2006b; Touma et al., 2001). While the test itself lasts for 16 days, it is commonly extended to 28 days.

3.5.1.5 Mitigated Accelerated Mortar-Bar Test (MAMBT) ASTM C 1567

A modified AMBT or Mitigated Accelerated Mortar-Bar Test (MAMBT) using fly ash is considered a method to evaluate the effectiveness of cement-aggregate-pozzolan combinations.

Reasonable correlations at 14 days between 70 different combinations of SCMs tested in both the CPT and AMBT were found (Thomas and Innis, 1999). Other evaluations concludes that this method "generally gives a good indication of the performance of SCM to control expansion due to ASR" (Fournier et al., 2004).

3.5.1.6 Concrete Prism Test ASTM C 1293

The Concrete Prism Test (CPT) is considered the gold standard of accelerated test methods and was developed in the 1950s to correct the short comings of the mortar bar test (ASTM C 227) (Swenson and Gillott, 1964). The benefit of this test over the AMBT is that it "tests a larger specimen, uses a full scale concrete mixture, and the testing environment is far less harsh than the AMBT" (Ideker et al., 2012). Thomas et al. (2006b) notes that to their knowledge "there are no aggregates that pass the current test conditions and performance limits that have caused damaging alkali-silica or alkali-carbonate reaction in concrete structures". It has been postulated that because the method boosts alkalis in the mix, that the method is still too severe and may result in false positives. However, this environment is still likely to occur in concrete used in highway structures (Thomas et al., 2006b). The reason the method is boosted is because throughout the duration of the test methods the alkalis leach out of the concrete subsequently causing a reduction in ASR expansion (Meissner, 1941; Rogers and Hooton, 1991). Fortunately, comparisons between the expansions of the CPT and the expansions of corresponding field exposure blocks show that the method is effective at predicting field performance (Fournier et al., 2004). A convenient aspect to this method is that it is capable of testing job specific combinations aggregate. However, the potentially reactive aggregate is typically isolated by coarse or fine, and supplemented with a nonreactive aggregate. The downside to this test is that it takes one year to complete and cannot determine the effect of concrete alkalinity on ASR due to alkali leaching (Thomas et al., 2006b).

3.5.1.7 Field Blocks

Utilizing outdoor exposure sites and large concrete blocks, while not formally standardized, is often considered the most accurate at assessing field performance of a mix. An FHWA report indicates that their use of field exposure sites is to provide data that can be used to calibrate laboratory tests (Thomas et al., 2013). Similar concepts and correlations between field performance and laboratory tests have been documented (Fournier et al., 2004; Ideker et al., 2012; Ideker et al., 2004; Rogers and Lane, 2000). However due to space limitations, and the length of time (5+ years), it is seldom performed (Rogers and Lane, 2000). One benefit of using larger concrete blocks in an outdoor environment is that alkali leaching becomes less likely due to longer transport distances and that the environmental changes are considered (Ideker et al., 2004; Rogers and Lane, 2000).

3.5.1.8 Autoclave Testing

To discover a single test method that meets the conditions of the "ideal test", there has been increased work utilizing an autoclave to evaluate the ASR potential of an aggregate. Several autoclaved methods have been proposed to rapidly evaluate the presence of ASR in as little as a few days (Berube, 1993; Duchene and Bérubé, 1992; Fournier et al., 1991; Liu et al., 2011; Nishibayahsi et al., 1996; Tang et al., 1983). These methods range from autoclaved microbars to

concrete prisms. In most cases, an increased alkali loading is used with a maximum of 4.0 percent Na_2Oeq by mass of cement. This increased alkali loading minimizes the effect of the high alkali cement (Giannini and Folliard, 2013). Some of these methods demonstrate good agreement with standard AMBTs and CPTs and acknowledge that the testing is limited (Duchene and Bérubé, 1992; Fournier et al., 1991; Giannini and Folliard, 2013; Liu et al., 2011; Nishibayahsi et al., 1996).

This research focuses primarily on extending the work published in Giannini and Folliard (2013) and the previous inter-laboratory study between the University of Wyoming (UW) and the University of Alabama (UA). The autoclaved concrete prism test (ACPT) method utilized in this research is a modified CPT procedure and is described in detail in chapter 5.

Throughout Giannini and Folliard (2013), two nonreactive aggregates and three highly reactive aggregates were tested in a pilot study, and followed up with six additional aggregates of varying reactivity. Expansions due to delayed ettringite formation (DEF) were ruled out because this type of expansion typically occurs after several weeks or months of moist storage (Giannini, 2012; Taylor et al., 2001). As autoclaved methods develop, classification limits have been roughly evaluated. Grattan-Bellew (1997) suggested that the overall expansion limit be greater than 0.05 percent. Giannini and Folliard (2013) who pioneered this method arrived at 0.08 percent to correctly classify two aggregate combinations as nonreactive. The rationale for the larger limit of 0.08 percent was also based on the observation that the ACPT may have some inherent expansive properties that are not yet understood (Giannini and Folliard, 2013).

3.5.1.9 ASTM C 618

This method governs the use of fly ash added directly to concrete. Within this standard, there are three classifications of fly ash based on the test results mandated in ASTM C 311:

- Class N – Raw or calcined natural pozzolans.
- Class F – Fly ash that has pozzolanic properties (and CaO content of less than 8 percent in CSA A3000-13 (2013)).
- Class C – Fly ash that has pozzolanic and some cementitious properties.

Essentially, the main chemical classification is based on the sum SiO_2+Al_2O_3+Fe_2O_3 as percentages by weight. Where the minimum for class C is 50 percent and class F and N is 70 percent. All class F fly ashes are also class C based on this definition. The main difference between these types in terms of ASR is that class C fly ash is less effective at mitigating ASR than class F. Interestingly, there is an inverse trend between this quantity and CaO content (Sutter et al., 2013). The CaO content is sometimes emphasized as the best indicator on the fly ash's behavior and recommended for fly ash classification (Shehata and Thomas, 2000; Thomas et al., 1999). The influence CaO content has on ASR behavior is viewed in Figure 6 based on Canadian classification criteria. While ASTM C 618 does not consider CaO content.

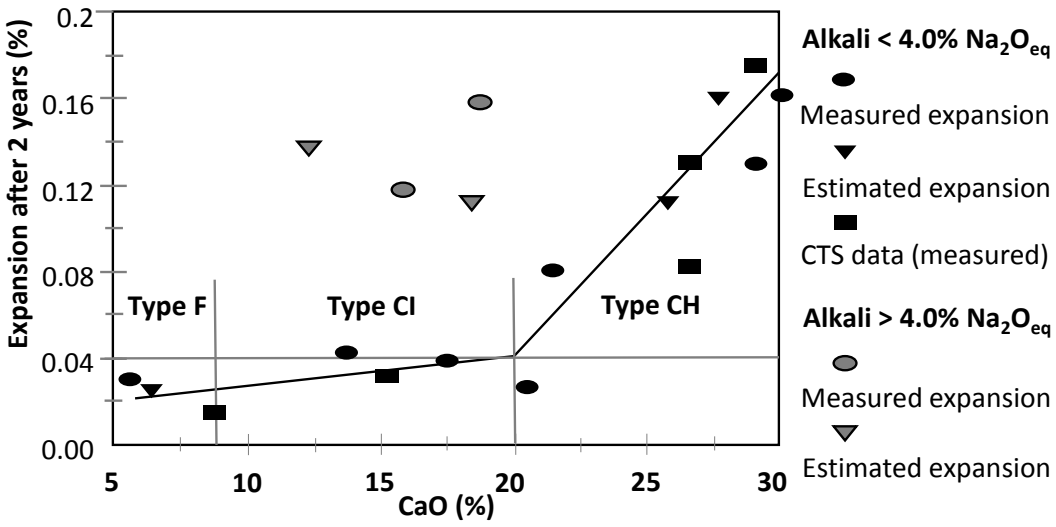

Source: Reproduced[2] from Shehata and Thomas, 2000.

Figure 6. Graph. Effect of CaO content and CPT expansion. Reactivity Classification of Aggregates.

While the CPT and AMBT standards recommend a binary, reactive-nonreactive criterion, it is beneficial to use a more detailed method to categorize the behavior of different aggregates. An effective categorization procedure has been produced by the Federal Highway Administration (Thomas et al., 2012). These categorization limits are illustrated in Table 3.

Table 3. FHWA classification limits.

Aggregate-Reactivity Class	**Description of Aggregate Reactivity**	**One-Year Expansion in CPT (%)**	**14-Day Expansion in AMBT (%)**
R0	Non-reactive (NR)	≤ 0.04	≤ 0.10
R1	Moderately reactive (MR)	> 0.04, ≤ 0.12	> 0.10, < 0.30
R2	Highly reactive (HR)	> 0.12, ≤ 0.24	>.0.30, ≤ 0.45
R3	Very highly reactive (VHR)	> 0.24	> 0.45

A better evaluation of an aggregate's potential of ASR is by evaluating them in a long term OEBs. Due to the lack of standardization of performing this type of test, uniform evaluation criteria is unavailable. Therefore, a preliminary evaluation system was developed at UW based upon the results for the boosted specimens for the virgin Wyoming aggregates which had naturally fallen in three groups (Kimble, 2015). The limits developed are presented in Table 4. Figure 50 and Figure 51 demonstrate the current OEB expansions, and illustrate these limits.

[2] Reprinted from Cement and Concrete Research, Volume 30, Issue 7, Medhat Shehata, Michael Thomas, "The effect of fly ash composition on the expansion of concrete due to alkali-silica reaction", pp. 1063-1072., Copyright (2000), with permission from Elsevier

Table 4. UW field exposure block classification.

Classification	Limit (percent expansion/year)	
	Unboosted	**Boosted**
NR	<0.01	<0.02
MR	0.01<x<0.03	0.02<x<0.06
HR	>0.03	>0.06

Source: Fertig, 2017.

Because several test methods exist, UW developed a composite evaluation method based on OEB, CPT and AMBT results. To quickly compare the results from each test method, a "failure ratio" was calculated by dividing the expansion from the test by a corresponding limit. The limits used are from the FHWA. The OEB contributed the most weight to the final classification, followed by the CPT and then the AMBT. Taking these factors into account, Figure 7 is proposed to calculate the final classification of the aggregate. When this equation is used, the results can be interpreted in the following way: x < 1 = NR, 1 < x <2.5 = MR, 2.5 < x < 4.5 = HR, 4.5 < x = VHR.

$$0.45 \cdot UBF + 0.4 \cdot CPT + 0.1 \cdot BF + 0.05 \cdot AMBT = x$$

Figure 7. Equation for composite classification calculation.

Where:
UBF=Unboosted field specimen failure ratio.
CPT=CPT failure ratio.
BF = Boosted field specimen failure ratio.
AMBT=AMBT failure ratio.

4 MATERIALS

The following sections describe the aggregates, cements and admixtures employed within each study.

4.1 Material Selection

The materials chosen for each testing program are explained here:

- **Unmitigated Testing**
  - All eight virgin Wyoming aggregates were tested to expand on the previous testing that involved all eight Wyoming aggregates. Additionally, WYDOT funded the majority of this work where these eight sources are specifically of interest.
  - BT aggregate was utilized as the nonreactive aggregate from AMBT testing.
  - The cement was required to be a high alkali cement per ASTM C1293.
- **Mitigated testing**
  - Twenty-five percent fly ash replacement was chosen because it represents the maximum amount of fly ash allowable by WYDOT. Fly ash was used to replace cement on a percent by mass basis per ASTM C1293. Additionally, 25 percent replacement has historically been able to fully mitigated ASR-induced expansions from each source.
  - FA1 was previously evaluated and shown to be effective in the AMBT. FA2 through FA5 represent alternative sources of interest due to their proximity to Wyoming DOTs.
  - GP, KR, LBG, LX, and WOR virgin aggregates were evaluated against each fly ash. These aggregate sources were chosen because they represent the reactive aggregate sources currently used by WYDOT. Additionally, they represent a range of reactivity which may demonstrate that the 25 percent replacement could be relaxed in future testing.
  - The cement was required to be a high alkali cement per ASTM C1293.
- **ACPT**
  - GP, KR, LBG, and WOR were chosen to represent moderately or highly-reactive aggregates and HP was chosen to represent a potentially nonreactive aggregate.
  - BT aggregate was utilized as the nonreactive portion because it has a good history in both field and AMBT testing. Additionally, the quality was consistent across shipments as opposed to previous testing using Beckman aggregate.
  - The cement was required to be a high alkali cement per the testing procedure.

4.2 Aggregates

The virgin aggregate used throughout this report comes from eight different locations throughout Wyoming. Virgin aggregates are aggregates that come directly from an aggregate source. This includes both course and fine aggregate along with any aggregate that has been crushed. Several shipments of aggregate from each pit have been delivered to UW engineering. Aggregate

properties, such as specific gravity, absorption capacity, unit weight, gradations etc., are reported in Table 19 and Table 20.

4.3 Cement

The high alkali cement came from Mississauga, Ontario in Canada was used within this report. The chemical composition of this cement is indicated in Table 5. Three shipments of the high alkali cement were received, one in 2015 and two in 2016. The 2015 shipment was used in the mitigated CPT investigation with fly ash. The first shipment in 2016 was shipped to UA to perform ACPTs, the remaining cement from this shipment was used in standard CPTs that separated the coarse and fine aggregates. The second shipment that arrived in 2016 was six months after the first. This cement was used to cast ACPTs at UW to compare with those cast at UA. Both 2015 and the first 2016 shipment are indicated in Table 5. Chemical compositions were not available for this second 2016 shipment, and were assumed to be the same as the first shipment. The bolded section Na_2Oeq is the governing factor when determining the total alkalis available in the cement paste matrix. The value is determined by: percent Na_2O + 0.658 times percent K_2O.

Table 5: Chemical analysis of cement

Chemical	**High alkali cement**	
	Shipment 2015 (%)	**Shipment 2016 (%)**
Na_2O	0.24	0.23
K_2O	1.16	1.16
SiO_2	19.2	19.1
Al_2O_3	5.2	5.3
Fe_2O_3	2.5	2.4
SO_3	3.8	4.1
CaO	62.9	62.1
MgO	2.4	2.5
C_3S	57	53
C_2S	11	14
C_3A	10	10
C_4AF	7	7
Na_2O_{eq}	**1.01**	**0.94**

Source: UW Tanner research group.

4.4 Fly Ash

The physical properties of each fly ash is given in Table 6 and the chemical makeup of each fly ash is given in Table 7.

Table 6: Relevant physical properties for fly ash.

Physical Property	FA1	FA2	FA3	FA4	FA5
SG	2.33	2.39	2.52	2.45	2.34

Source: UW Tanner research group.

Table 7: Fly ash chemical composition according to ASTM C618.

Chemical	FA1 (%)	FA2 (%)	FA3 (%)	FA4 (%)	FA5 (%)
SiO_2	54.4	60.63	52.42	52.86	60.66
Al_2O_3	23.48	18.08	16.30	19.62	21.24
Fe_2O_3	4.28	4.68	6.10	5.68	5.02
SO_3	0.40	0.80	0.69	0.56	0.42
CaO	9.67	6.02	13.03	13.66	5.24
MgO	2.15	2.14	4.53	3.04	1.39
Na_2O	0.70	3.07	1.85	0.52	1.92
K_2O	1.09	1.18	2.45	1.05	1.42
TiO_2	0.85	1.01	0.66	1.27	1.12
P_2O_5	1.24	0.54	0.24	0.26	0.19
Na_2O_{eq}	**1.42**	**3.85**	**3.46**	**1.21**	**2.86**

Source: UW Tanner research group.

4.5 Additional Materials

For the AMBT and CPT methods, alkalis needed to be added to the system to reach a total alkali content of 1.25 percent. This was done by adding sodium hydroxide (NaOH) pellets in the mixing water.

To achieve the correct workability in the CPT mixes, a superplasticizer was used. Specifically, Sikament 686 which is a high range water reducing admixture, but can also be used as a mid-range water reducing admixture in lower dosages. It is also a poly-carboxylate, which has been shown not to affect ASR (Leeman et al., 2010). Each form was sprayed with WD-40 to lubricate the molds before casting.

5 TESTING PROCEDURES AND EQUIPMENT

A list of the test methods described in this section and summary of what was done in each method is presented in Table 8. Virgin Wyoming aggregates consist of Black Rock (BR), Devries Farm Pit (DF), Goton Pit (GP), Harris Pit (HP), Knife River (KR), Labarge (LBG), Lamax (LX), and Worland (WOR). The non-reactive aggregate is labeled BT. The XX designation for the separated coarse and fine CPT is a place holder for the potential aggregate used. As an example, a specimen set cast with Knife River fines would be KR-F. The coarse aggregate would be the nonreactive BT.

Table 8. Project descriptions.

Testing Type	Specific Category of Testing	Description of Test
Field Specimens	-	Continuation of measuring existing outdoor exposure blocks OEBs.
CPT	Mitigated or MCPT	Uses aggregate from the same pit for both coarse and fine sized fractions to explore the effects of four different fly ashes on five Wyoming aggregate combinations.
	Separated Coarse and Fine	Separates the potentially reactive aggregate into coarse and fine sized fractions to test their individual reactivity. Each fraction is supplemented with a nonreactive aggregate. For example, a potentially reactive coarse aggregate would be paired with nonreactive fine aggregate and vice versa.
AMBT	Recycled Concrete Aggregate (RCA)	Recycled concrete aggregate was used to perform AMBTs at a variety of laboratories.
	Precision Statements	The results from the RCA AMBT inter-laboratory study are analyzed using statistical methods to produce a guiding precision statement for the use of the AMBT with RCA.
Autoclaved Concrete Prism Test	Separated Coarse and Fine	This test is performed on separated coarse and fine aggregates just as the separated coarse and fine CPT. However, the test is completed over the period of four days through the use of an autoclave.
Predictive modeling	-	Models have been developed based on the AMBT and the CPT for use with fly ash mitigation methods. These models have been employed and compared against the results of this and previous work with fly ash and Wyoming aggregates.

Source: UW Tanner research group.

5.1 Outdoor Exposure Blocks

Although less commonly performed, large scale field testing of ASR has been a priority at UW because these specimens represent field performance more closely. The original OEBs were cast in 2008. The coarse and fine aggregate are from the same pit. OEBs can be used as benchmark ASR assessments for accelerated testing. This is because both the AMBT and CPT are stored in a controlled environment, which limits their ability to predict the true reactivity of aggregates (Ideker et al. 2012). The lack of control of the environmental exposure to the field specimens makes understanding all the factors that go into ASR difficult. However, each of those factors affect concrete used in the real world, and that is where the true value of the field expansions begins to emerge. An image of the outdoor exposure site and schematic showing measurement locations is illustrated in Figure 8 and Figure 9.

Source: UW Tanner research group.

Figure 8. Photo. Outdoor Exposure site.

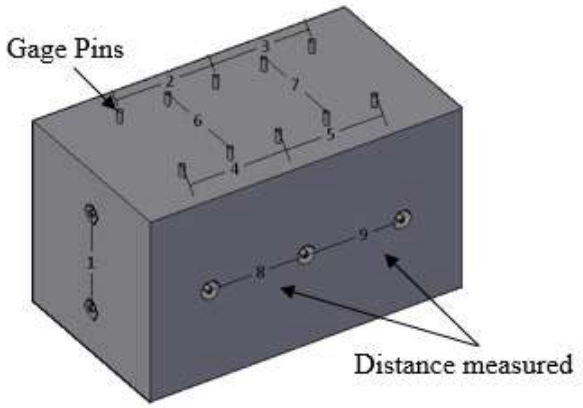

Source: UW Tanner research group.

Figure 9. Photo. Field block measurement locations.

The blocks rest on 3/4 inch (19.5 mm) angular gravel atop a bed of 4 inch (101.6 mm) rock to ensure a level surface and a properly drained foundation. Each specimen was cast in 15 x 15 x 26 inch (380 x 380 x 660 mm) plywood forms. The forms were coated with a debonding agent and the edges and corners were caulked to prevent moisture loss during curing. Threaded steel inserts were utilized to create 12 measurement locations for each block. The measurement locations are

illustrated in Figure 9. Four longitudinal and two transverse measurements are on the top, two longitudinal measurements are along each side and one vertical measurement on the ends.

Measurements are taken utilizing a Demec mechanical strain gage, and are recorded to the nearest 3.9x10-5 inches (0.001 mm). The Demec and reference bar are presented in Figure 10 and Figure 11. Care was taken to use the instrument in the same manner every time. Suggestions for measuring consistently with this device is outlined in Kimble (2015):

1. Expose the Demec, thermostat and the reference bar to field conditions to avoid discrepancies due to thermal changes in the measurement equipment. If it is sunny, shade the equipment and the block for at least twenty minutes prior to measuring to reduce thermal gradients.
2. After the instrument and reference bar have normalized to the outdoor temperature, turn on the instrument and measure the reference bar to obtain the reference measurement.
3. On the block, measure each distance between studs at least three times, and confirm that the difference in measurements is less than 0.2 x 10-3 inch (0.005 mm) each time.
4. Record the average of these three measurements.
5. Repeat steps 2 through 4. The second series of measurements should be completely independent of the first measurement series.
6. If the difference between related measurements in the two series is more than 0.59 x 10-3 inch (0.015 mm) (equivalent to 0.0075 percent expansion) then that location on the specimen should be measured again.

An analysis of measurement error using the device was conducted with the supplied reference bar. The error was found to be 0.47 x 10-6 inch (1.2 micrometers). A separate analysis was also conducted to determine the effects of rotation on the readings. It was found that measurements at 5 degrees of rotation did not show significant variation while measurements with a rotation greater than 5 degrees did" (Kimble, 2015). The device was constructed using invar to reduce thermal expansions. Furthermore, thermal effects based on ambient temperature were accounted for by recording the surface temperature at the time of recording and adjusting measurements to a constant 70 degrees F (21 degrees C); the coefficient of thermal expansion used was 5.5 x 10-6/(degree F) (11.7 x 10-6/(degree C). The final expansion is the average of the twelve measurements.

The Demec gage has conical measurement points, which fit inside pin holes on both the reference bar, and the ends of the threaded rods in each specimen. Images of the measurement points are provided in Figure 12. Photo. OEB gage pin The Demec instrument has a fixed maximum length that can be measured, therefore two measurement points were placed in each threaded rod. This allows the measurement points to be adjusted as the blocks expand, should the original measurement points become too large for the Demec gage.

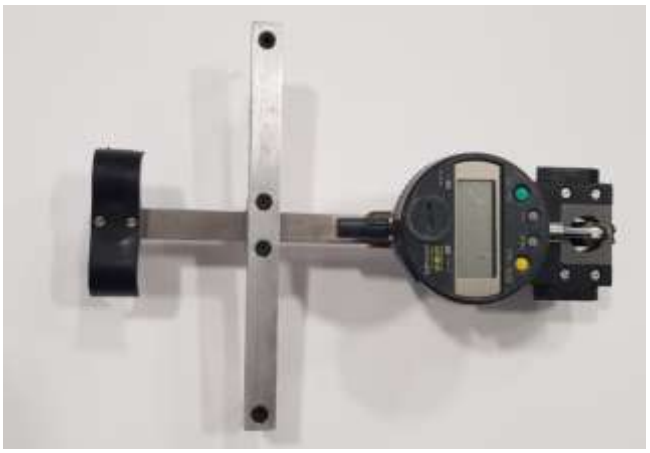

Source: UW Tanner research group.

Figure 10. Photo. Mechanical strain gage instrument.

Source: UW Tanner research group.

Figure 11. Photo. Reference bar.

Source: UW Tanner research group.

Figure 12. Photo. OEB gage pin.

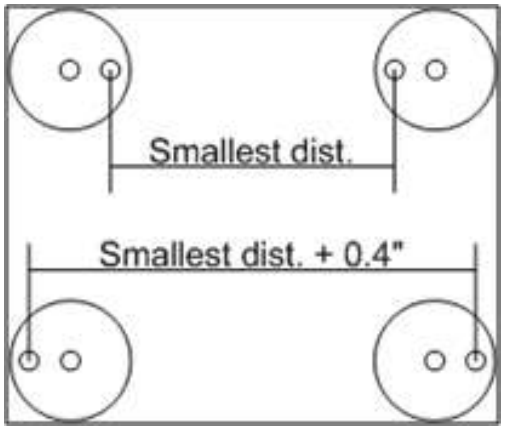

Source: UW Tanner research group.

Figure 13. OEB measurement points.

Aggregate gradations for each specimen were the same as the gradation of the as received aggregate from each source (Fertig, 2010). In addition, the aggregate used for both coarse and fine came from the same source pit. A poly-carboxylate superplasticizer was utilized to achieve the desired workability. Generic material quantities are displayed in Table 9. Specific quantities of material for each specimen are displayed in the

Appendix G: OEB Data, in Table 40. At least one specimen from each aggregate source used NaOH to boost the cement alkalinity to a Na_2O_{eq} of 1.25 percent to accelerate the test and represent an upper bound of the aggregate's reactive potential.

Table 9. Material quantities common to all field specimens.

Material	Quantity (lb.)
Coarse Aggregate	305
Fine Aggregate	196
Cement	124

Source: Fertig, 2010.

5.2 CPT unmitigated and mitigated (ASTM C 1293)

There are two types of CPTs that were explored in this project: standard aggregate analysis and mitigation with various fly ashes. While each test fits within the same ASTM standard, there are some differences in the execution of each type of test. These differences are described in this section. The mitigated CPTs (MCPT) assess the ASR potential of five different aggregates of varying ASR potential with four different fly ashes for a total of twenty combinations. This study evaluates the effectiveness of each fly ash to mitigate ASR. The standard CPT assess the ASR potential of each of the eight aggregate sources in Wyoming in either its coarse or fine fraction for a total of 16 tests. Additionally, this test provides a benchmark for the ACPTs.

5.2.1 Basic Test Method

The CPT as defined by ASTM C1293 is carried out over one year for normal concrete specimens and two years for concrete specimens containing SCMs. The test uses three 3 x 3 x 11.25 inch (75 x 75 x 285 mm) prisms with a water-to-cement ratio between 0.42 and 0.45. An additional fourth specimen was created for redundancy. These molds are depicted in Figure 14.

Source: UW Tanner research group.

Figure 14. Photo. CPT molds.

One set is considered three or four specimens depending on how many are cast from the same batch. A specific proportion of coarse aggregate and cement content is used in conjunction with the absolute volume method described in Design and Control of Concrete Mixtures (Kosmatka et al., 2003). The cement content is 707.94 lb/yd3 (420 kg/m3). The cement is also required to have a base total alkali content of 0.9±0.1 percent Na_2O equivalent, which is boosted to 1.25 percent by mass of cement through the addition of NaOH. The specimens themselves have a steel gage pin on each end for measuring the expansion with a comparator shown in Figure 16. Photo. Comparator with specimen. The specimens are stored at 100 percent relative humidity in an oven maintained at 100 degrees F (38 degrees C). Two types of ovens are used. They are displayed in Figure 15. The second type of oven is a 4 x 8 ft (1.2 x 2.4 m) box, sheathed with OSB on the outside and cement board on the inside. Two-inch thick insulation fully encapsulates the structure. A temperature controlled space heater is used to maintain a constant temperature, and a fan is used to circulate the air within the room.

a)Type one b) Type two

Source: UW Tanner research group.

Figure 15. Photo. Oven.

Source: UW Tanner research group.

Figure 16. Photo. Comparator with specimen.

Source: UW Tanner research group.

Figure 17. Photo. Comparator with reference bar.

One hundred percent relative humidity is achieved by suspending the specimens over approximately 1 inch of water at the bottom of a 5-gallon bucket.. A top rack is also used to secure and separate the specimens. A wicking fabric is used to line the inside of the bucket to help maintain a constant humidity. A screw top lid is used to seal the bucket and trap the moisture allowing for the humidity to build when the buckets are stored in the oven. The expansion limit for the CPT is 0.04 percent at one year to classify the aggregate as potentially deleteriously reactive aggregate. If supplementary cementitious materials (SCMs) are used, the

limit is 0.04 percent after two years. A storage container and the supporting racks can be seen in Figure 18.

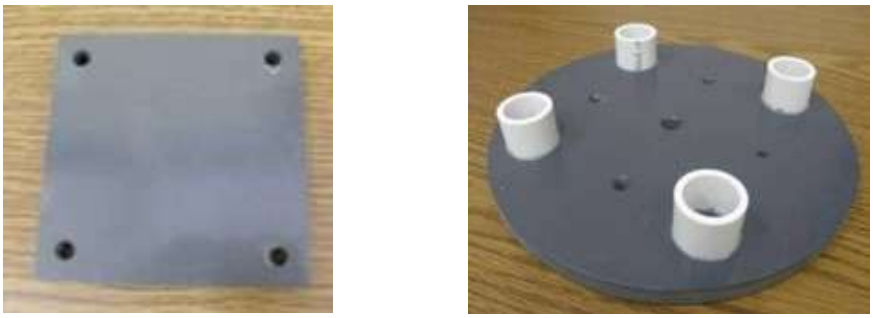

a) Top rack b) Bottom rack (upside-down)

Source: UW Tanner research group.

Figure 18. Storage container and the supporting racks.

5.2.2 Aggregate Preparation

The coarse aggregate is separated into 1/2 inch (12.5 mm), 3/8 inch (9.5 mm) and No. 4 (4.75 mm) sized fractions and the fine aggregate are separated into No. 8 (2.36 mm), No. 16 (1.180 mm), No. 30 (0.600 mm), No. 50 (0.300 mm) and 100 (0.150 mm) sized fractions. Once separated, the aggregate is then reassembled based on the quantities outlined in Table 10 and Table 11. The test is designed to assess the ASR reactivity of either a fine aggregate, or a coarse aggregate, by supplementing the concrete mix with non-reactive aggregate. This means that if the potential reactivity of a coarse aggregate is being tested, then a known non-reactive fine will be used and vice versa if the potential reactivity of a fine aggregate is being tested.

Table 10. CPT coarse aggregate grading requirements.

Gradation	
Size (mm)	Mass fraction
1/2 in. (12.5)	1/3
3/8 in.(9.5)	1/3
No. 4 (4.75)	1/3

Source: UW Tanner research group.

Table 11. CPT fine aggregate grading requirements.

Gradation (ASTM C 33)	
Size (mm)	Percent Passing (%)
No. 8 (2.36)	80 to 100
No. 16 (1.180)	50 to 85
No. 30 (0.600)	25 to 60

No. 50 (0.300)	5 to 30
No. 100 (0.150)	0 to 10

Source: UW Tanner research group.

Because WYDOT combines coarse and fine aggregate from the same source. Therefore, these prisms are testing for the mitigated ASR behavior of the coarse and fine aggregate combination. The fine aggregate in this test conformed to Table 11. For all cases the No. 100 (0.150 mm) percent passing was taken to be 0 percent. The aggregate was not washed before casting. For this test, four prisms were cast. The actual MCPT gradations used are given the Appendix A: Physical property tests and batch quantities in Table 21.

The aggregate for the separated CPT investigation was washed before casting. This was done by weighing out the dry material on the appropriate sieve and running water over the aggregate until the water ran clear. To expedite washing time, a wash frame was built and is illustrated in Figure 19. Once each sieve was loaded, they were stacked in the frame with the largest size on top. Water was poured over the top of the largest size. Once the water ran clear, that sieve was removed and the next smallest size was washed. This process was followed until all the aggregate sizes were washed. The coarse aggregate was washed on top of the inclined shoot.

a) Front b) Side

Source: UW Tanner research group.

Figure 19. Photo. Aggregate wash frame.

After washing, the aggregate was mixed in its wet state in a large metal container. As much of the excess water was drained as possible and then the aggregate was placed in the oven. The aggregate was dried to a target point of Saturated Surface Dry (SSD). The purpose of leaving the aggregate wet was to promote workability throughout the casting process (Poon et al., 2004). Additionally, testing at the University of Alabama (UA) shows a nonreactive dry aggregate will exhibit larger expansions than the same aggregate that is cast in a state near SSD. It is postulated that the dry aggregate absorbs the alkali boosted mixing water, promoting an exacerbated reaction from within the pores of the aggregate. This type of behavior has been observed in the CPT with RCA (Scott and Gress, 2004). Variances in moisture content in each mix design is due to becoming acquainted with the method and judging an SSD state visually.

Once the aggregate was dried, a representative sample was taken and placed in the oven at 230 degrees F (110 degrees C) for at least 16 hours to determine the moisture content of the aggregate. The rest of the material was placed in a bucket with a screw top lid, where moisture loss was assumed to be negligible.

5.2.3 Casting Method

Both the MCPT and CPTs utilized the following casting method according to ASTM C192(ASTM C192, 2016).

5.2.4 Physical Property Tests and Molding

The specimens were tested for slump, unit weight and air content according to ASTM C 143 and ASTM C 138 respectively then placed in the appropriate molds according to ASTM C 157 (ASTM C138, 2016; ASTM C143, 2015; ASTM C157, 2014).

5.2.5 Curing

Companion cylinders were cast to check quality control of the concrete for the separated coarse and fine CPTs. Twenty-four hours after casting the prisms or cylinders, they are demolded. Once demolded, the prism lengths were measured, and placed in the storage buckets which were then placed in the oven.

5.2.6 Measurements

Prism measurement intervals are: initial measurement on days 1, 7, 28, 56, 3 months, and every subsequent three months until the completion of the test. Cylinders are tested on day 28. The prism lengths are measured by turning on the comparator and zeroing it out using the reference bar, then placing gauge pins of the specimen into the comparator and giving it a light spin. The lowest number is read off the comparator. The specimens were marked with an arrow in order to maintain the same orientation at each measurement. After each specimen was measured, they were flipped upside down and returned to the storage container to reduce alkali leaching.

The cylinders were tested according to ASTM C 39 in a 400 k (1780 kN) Forney test machine (ASTM C39, 2016).

5.3 Accelerated Mortar Bar test (AMBT)

This test is normally conducted using virgin aggregate as defined by ASTM C1260. The AMBT is a relatively quick way to assess whether an aggregate will exhibit deleterious ASR expansions. Reactivity can be determined 16 days after the initial casting, although many investigators extend the duration to 28 days. The test is limited to fine aggregate based on the size of the specimens and is often criticized for the harsh environment in which the specimens are stored. If coarse aggregate is tested using this method, it should be crushed to the appropriate size. It prescribes the amount of cement and aggregate to be 440 and 990 g, respectively. The water to cement ratio is maintained at 0.47. The materials are used to cast three 1 x 1 x 11.25-inch (25 x 25 x 285 mm) mortar bars; this defines one set. These molds are illustrated in Figure 20.

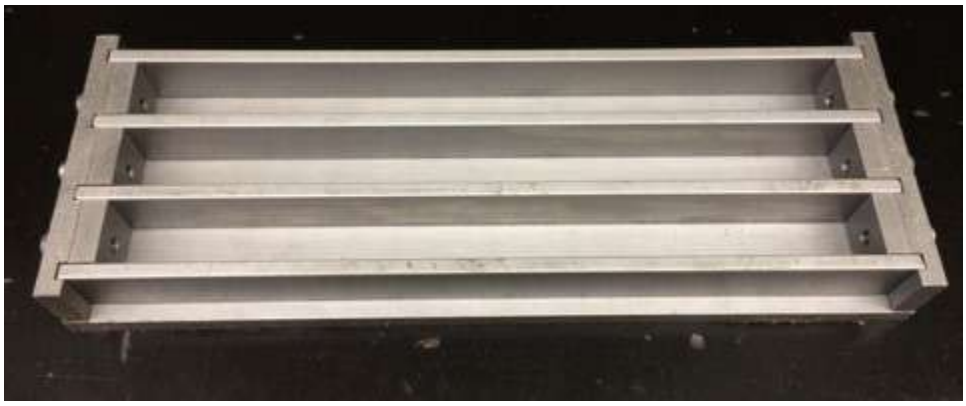

Source: UW Tanner research group.

Figure 20. Photo. AMBT mold.

Each bar has a steel gauge stud on the ends to measure expansions with the length comparator illustrated in Figure 16. Fine aggregate is washed to remove adhered extra fine particles and provide consistency among materials sent to other laboratories.

All the aggregate was washed, dried back to an oven dry state and sent to the participating laboratories. Each lab assembled the separated aggregate by mass as defined in Table 12. The mixer used for this test method is shown in Figure 21. A modified mixing procedure was suggested to eliminate early expansions due to an increased absorptivity exhibited by RCA (Adams et al., 2013).

Table 12. AMBT Grading Requirements.

Size (mm)	Mass (%)
No. 8 (2.36)	10
No. 16 (1.180)	25
No. 30 (0.600)	25
No. 50 (0.300)	25
No. 100 (0.150)	10

Source: UW Tanner research group.

Source: UW Tanner research group.

Figure 21. Photo. AMBT mixer.

For this study, the standard mixing procedure in ASTM C305 was used and is summarized here (ASTM C305, 2014):

- The green mortar is placed in the molds within 2 minutes and 15 seconds after completion of mixing the mortar. The molds are filled in two layers and compacted with a tamper. The molds are struck off with a trowel. These specimens were then covered in plastic and transported to the fog room for curing.
- 24 ± 2 hrs. after casting, the specimens are demolded, an initial measurement is taken, and then they are placed in a container full of water at room temperature. This measurement is the initial measurement.
- The specimens are then placed in an oven at 176 ± 3.6 degrees F (80 degrees C ± 2.0 degrees C) for 24 ± 2 hrs. The mortar bars are then measured as day zero and placed in a 1 N NaOH solution that is already at 176 ± 36 degrees F (80 degrees C ± 2.0 degrees C). The bars are measured periodically throughout a 14-day period from day zero. For this study, the measurements were extended to 28 days. The target days were: 0, 3, 5, 7, 10, 12, 14, 17, 19, 21, 24, 26, and 28.
- Expansions below 0.1 percent are considered innocuous and expansions larger than 0.2 percent is indicative of potentially deleterious expansions. Expansions between 0.1 percent and 0.2 percent include aggregate that may have innocuous or deleterious expansions in field performance (ASTM C1260). In practice, the 0.1 percent limit is used to judge an aggregates ASR potential as reactive or innocuous.

5.4 Autoclaved Concrete Prism Test (ACPT)

Work in this area was started at UT Austin by Giannini and Folliard (Giannini and Folliard, 2013). It was continued by comparing data at UW and the University of Alabama (UA). Initial comparison tests showed strong correlation for coarse aggregate but some discrpency in expansions for fine aggregates. This is primarily attributed a low strength non-reactive coarse aggregate quality. As a result, procedures were compared and testing was continued in hopes of obtaining better inter-laboratory repeatability thereby adding merit to a test that significantly reduces exposure time compared to the CPT (4 days versus 1 year).
This test follows the same procedure as the standard CPT with the following exceptions:

- After gaining experience from the separated CPT wash procedure, the aggregate was washed, dried back to oven dry state, and then recombined according to the AMBT gradation. Water was mixed into the combined aggregate to achieve a moisture content slightly above saturated surface dry and sealed in a screw top bucket.
- Total alkalis are raised to 3.0 percent.
- Specimens cure another 24 hours after demolding.
- An initial measurement is made at this point.
- The specimens are placed in an autoclave for 24 ± 3 hours at 29 psi (0.2 MPa) with the temperature set at 133 degrees C.
- After the specimens are autoclaved, the specimens are cooled from approximately 194 degrees F (90 degrees C) to 73.4 degrees F (23 degrees C) over about 1 hour by submerging them in 194 degrees F (90 degrees C) water and running cool water through the tank. This was achieved by placing a five-gallon bucket full of water with its lid on into the oven at 230 degrees F (110 degrees C) at the same time the specimens are placed in the autoclave.
    - It is optional to measure the pH of the water that remains in the autoclave.
- The final measurement is taken once the prisms are cool.
- The expansion limit is 0.08 percent.

The autoclave is shown in Figure 22. Batch quantities and physical property test results are given in the Appendix A: Physical property tests and batch quantities in Table 27 and Table 28.

a)Exterior b) Interior

Source: UW Tanner research group.

Figure 22. Photo. Autoclave.

6 RESULTS AND DISCUSSIONS

6.1 CPT – Separated Coarse and Fine

This experiment separates the potentially reactive aggregate into coarse and fine sizes. A semi-local nonreactive aggregate was paired with each potentially reactive aggregate. The merit in performing the CPT in this way allows the results to be used as a benchmark for the experimental ACPT. Furthermore, it is a more detailed assessment of the ASR potential exhibited by each type of aggregate source. In previous testing at UW the coarse and fine aggregates were tested in combination from the same source because this is how WYDOT specifies concrete mixtures.

Results of this work are provided in Figure 23. The legend is organized by decreasing expansion, with the top label having the most expansion. Each potentially reactive source is named and the marker type is consistent with the rest of this thesis. Open or unfilled markers indicate fine aggregates and closed or filled markers represent coarse aggregates. The same line style is used for fine and coarse aggregates form the same pit. An overall trend can be seen in the legend of Figure 23 where the fine aggregates have larger expansions than their companion coarse aggregates because of the larger surface area for each particle.

An additional comparison between the combined and separated aggregate sources is given in Figure 24, where combined coarse and fine CPTs have a lower observed reactivity in all but two cases. These are for KR and LBG aggregates. This is attributed to a pessimum effect.

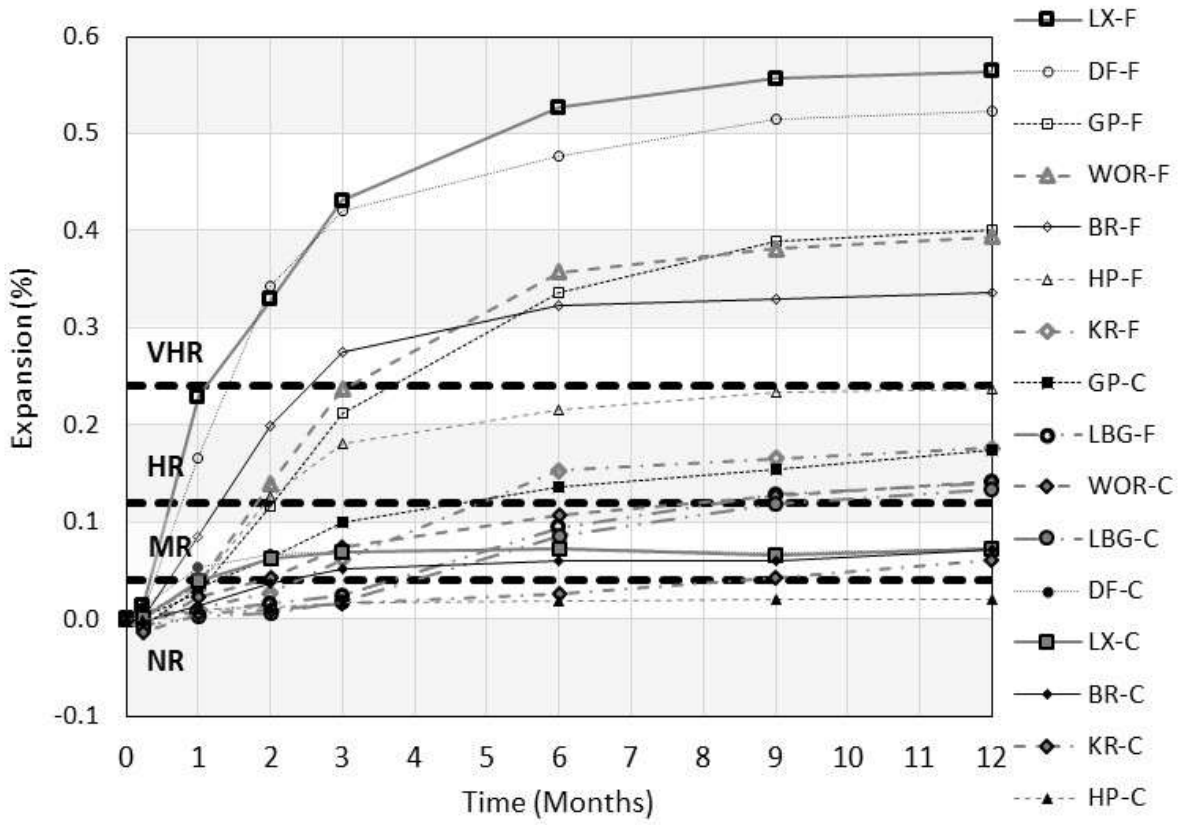

Source: UW Tanner research group.

Figure 23. Graph. Separated coarse and fine CPT results.

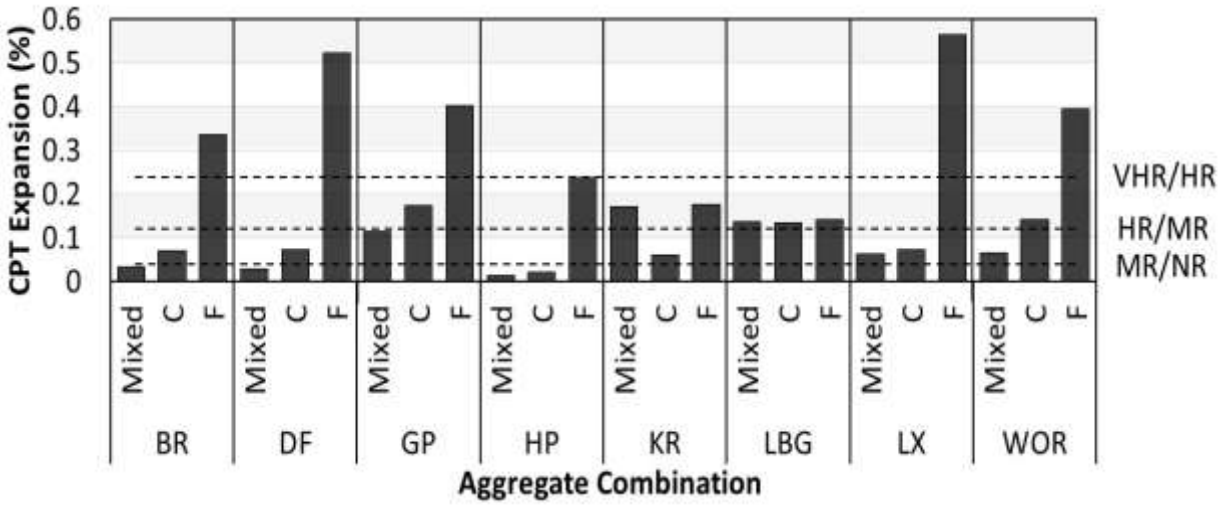

Source: UW Tanner research group.

Figure 24. Chart. Comparison of separated CPT and combined CPT.

During testing, two historically non-reactive aggregates showed early reactivity when the coarse and fine fractions were separated. These aggregates are DF-F, DF-C and HP-F. Therefore, targeted replicate specimens were cast to verify the behavior. The results of the replicate specimens are compared against the original sets in Figure 25. The overall expansion behavior between the two castings appears to be the same except for HP-F. Where the replicate specimen is showing less expansions than the original. Currently, DF-F is VHR, DF-C is MR and HP-F is VHR based on AASHTO PP65. Previous AMBT classifications indicate that DF is VHR and HP is moderately reactive. This is further explored in Figure 27.

Source: UW Tanner research group.

The compressive strengths of each CPT and ACPT mix can be seen in Figure 42 for comparison. Here HP-F and DF-F replicates have a lower strength than the original sets. Figure 26 illustrates that the nonreactive aggregate has CPT expansions of 0.025 percent which is less than below the reactive classification limit of 0.04 percent.

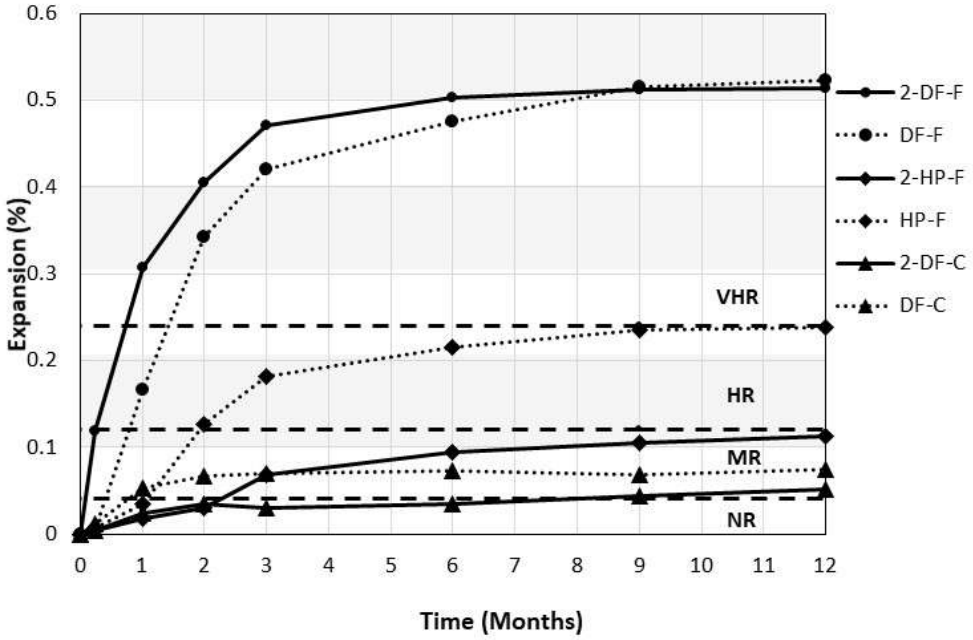

Source: UW Tanner research group.

Figure 25. Graph. Comparison of replicate specimens.

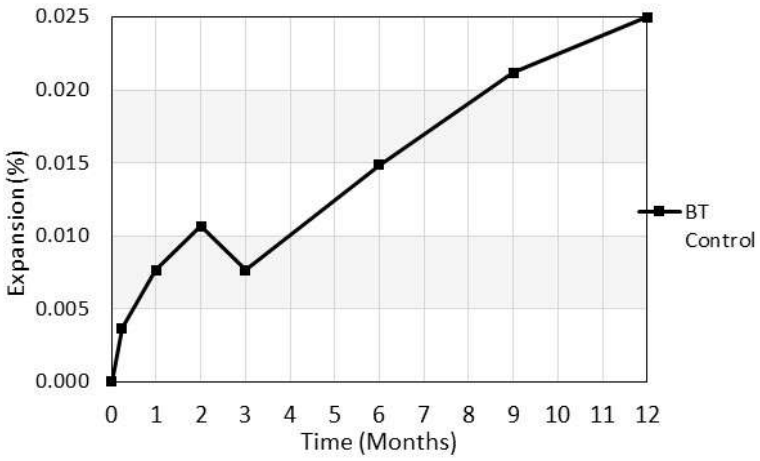

Source: UW Tanner research group.

Figure 26. Graph. BT control CPT expansions.

By comparing expansions of the mixed and separated CPTs, it is seen that reactive aggregates can be used as an effective ASR suppressant for DF and HP (Ichikawa, 2009). Additionally, the surface area of aggregate has an effect on ASR; fine aggregate fractions tend to exhibit greater expansions with the coarse fractions.

Source: UW Tanner research group.

Figure 27 indicates that AMBT results, shown in white, generally agree with the CPT-F results, shown in black. This makes sense because the AMBT was designed to evaluate fines only. Such results help to explain the previous disagreement in AMBT and CPT results because the AMBT is unable to consider the influence of coarse aggregate.

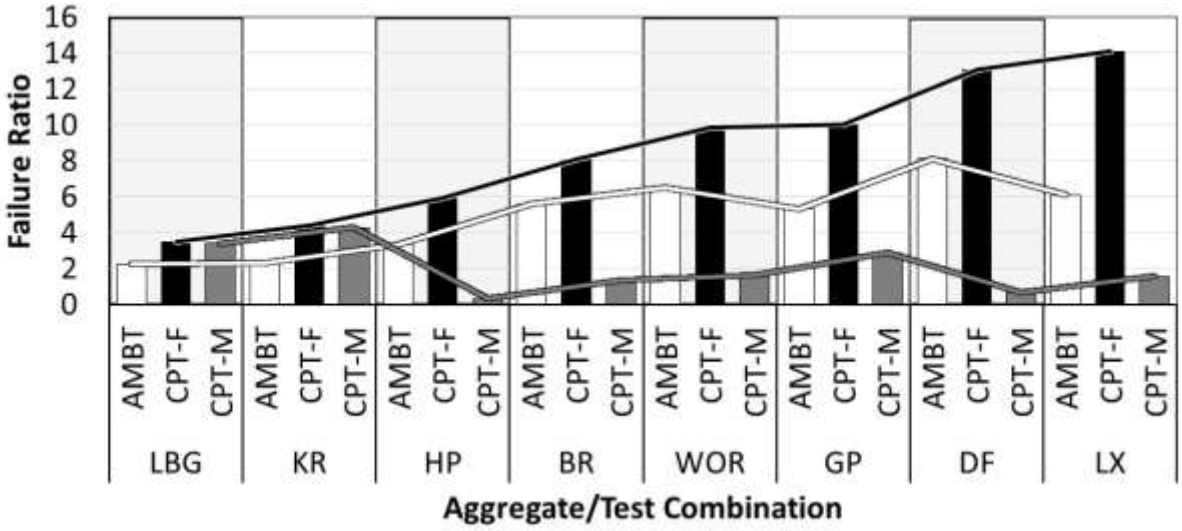

Source: UW Tanner research group.

Figure 27. Chart. CPT vs AMBT failure ratio.

6.2 MCPT – Fly Ash Specimens

The CPT specimens to evaluate mitigation (MCPT's) used a 25 percent fly ash replacement mix and with a 2-year exposure period. This experiment has been performed to provide data on the ASR mitigating efficacy of four sources of fly ash – FA2, FA3, FA4 and FA5 using a variety of reactive aggregates. FA1 has been previously evaluated in AMBT and CPT (Kimble, 2015), but due a difference in mixture proportions, it is not included for comparison. This will provide additional options for future projects, and potentially allow for matching a fly ash with an aggregate's level of reactivity.

AMBT and CPT expansions are provided in Table 13 along with the mitigated results for comparison. Any expansions greater than the 0.04 percent CPT limit or the 0.1 percent AMBT limit are displayed in bold italic font.

Table 13. Expansion comparisons between mitigated and unmitigated test results.

Source	CPT (%)	MCPT (%)				AMBT (%)	MAMBT (%)
		FA2	FA3	FA4	FA5		FA1
BR	***0.054***	N/A	N/A	N/A	N/A	***0.56***	0.039
DFP	0.026	N/A	N/A	N/A	N/A	***0.81***	0.095
GP	***0.114***	0.021	0.022	0.035	0.006	***0.53***	0.039
HP	0.011	N/A	N/A	N/A	N/A	***0.33***	0.024
KR	***0.172***	**0.046**	***0.050***	0.023	0.031	***0.23***	0.032
LBG	***0.136***	0.025	0.035	0.023	0.018	***0.22***	0.004
LX	***0.063***	0.024	0.031	0.006	0.005	***0.61***	0.083
WOR	***0.065***	0.027	0.026	0.014	0.004	***0.65***	0.031

Source: UW Tanner research group.

Figure 28 displays how effective each fly ash treatment is for each aggregate source. For reference, CPT values are included and the data is sorted by fly ash type, and then by increasing expansion. Expansion values are the most current measurement for each specimen set. The horizontal lines show the average expansion of each aggregate source for each fly ash. While the value of these horizontal lines is related to the aggregates sources, they illustrate the overall behavior of each fly ash. The larger the average expansion value, the less effective a 25 percent fly ash replacement is at mitigating ASR for all the aggregates in this study. Test results shows FA5 and FA4 are the most effective, followed by FA2 and ending with FA3. Despite these trends, all four fly ashes have successfully mitigated ASR below the 0.04 percent limit except FA2 and FA3 combined with Knife River exceeded the expansions limit.

Source: UW Tanner research group.

Figure 29 organizes the data in terms of aggregate source. Each plot shows the relationship between each fly ash on the indicated aggregate source over time. Figure 30 separates the data in terms of the type of fly ash being utilized. The graphs are intended to illustrate the relationship between aggregate sources and their individual expansions when using the specified fly ash treatment.

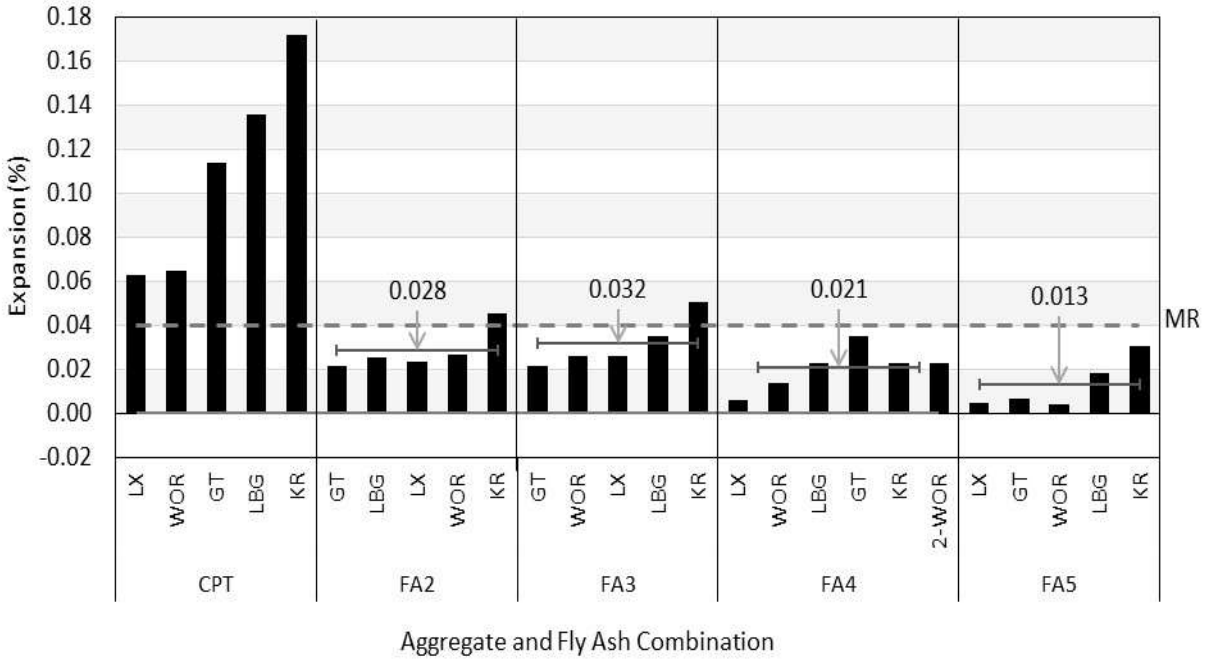

Source: UW Tanner research group.

Figure 28. Graph. Fly ash effectiveness with aggregate source.

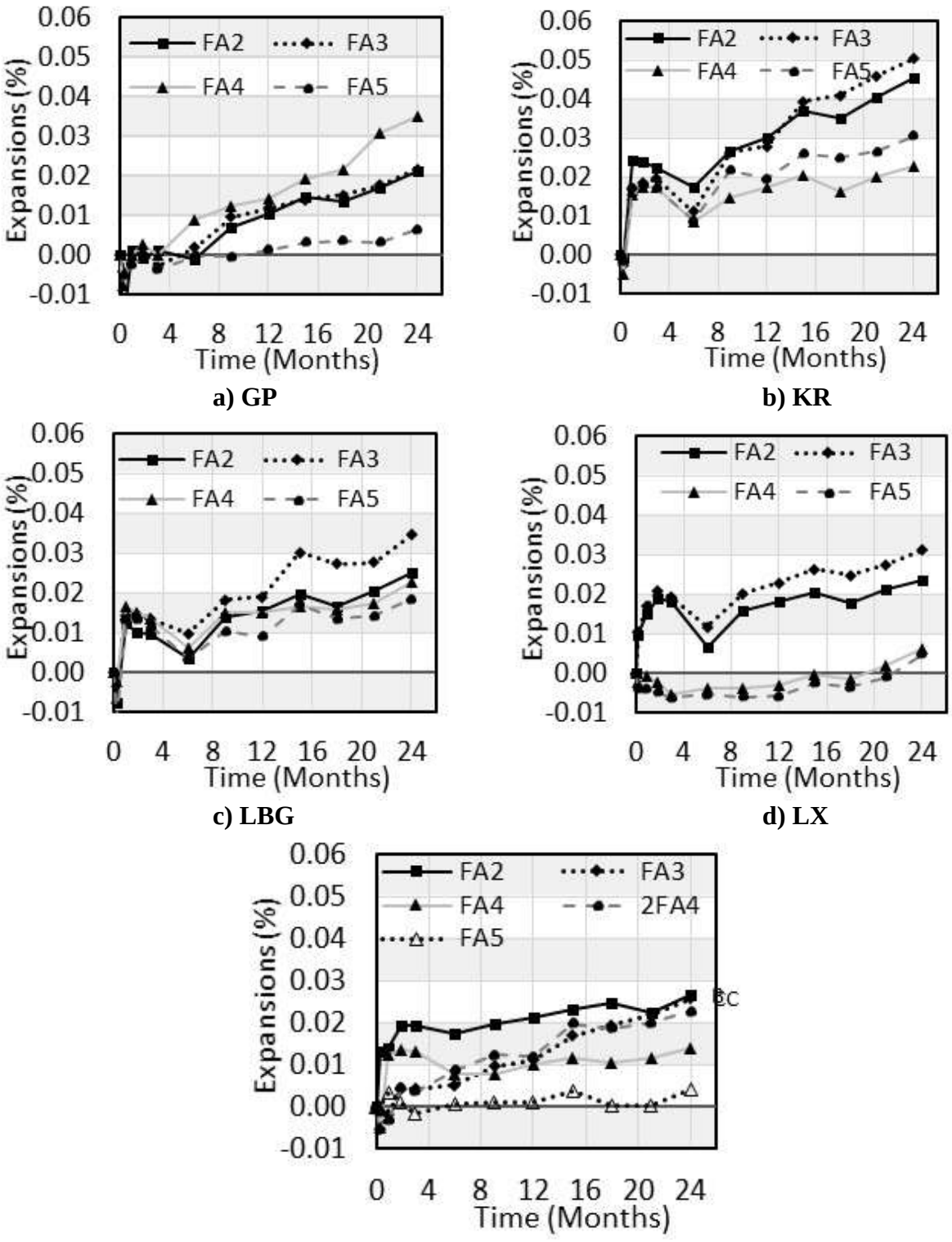

a) GP

b) KR

c) LBG

d) LX

e) WOR

Source: UW Tanner research group.

Figure 29. MCPT expansions for GT, KR, LBG, LX and WOR aggregates.

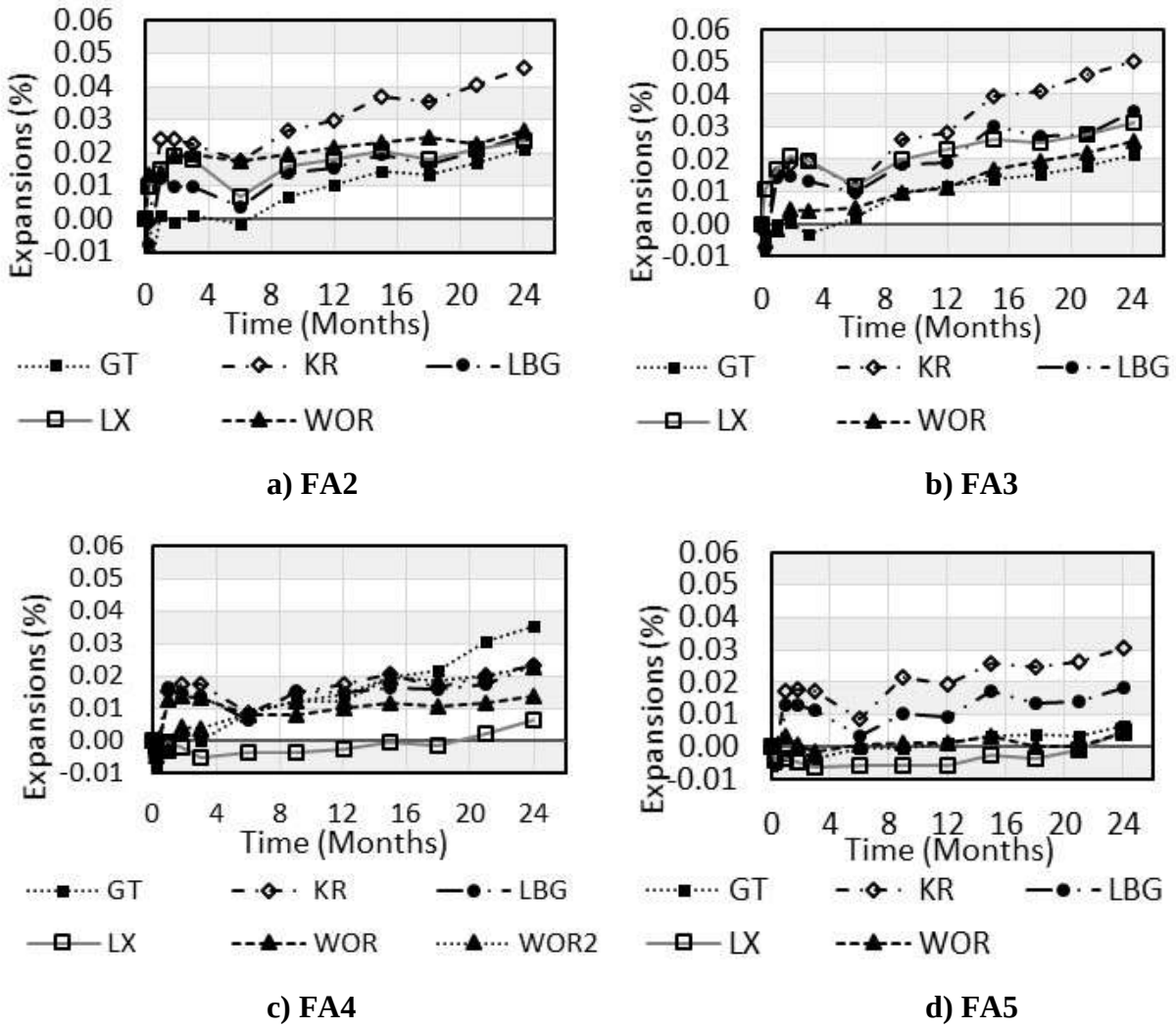

Source: UW Tanner research group.

Figure 30. Effect of different types of fly ashes on MCPT expansions.

6.3 Fly ash dosage prediction, mitigation, evaluation and assessment

Fly ash dosage predictions are available based on two different models that use the chemical composition of the fly ash and cement used in the concrete mix. The Malvar and Lenke model, uses AMBT expansion data to predict fly ash dosages that will mitigate AMBT expansions to below 0.08 percent. For a given fly ash, users should take measured AMBT expansion data (x-axis) and read a corresponding fly ash dosage (y-axis) to mitigate ASR to below the threshold. This limit shows some conservatism as the AMBT classification limit for innocuous behavior is 0.10 percent. Furthermore, two levels of certainty are considered: 50 and 90 percent reliability, shown in Figure 31 and Figure 32, respectively. While 50 percent reliability equation most closely matches the data used to develop the equation; the 90 percent reliability has additional conservatism embedded in the equation (Schumacher and Ideker, 2014). Because the equations are based on Class F fly ashes, this equation is not considered useful for class C fly ashes. (Malvar and Lenke, 2006; Vayghan et al., 2016).

More reactive aggregates require larger quantities of FA replacement. At both levels of reliability, the most effective fly ash is FA5 and FA3 is the least effective. Within these figures, unmitigated AMBT expansions for GP, KR, LBG, LX and WOR are shown for a 25 percent fly ash replacement. If the data points fall above, or to the left of the fly ash dosage prediction curves, it means that more fly ash was used than the minimum predicted by the model. Conversely, any data point that is beneath, or to the right of the dosage curve, means that more fly ash could be required to mitigate ASR beneath the corresponding limit.

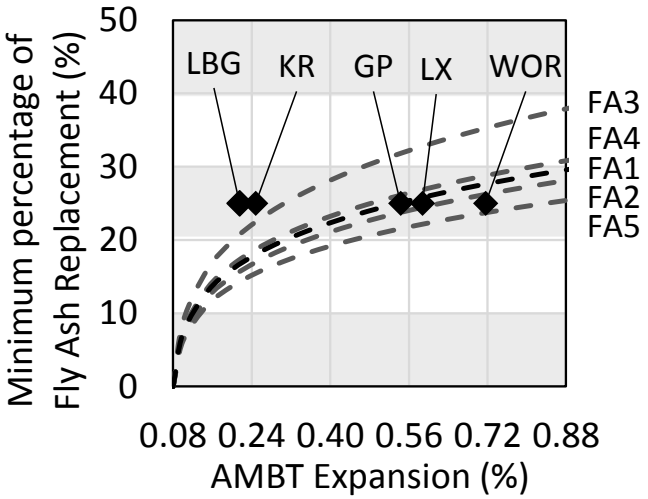

Source: UW Tanner research group.

Figure 31. Chart. Malvar and Lenke 50 percent reliability model.

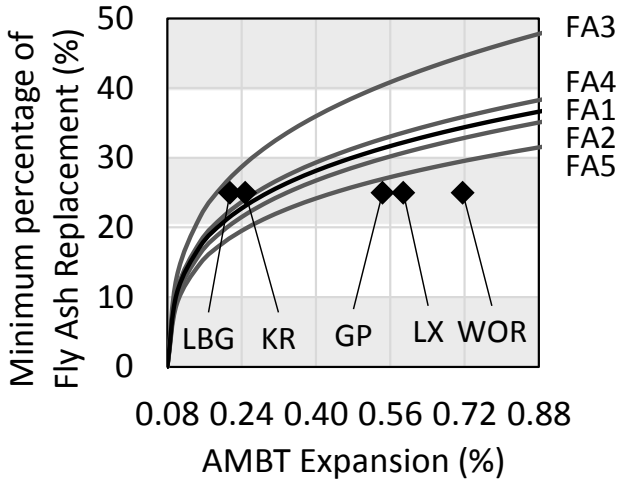

Source: UW Tanner research group.

Figure 32. Chart. Malvar and Lenke 90 percent reliability model.

A similar study was conducted by Vayghan et al (2016); their predictive equation is illustrated in Figure 33. As with the Malvar and Lenke model, the curve is based on the chemical composition of the fly ash and cement. It uses CPT expansion data to predict fly ash dosages that will mitigate ASR to below the 0.04 percent CPT limit. The most effective fly ash is FA5 with FA1 is the least

effective. Also, a 25 percent fly ash replacement for LBG and KR may not be sufficient to fully mitigate their ASR potential when FA3 and FA4 is used. Another benefit to the Vayghan equation is that it is applicable for both class C and class F fly ashes, making it more flexible than the Malvar and Lenke model. Additionally, the CPT expansions for each aggregate indicate a different order of reactivity as that predicted by AMBT expansions shown in Figure 31 and Figure 32. This could be related to the mixing of coarse and fine aggregates. If indeed the AMBT is not capable of considering coarse aggregates, it is prudent to use only the Vayghan model for comparison.

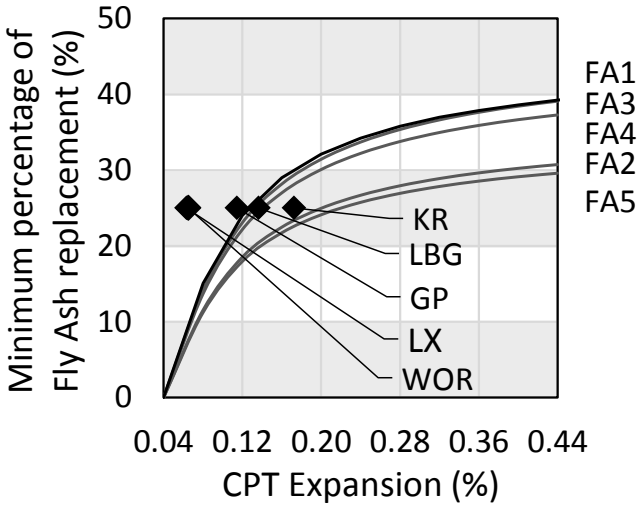

Source: UW Tanner research group.

Figure 33. Chart. Vayghan Model.

Figure 34 back calculates the maximum predicted expansion for each fly ash that can be mitigated below the 0.04 percent expansion limit. This allows for a straightforward comparison of predicted results to experimental results. The white bars indicate the unmitigated experimental results, which are intended to be compared against the black horizontal predicted max expansions. If the tested expansion is greater than this predicted horizontal bar, then the model predicts that 25 percent fly ash replacement is not enough to fully mitigate. If the model is reflecting the experimental data well, the trend of the black bars should follow the white bars. In this way, most of the MCPT results are performing similar or better than predicted. The combination FA2-KR and FA3-KR exceeded the classification limit of 0.04 percent. This is an un-conservative contradiction of the model. FA1 was not included in this comparison because the aggregate quantities were different for this particular fly ash.

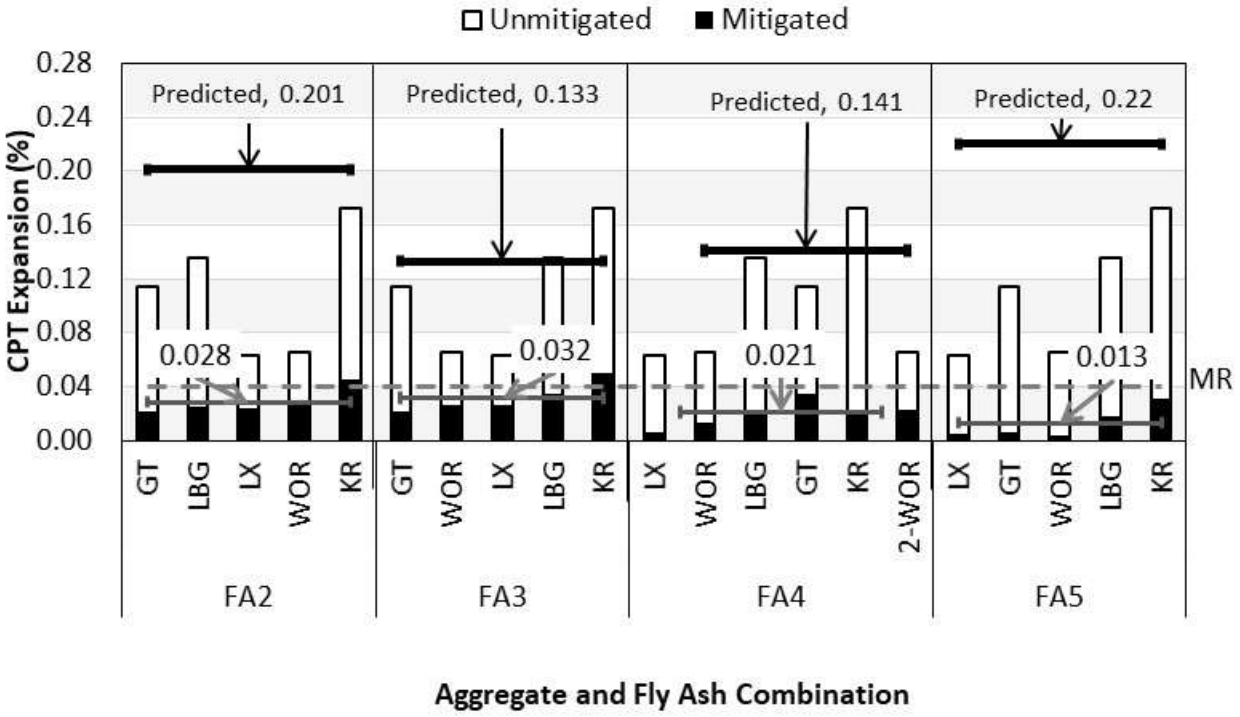

Source: UW Tanner research group.

Figure 34. Comparison of Fly Ash Predictions and Experimental Results.

The minimum fly ash dosage as predicted by each equation is presented in Table 14. The 50 percent reliability equation from Malvar and Lenke is used here because it has less conservativism. Any predicted dosage greater than 25 percent is shown in italic, bold font. Due to the different classifications for reactive aggregate between the CPT and AMBT methods, there is no overlap between equations for fly ash dosages that are greater than 25 percent. Because KR expansions exceeds the 0.04 percent limit, Vayghan suggests a 29.3 percent replacement with each of these fly ashes would be adequate. This roughly matches the experimental data because some expansions exceed the 0.04 percent limit. The Malvar and Lenke equation predicts approximately 20 percent. This is because of the low AMBT expansions.

Experimentally, FA1 was able to reduce each of these aggregate source expansions below the reactive limit in the AMBT at a 25 percent fly ash replacement level. This compares very well to the predictions in Table 14 where the greatest predicted dosage is 27 percent. This illustrates the conservatism in the equation even within the 50 percent reliability model.

Table 14. Minimum fly ash requirements.

Aggregate		GP	KR	LBG	LX	WOR
FA1	V Dosage (%R)	23.0	***30.1***	***26.3***	8.8	9.6
	ML Dosage (%R)	***25.1***	18.0	16.7	***25.8***	***27.62***
FA2	V Dosage (%R)	17.8	23.3	20.4	6.7	7.3
	ML Dosage (%R)	23.8	17.0	15.7	24.5	***26.2***
FA3	V Dosage (%R)	22.1	***29.3***	***25.4***	8.1	9.0
	ML Dosage (%R)	***31.8***	22.5	20.8	***32.8***	***35.3***
FA4	V Dosage (%R)	21.2	***28.1***	24.4	7.9	8.7
	ML Dosage (%R)	***26.1***	18.7	17.3	***26.9***	***28.8***
FA5	V Dosage (%R)	17.2	22.6	19.7	6.5	7.1
	ML Dosage (%R)	21.5	15.5	14.3	22.2	23.7

*Note: V = Vayghan fly ash dosage, %R = percent replacement of cement, ML = Malvar and Lenke fly ash dosage at 50 percent reliability.

Source: UW Tanner research group.

While FA1 was previously evaluated with reduced fines, the cement fly ash combination creates useful discussion towards the differences between Malvar and Lenke and Vayghan. Between the two models, FA1 is the only fly ash that occurs out of relative order. For example, in Figure 31 though Figure 33 the Malvar and Lenke equation predicts FA1 is in the middle of the group, yet the Vayghan indicates that FA1 is the least effective of the five fly ashes. Figure 35 through Figure 41 illustrate all the equations for promotors and suppressors.

$$\frac{CaO_{eq}}{SiO_{2eq}} = \frac{\text{Promotors}}{\text{Suppressors}} = \frac{CaO + 6.0(0.905Na_2O + 0.595K_2O + 1.391MgO + 0.7SO_3)}{SiO_2 + 1.0(0.589Al_2O_3 + 0.376Fe_2O_3)}$$

Figure 35. Equation. Malvar and Lenke Chemical Index.

$$C_b = \frac{f(CaO_{eqfa}) + (1-f)(CaO_{eqc})}{f(SiO_{2eqfa}) + (1-f)(SiO2_{eqc})}$$

f = fly ash replacement percentage, fa = fly ash. C = cement

Figure 36 . Equation. Malvar and Lenke Vulnerability Index.

$$P_c = 0.13CaO + 0.7Na_2O + 0.18K_2O + 0.19MgO$$

Figure 37. Equation. Vayghan Cement Promotors.

$$S_c = 0.17SiO_2 + 1.22Fe_2O_3$$

Figure 38. Equation. Vayghan Cement Suppressors.

$$P_{fa} = 0.2CaO + 0.44MgO + 0.34SO_3$$

Figure 39. Equation. Vayghan Fly Ash Promotors.

$$S_{fa} = 0.67SiO_2 + 0.12Al_2O_3 + 0.17Fe_2O_3$$

Figure 40. Equation. Vayghan Fly Ash.

$$V_b = \frac{Blended\ Promotors}{Blended\ Suppressors} = \frac{(1-f)P_c + f \cdot P_{fa}}{(1-f)S_c + f \cdot S_{fa}}$$

Figure 41. Equation. Vayghan Vulnerability Index. f = fly ash replacement.

Table 15 presents the results of the previous equations for the fly ashes used in this study normalized to the cement in each mix. Normalization allows for a consistent comparison when different cements are used, as is the case with FA1. Therefore, C_c and V_c are evaluated when the fly ash replacement is 0 percent in Figure 35 through Figure 41, respectively. C_b and V_b evaluate the blend of cement and fly ash at twenty-five percent fly ash replacement to reflect the experiments. Larger numbers indicate that the fly ash is less effective at mitigating. Here it is clearly seen that the two equations assess the vulnerability of the fly ash and the vulnerability of the cement in a similar way. Therefore, CM2 is less vulnerable to ASR by both the Malvar and Lenke, and Vayghan models. Similarly, FA1 is the least vulnerable followed by FA5, FA2, FA4 and FA3 in Malvar and Lenke, while Vayghan assesses that FA5 is the least vulnerable by 0.01 followed by FA1, FA2, FA4, and FA3. The main reason FA1 occurs out of relative order between the Malvar and Lenke equation in Figure 31 and Figure 32 and the Vayghan equation in Figure 33 is due to normalizing the calculated cement parameters with the fly ash parameters.

Once normalized, FA1 is shown to be less effective in Vayghan, and between FA2 and FA3 for Malvar and Lenke. This is consistent with what is observed in Figure 31 through Figure 33. The effect normalizing has on the vulnerability indexes can be understood as the vulnerability of ASR is in terms of the effectiveness of the fly ash relative to the cement. This means that if the cement used promotes ASR heavily then the fly ash will have less of an impact than it would on

the same cement that did not promote ASR as much. It is apparent that the influence of the cement in the Vayghan equation is greater than that in Malvar and Lenke. In fact, if FA1 was evaluated experimentally using the high alkali cement, FA1 would be only slightly less effective than FA5 with a V_b/V_c value of 0.36, while the C_b/C_c calculated with Malvar and Lenke would be 0.56, which is only a slight improvement. This is most likely because Malvar and Lenke assume that the reactivity and effect of all ASR promoting oxides is the same. Furthermore, Malvar and Lenke consider the contributions of alkalis from the fly ash, which range from 1.21 to 3.85. Vayghan has assessed that the effect these alkalis has is negligible towards inducing ASR (Vayghan et al., 2016).

Table 15. Chemical Index Comparisons at 25 percent replacement.

Cementitious Materials	**ML C_b**	**ML C_b/C_c at**	**V V_b**	**V V_b/V_c**
C_c & V_c with Shipment 2015	4.5	1.0	1.42	1.0
FA1	2.23	0.58	0.46	0.40
FA2	2.53	0.56	0.47	0.33
FA3	2.88	0.64	0.56	0.39
FA4	2.65	0.59	0.54	0.38
FA5	2.40	0.53	0.45	0.32

Note: ML = Malvar and Lenke, V = Vayghan

Source: UW Tanner research group.

Figure 34 indicates that FA2 and FA4 show behavior that is different than predicted, emphasizing the considerable amount of variability in ASR behavior and importance of experimental testing. All the fly ashes have successfully mitigated below the 0.04 percent limit with the exception of KR-FA2 and KR-FA3 combinations.

The importance of the Vayghan model cannot be understated, especially in this instance where all five of the aggregates switched behavior between AMBT and CPT results likely due to the presence of mixed coarse and fine aggregates. This is demonstrated in the order of aggregate expansions (diamond markers) from the left to right in Figure 31 and Figure 32. The Malvar and Lenke relationship is only as reliable as the AMBT data.

Both FA3 and FA4 are considered class CI fly ash by the Canadian standard (CSA A3000-13, 2013). This explains the distinct difference in mitigation effectiveness between FA3 and FA4; and FA2 and FA5 in Figure 33. Experimentally, FA5 is performing the best and is followed by FA4; both of these sources mitigate all of the aggregate sources in this study. This illustrates how the current classification system used may disregard effective fly ashes for mitigation (Vayghan et al., 2016).

Clearly chemical index models are useful tools and can serve to guide DOT work at times when experimental testing is not possible, or in cases where field history is not available.

6.4 Autoclaved Specimens

Each of the previously discussed test methods have their own shortcomings. As a result, the research community is still seeking better options. Some researchers have placed concrete specimens in an autoclave in hopes of accelerating the exposure and significantly decreasing the test duration (Berube, 1993; Duchene and Bérubé, 1992; Fournier et al., 1991; Liu et al., 2011; Nishibayahsi et al., 1996; Tang et al., 1983). In 2013, UW and UA collaborated to evaluate one such method. Preliminary results were promising for coarse aggregates but not as good for fine aggregates. This was attributed to a poor quality nonreactive coarse aggregate and honeycombing of the specimens resulting in low compressive strengths (Kimble, 2015). In 2016, work with this autoclave procedure was rekindled using a different nonreactive aggregate from the same shipment and a consistent casting methodology. The preliminary limit of 0.08 percent was used to evaluate the expansions (Giannini and Folliard, 2013). These improvements are evident in the tested compressive strengths and expansions discussed in the following paragraphs.

Figure 42 illustrates the 2013 and 2016 compressive strengths. The overall average compressive strengths for each study are presented to the right of the graph. The UW-2013 compressive strengths are all uncharacteristically low at 2.5 ksi (17.2 MPa), where UA determined a strength of 5.03 ksi (34.7 MPa) in the same study. Because of the uniform procedures, the range of 2016 strengths was improved from the 2013 data. The 2016 range is from 3.92 ksi (27.0 MPa) to 4.23 ksi (29.2 MPa). The average tested compressive strength for the ACPT specimens are less than the CPTs because of the added alkalis which is consistent with Smaoui et al. (2005). This data is also available in Appendix E: ACPT Data in Table 38. Coefficient of variations are also provided.

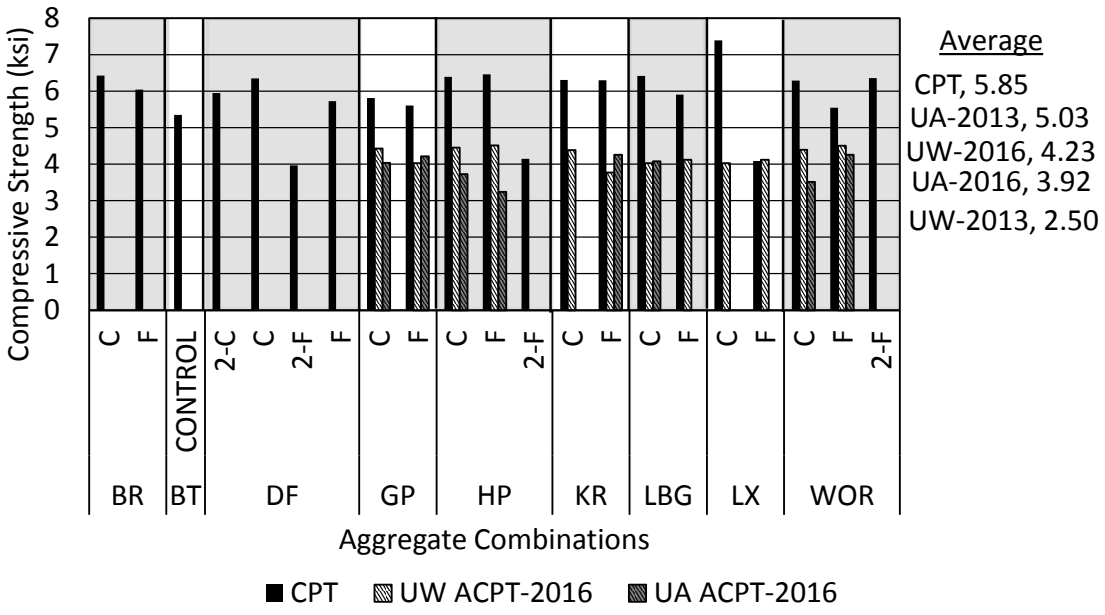

Source: UW Tanner research group.

Figure 42. Chart. Concrete compressive strengths.

Figure 43 illustrates a linear regression for ACPT measurements from each set of data. Classification agreement is identified by the shaded regions. Unfilled markers represent fine reactive aggregate while filled markers represent coarse aggregate. The black data and trend line indicate the relationship from the 2013 data, while the grey data and trend line indicates the relationship from the 2016 data. With the new aggregate and changes in procedure, the slope has changed dramatically for data collected in 2016. A slope of one paired with an R^2 of one would indicated perfect agreement between labs or 100 percent reproducibility of the test data.

Figure 44 illustrates the failure ratios for each aggregate source, organized by increasing reactivity, for both schools and both years data was obtained. As observed with CPT data, coarse aggregates generally have lower expansions than the fine aggregates. Additionally, there is less variation in the 2016 data than the 2013 data.

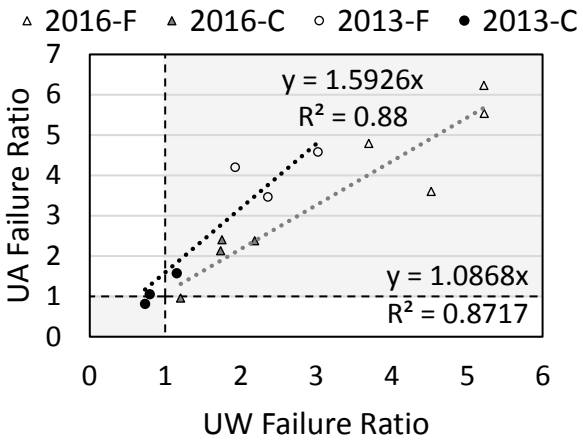

Source: UW Tanner research group.

Figure 43. Graph. Comparison of 2016 and 2013 ACPT failure ratios.

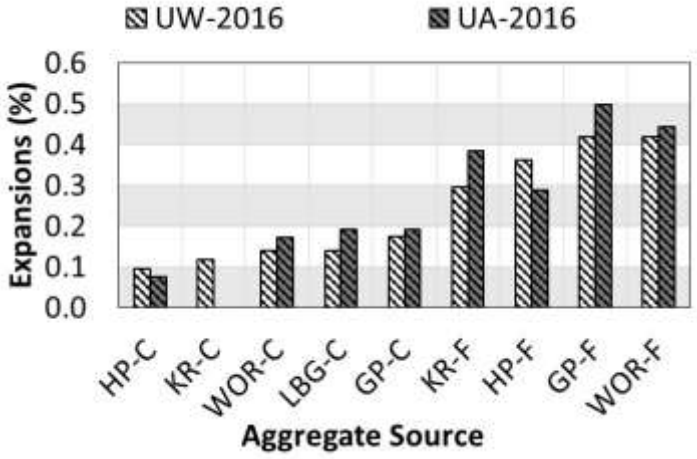

Source: UW Tanner research group.

Figure 44. Chart. Comparison of 2016 ACPT expansions.

Table 16 includes a summary of all the test results. Figure 45 shows the repeatability measurements between UW and UA. Additionally, a coefficient of variation (CV) for UW and UA is given for each material in Table 17. The asterisk (*) represents data that was collected but was removed due to procedural concerns. UA indicated that KR-C incorporated too much superplasticizer which caused segregation problems in the mix. For LBG-F, the moisture content of the aggregate was unaccounted for by UA. For the same mix at UW, the mixer broke during the mixing cycle, and was completed manually. The CVs given for UW and UA represent the variation of the expansion obtained between the three specimens in the batch for each material. They range 0.4 to 22.5 percent. The third column (UW and UA 2016) provides the inter-laboratory CV which ranges from 6 percent to 22 percent. By using BT as the nonreactive aggregate, and incorporating a standard washing procedure, the current UW failure ratios are much closer to the failure ratios obtained by UA.

Table 16. Autoclaved CPT expansion results.

Aggregate	UW-2016		UA-2016	
	Expansion (%)	Failure Ratio	Expansion (%)	Failure Ratio
GP-F	0.42	5.22	0.50	6.23
GP-C	0.17	2.18	0.19	2.38
HP-F	0.36	4.52	0.29	3.60
HP-C	0.10	1.20	0.08	0.96
KR-F	0.30	3.70	0.38	4.79
KR-C	0.12	1.48	*	*
LBG-F	0.36 **	4.52 **	*	*
LBG-C	0.14	1.75	0.19	2.40
WOR-F	0.42	5.23	0.44	5.54
WOR-C	0.14	1.73	0.17	2.13

*Data not included because of concern with mixing procedure.

**Concrete was mixed manually.

Source: UW Tanner research group.

Table 17. Autoclaved CPT expansion CV results.

Aggregate	UW-2016	UA-2016	UW and UA 2016
	CV (%)	CV (%)	CV (%)
GP-F	1.5	11.6	12.5
GP-C	1.8	11.1	6.0
HP-F	7.3	1.8	16.0
HP-C	7.8	22.5	16.1
KR-F	2.4	2.1	18.2
KR-C	0.4	*	*
LBG-F	2.7 **	*	*
LBG-C	18.0	6.7	22.3
WOR-F	3.1	4.7	4.1
WOR-C	4.2	1.8	16.6
Average	5.5	7.8	14.0

*Data not included because concrete was mixed manually.

Source: UW Tanner research group.

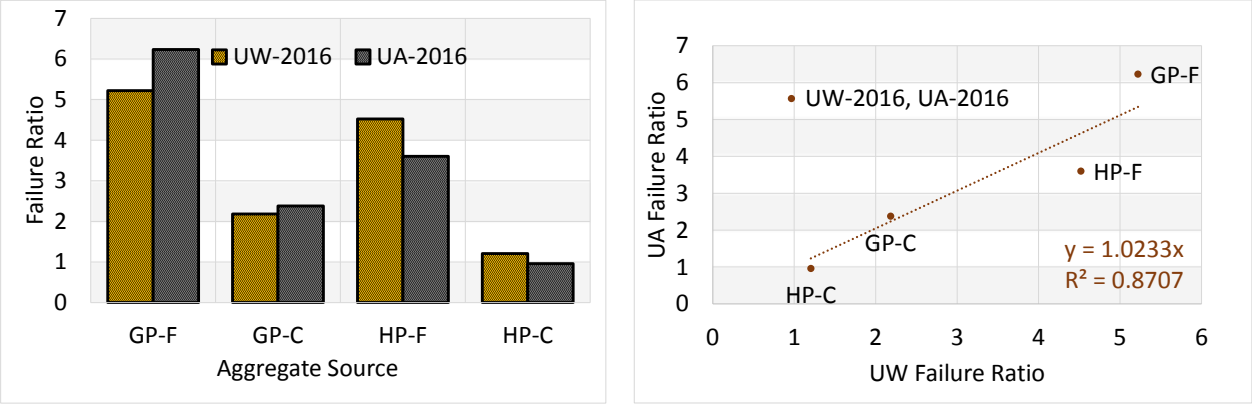

a) Bar graph b) Scatter Plot

Source: UW Tanner research group.

Figure 45. Graph. Repeatability measurements between UW and UA.

6.4.1 CPT and ACPT Comparison

Figure 46 shows two linear regressions of the ACPT and CPT expansion data obtained in this study. The grey dots represent data from UA and the black dots are data from UW. Unfilled, markers represent fine while filled markers represent coarse aggregate as the potentially reactive constituent. Classification agreement is identified by the shaded regions. The slope of the trend line relates the ACPT expansions to those obtained from the CPT. The regression with a y-intercept has the best correlation (R^2=0.84). A slope of 0.99 suggests that the ACPT and CPT expansions are very similar, which is consistent with the comparison in Figure 49. The intercept may indicate the potential for inherent expansions in the test method for a nonreactive aggregate of 0.06 percent when CPT expansions are 0 percent. Giannini and Folliard (2013) also mention the possibility of an inherent expansion in the ACPT test. The trend line without the intercept illustrates a theoretical relationship that the ACPT produces zero expansion when the CPT produces zero expansion for a nonreactive aggregate. In this case, the ACPT is predicted to produce expansions approximately 20 percent greater than CPT expansions.

While both regressions gain insight into the relationship of the CPT and ACPT, any intercepts are a product of the choice to use CPT as the independent variable. As an academic exercise, if these were switched, the intercept would be -0.03 percent. This implies that the CPT has an inherent shrinkage, which is highly unlikely based on the curing temperature and a myriad of test data available. Therefore, a better comparison of the two models is the correlation coefficient, or R value (square root of R^2 value). For the best fit regression, the correlation coefficient is R=0.92 and R=0.89 for the regression without the intercept. This value can be compared to 1, which corresponds to a perfect positive fit while an R of zero indicates no linear correlation.

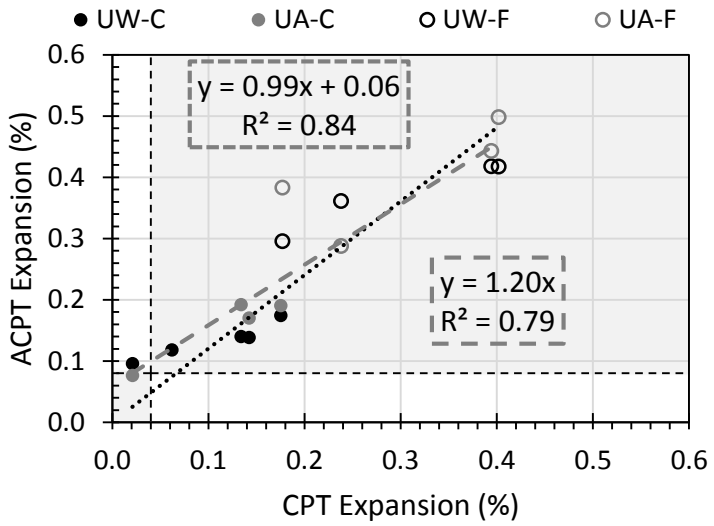

Source: UW Tanner research group.

Figure 46. Chart. Comparison of ACPT and CPT failure ratios.

The validity conditions for the best fit model is assessed here. The histogram in Figure 47 should show a normal distribution, or have sufficiently large sample size to assume normality. The Residual versus fitted value plot in Figure 48 should not display curvature and should have uniform scatter. An example of unequal scatter is fanning or uneven spreading of residuals

across fitted values. The residuals plot in Figure 47 is difficult to interpret because of the small sample size of 17. However, the Anderson-Darling test for normality yields a P-value of 0.076 (>0.05) which confirms that the distribution is normal. Additionally, with 17 data points the central limit theorem begins to take effect which helps in confirming normality. The residuals plotted in Figure 48 show that the assumptions for a linear regression of no curvature and uniform scatter are appropriate. While Figure 48 indicates there may be a possible outlier, that data point is not highly influential in the model.

The data was also analyzed to verify that the UA regression was not statistically different from the UW regression. The P-value for the categorical predictor, which is the difference between the intercepts in both regressions, was 0.4 which indicates that the difference in intercepts is not significant. Finally, the slope was tested by including an interaction term between CPT expansion and the categorical predictor. The P-value for this term was 0.664 which is also not significant. While there is no indication that a quadratic would be a good fit, the P-value for a quadratic term was evaluated and found to be 0.704. This indicates that a quadratic would not be a better fit than the linear regression which is the best fit in this case. Therefore the two sets of data can be combined to estimate the relationship between CPT and ACPT expansions.

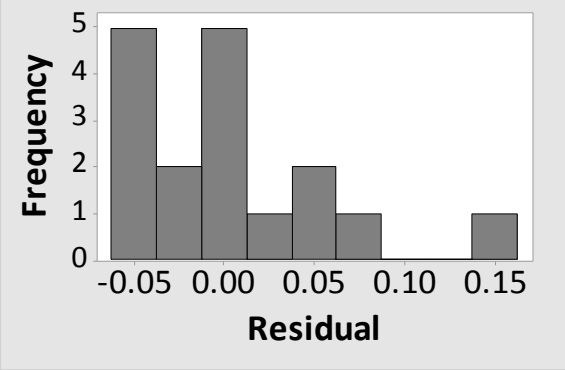

Source: UW Tanner research group.

Figure 47. Graph. Histogram of residuals for CPT vs ACPT regression with Y intercept.

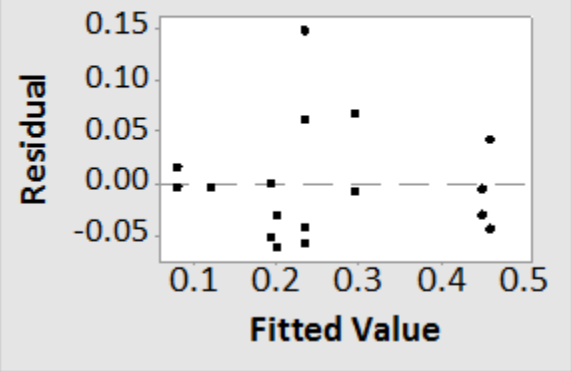

Source: UW Tanner research group.

Figure 48. Graph. Residuals vs. Fits for CPT vs ACPT regression with Y intercept.

Figure 49 shows the same expansion data to compare the CPT data to the ACPT data. The grey bars show the 65 percent error limit defined by the CPT as a potential estimate of the variation one might expect in the ACPT. Both the CPT limit of 0.04 percent and the ACPT limit of 0.08 percent are also portrayed in the figure. For most of the data, the CPT precision includes the ACPT expansions. The only exception is HP-C and KR-F. Furthermore, HP-C is the only aggregate that does not agree with the CPT classification of nonreactive by using the expansion limit of 0.08 percent. KR-C is also close since the CPT expansions are just over the reactive limit.

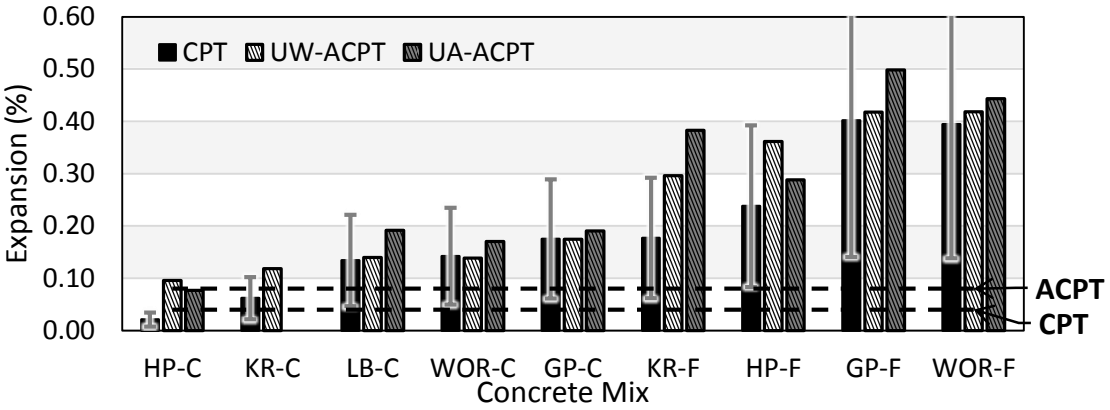

Source: UW Tanner research group.

Figure 49. Chart. Comparison of ACPT and CPT expansions.

The slope of the trend line in Figure 46 indicate that the ACPT expansions are very nearly the expansions obtained from the CPT. As is the case with any classification limit, natural variations in test results may result in disagreement in aggregate classification between test results. For example if a particular aggregate's expansions are near a limit, one test could indicate the material is nonreactive, and a subsequent test could indicate reactive material, good experimental methodologies need to be used in proper classification. This is especially true for highly variable materials and aggregates that reach expansions that are close to a classification limit. The range of CVs for this test goes from 4.11 to 22.3. This range is below the 23 percent limit defined in CPT and is indicative of promising interlaboratory agreement.

The difference in compressive strengths between CPT and ACPT cylinders made from the same aggregate is notable. With the exception of LX-F, there was an approximate reduction in strength by 65 percent for the ACPT results. Smaoui et al. (2005) indicates that increasing concrete alkali content from 0.6 percent to 1.25 percent is harmful to most of the mechanical properties in concrete. Therefore, this reduction in strength may be due to the heightened alkalinity of the ACPT concrete pore solution of 3.0 percent versus 1.25 percent in the CPT.

6.5 Outdoor exposure blocks

While OEBs are considered a very reliable method for evaluating ASR, they take at least five years before detection is possible (Rogers and Lane, 2000). Additionally, secondary effects like freeze thaw are uncontrollable, and often unquantifiable. For the past nine years, UW has been monitoring the ASR expansions for the original eight aggregate sources. These measurements are part of a long term experimental field block test site. Typically, measurements occurred every

six months, once in May or June and once near the end of the year. Currently more emphasis is being placed on more frequent measurements during the winter months to document more localized expansions and possible freeze thaw effects. By observing expansions between the shorter intervals, it can be assumed that ASR is at a minimum.

Figure 50 and Figure 51 illustrate the expansions to date for the outdoor exposure blocks. Figure 50 plots the results for specimens that were cast with boosted levels of alkalinity while Figure 51 represents the specimens that were cast without additional alkalis. The legends in both figures are listed at the top. The two solid diagonal lines are divisions between proposed aggregate classifications. The top line separates highly and moderately reactive aggregates while the lower line distinguishes between moderately and nonreactive aggregates as described by Table 4 (Fertig et al. 2010).

The classification lines are a linear functions of time, while the expansions will eventually approach a final limit when the reaction is complete (Multon et al., 2010). Therefore, the final aggregate classification is the most severe classification at any point in time. A good example of this case is KR in Figure 50 where the rate of expansion has decreased relative to the classification line thereby placing KR right on the limit. If KR's trend continues, it would receive a lower classification. However, because it has already been classified as HR, it will never be demoted. Table 18 summarizes the OEB classifications.

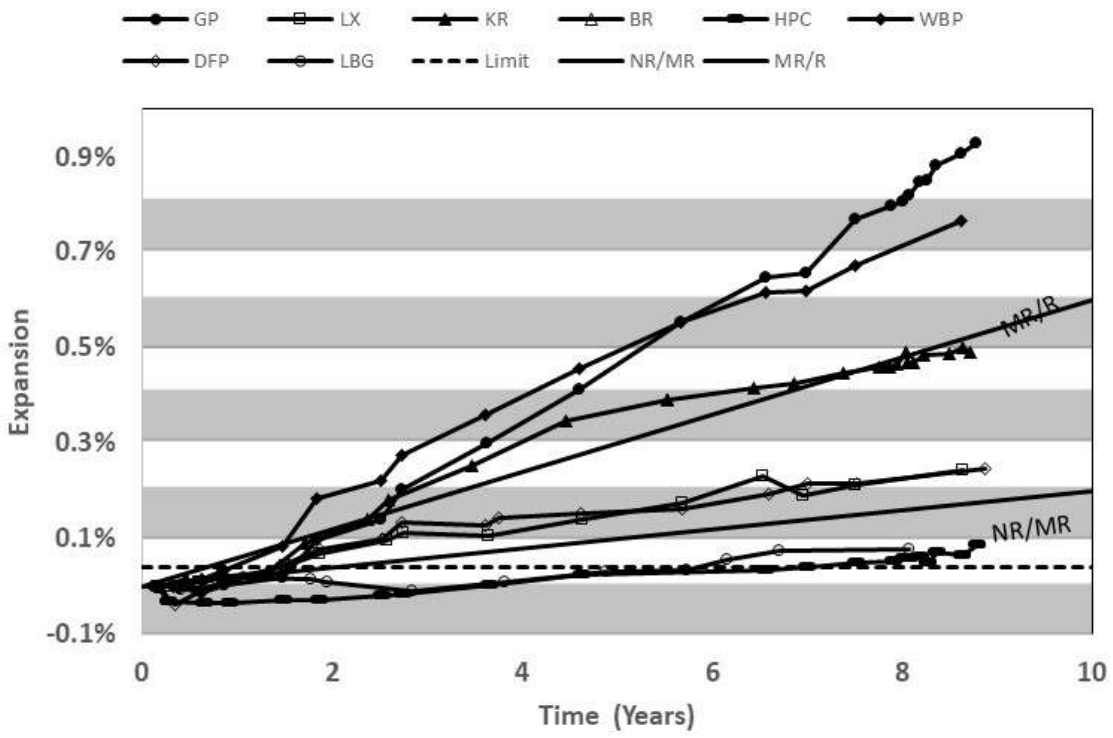

Source: UW Tanner research group.

Figure 50. Graph. OEB boosted expansions.

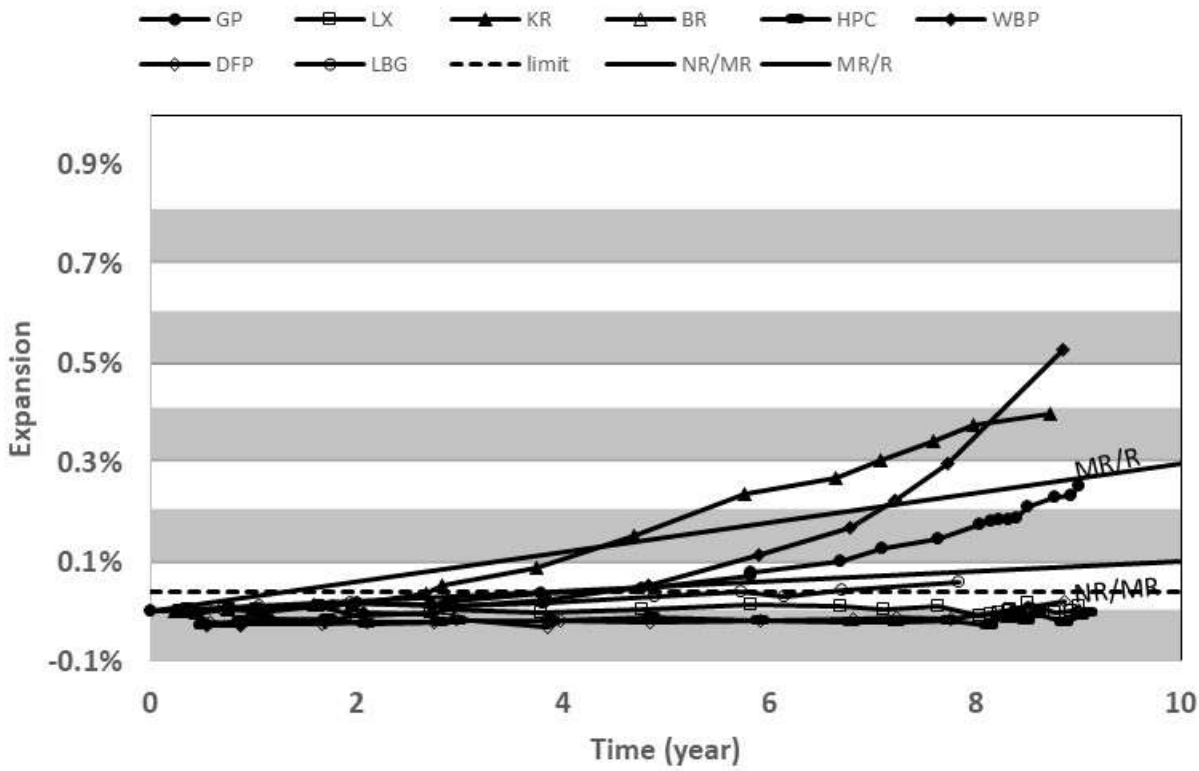

Source: UW Tanner research group.

Figure 51. Graph. OEB unboosted expansions.

Table 18. OEB classification.

Aggregate Source	BR	BT	DF	GP	HP	KR	LBG	LX	WOR
Unboosted	NR	NR	NR	MR	NR	HR	NR	NR	HR
Boosted	HR	MR	MR	HR	NR	HR	NR	MR	HR

Source: UW Tanner research group.

7 CONCLUSIONS AND FUTURE WORK

7.1 CPT Data

Mitigated

Based on CPT results, all the fly ashes at 25 percent replacement levels are capable of reducing the ASR potential down to innocuous for all aggregate sources except for KR. However, both the FA3-KR and FA2-KR exceeded the reactive limit 0.04 percent. Therefore, 25 percent fly ash replacement was not adequate to fully suppress the ASR potential of KR for these combinations.

The effectiveness of fly ash dosage models will only be as accurate as the available test results. The AMBT has known reliability concerns when compared to CPT results. Thus, the Vayghan model is a step in the right direction. For FA2 through FA5, the Vayghan model trends match the experimental data.

Combined Coarse and Fine Aggregate Fractions

Previous CPT data combined coarse and fine aggregate components. In this study, the potentially reactive coarse and fine aggregates were separated. Additionally, the overall CPT expansions for fine aggregate were greater than the mixed CPT results for five of the eight aggregate sources. KR-C was the only aggregate that showed a marked reduction in expansion when it was paired with a nonreactive fine. As observed in Ichikawa (2009), combining two reactive aggregates may suppress ASR through a pessimum effect.

Future Work for CPT

Additional testing could be conducted using different fly ash replacement levels. This data could develop curves that express expansions versus various levels of fly ash replacement.

7.2 ACPT

The ACPT is reproducible between two independent laboratories with at least as much precision as the CPT. When using an initial limit of 0.08 percent for the ACPT there was less success in classifying aggregates. Furthermore, based on the linear regression, the ACPT data have average expansions of 0.06 percent at a CPT expansion of 0 percent. This may be due to a potential inherent expansion that results from the autoclaving temperature. Alternately, these inherent expansions may be due to the dissolution of stable mineral structures from the harsh test environment. This means that ASR may be occurring from both the reactive portion and the nonreactive portion of the aggregate. Both values of expansion suggest that a higher classification limit should be used.

Future Work for ACPT

The study should be expanded to consider a larger source of non-, moderately-, and highly-reactive aggregates. Due to the long exposure time in the CPT, nonreactive aggregates that have already been published with CPT data may also be compared. Completing a larger inter-laboratory study would also be helpful to further validate the proposed test method. If it becomes widely accepted, appropriate precision statements for the ACPT should be evaluated.

7.3 OEB

In this study, short term expansions resulting from freeze thaw cycles were not obvious when the OEBs were monitored more frequently during the winter months. While the investigation is of interest to study how much freeze thaw impacts the total expansions, a distinction between freeze thaw expansions and ASR expansions is not necessary since the goal of the field blocks is to represent field conditions.

Future Work for OEB

While OEBs are continuously cited as the best evaluation tool, the ASR research community lacks a unifying approach to consolidate the data. As a result, it can be recommended that laboratories with OEB data collaborate to produce evaluation criteria and a potential database of information on OEBs.

APPENDIX

Appendix A: Physical property tests and batch quantities

Table 19. Accumulated property test data of potentially reactive aggregates.

Aggregate	Coarse Aggregate				Fine Aggregate	
	Specific Gravity (SSD)	Absorption (%)	Unit Weight (pcf)	Unit Weight (kg/m^3)	Specific Gravity (SSD)	Absorption (%)
BR 2008	2.59	1.80	97.7	1565.5	2.60	2.15
BT 2015	2.54	0.88	101.0	1617.2	2.63	0.66
BT 2015 – 2	2.55	0.87	100.6	1610.8	N/A	N/A
DF 2015	N/A	N/A	N/A	N/A	2.55	2.66
DF 2008	2.52	2.19	96.6	1547.1	N/A	N/A
GP 2015	2.56	0.64	97.5	1562.2	2.61	1.23
GP 2008	2.58	1.07	99.0	1585.2	2.63	1.01
HP 2008	2.60	1.83	97.2	1556.2	2.62	2.25
HP 2008-2	2.56	2.13	96.5	1545.5	2.63	2.73
KR 2008	2.66	0.67	98.8	1581.8	2.63	0.91
LBG 2008	2.60	0.67	98.8	1583.2	2.62	1.05
LBG 2008-2	2.52	0.95	101.9	1632.6	2.59	0.99
LX 2008	2.54	2.02	97.7	1565.1	2.60	1.81
LX 2015	2.57	1.88	99.0	1585.2	N/A	N/A
WOR 2008	2.55	1.45	99.0	1586.4	2.61	1.56
WOR 2015	2.55	1.76	97.9	1568.6	2.41	1.64

Source: UW Tanner research group.

Table 20. As received aggregate gradations

	Coarse (% passing)			Passing (% passing)					
	3/4 in. (19 mm)	1/2 in. (12.5 mm)	3/8 in. (9.5 mm)	#4 (4.75 mm)	#8 (2.36 mm)	#16 (1.18 mm)	#30 (0.6 mm)	#50 (0.3 mm)	#100 (0.15 mm)
BR-2008	90	45	24	100	84	66	45	13	1
BT-2015	94	64	40	100	92	64	38	11	4
BT-2015-2	88	52	31	100	91	63	37	8	2
DF-2008	73	33	16	97	82	69	46	9	1
DF-2015	N/A	N/A	N/A	92	56	36	25	17	11
GP-2008	93	58	30	100	88	79	64	18	0
GP-2015	N/A	N/A	N/A	98	85	72	51	16	3
HP-2008	86	38	10	100	83	60	43	22	7
HP-2008-2	84	36	12	100	86	62	39	13	1
KR-2008	81	26	11	100	96	72	43	18	7
LBG-2008	91	44	22	100	90	78	62	27	8
LBG-2008-2	89	49	31	100	86	62	39	13	1
LX-2008	94	55	25	100	76	61	48	16	1
LX-2015	78	37	19	N/A	N/A	N/A	N/A	N/A	N/A
WOR-2008	82	36	16	98	90	79	52	6	0
WOR-2015	30	15	1	97	82	68	46	16	4

Source: UW Tanner research group.

Table 21. As batched MCPT gradation.

	Coarse Fraction (% passing)			Fine Fraction (% passing)				
	1/2 in. (12.5 mm)	3/8 in. (9.5 mm)	#4 (4.75 mm)	#8 (2.36 mm)	#16 (1.18 mm)	#30 (0.6 mm)	#50 (0.3 mm)	#100 (0.15 mm)
KR	33	33	33	96	72	43	18	0
LBG	33	33	33	90	78	60	27	0
LX	33	33	33	80	64	52	24	0
WOR	33	33	33	90	79	52	7	0
GP	33	33	33	89	79	60	19	0

Source: UW Tanner research group.

Table 22. As batched separated CPT and ACPT gradation.

	Coarse Fraction (% passing)			Fine Fraction (% passing)				
	1/2 in.	3/8 in.	#4	#8	#16	#30	#50	#100
BR-F	33	33	33	84	65	44	12	0
BR-C	33	33	33	91	62	35	7	0
BT-	33	33	33	91	62	35	7	0
DF-2C	33	33	33	91	62	35	7	0
DF-2F	33	33	33	82	70	46	8	0
DF-C	33	33	33	91	62	35	7	0
DF-F	33	33	33	82	70	46	8	0
GP-C	33	33	33	91	62	35	7	0
GP-F	33	33	33	86	71	50	14	0
HP-2F	33	33	33	86	62	39	13	0
HP-C	33	33	33	91	62	35	7	0
HP-F	33	33	33	86	62	39	13	0
KR-C	33	33	33	91	62	35	7	0
KR-F	33	33	33	95	69	37	11	0
LBG-C	33	33	33	91	62	35	7	0
LBG-F	33	33	33	82	67	48	7	0
LX-C	33	33	33	91	62	35	7	0
LX-F	33	33	33	77	61	48	16	0
WOR-2F	33	33	33	82	66	43	12	0
WOR-C	33	33	33	91	62	35	7	0
WOR-F	33	33	33	82	66	43	12	0

Source: UW Tanner research group.

Table 23. Batch quantities for MCPTs.

Fly Ash	Agg.	Coarse lb (kg)	Fine lb (kg)	Cement lb (kg)	Water lb (kg)	Super-plasticizer (mL)
FA2	GP	25.99 (11.79)	13.67 (6.2)	7.38 (3.35)	4.52 (2.05)	10
FA3	GP	25.99 (11.79)	13.81 (6.26)	7.38 (3.35)	4.52 (2.05)	8
FA4	GP	25.99 (11.79)	13.74 (6.23)	7.38 (3.35)	4.52 (2.05)	7
FA5	GP	25.99 (11.79)	13.61 (6.17)	7.38 (3.35)	4.52 (2.05)	10
FA2	KR	25.97 (11.78)	14.7 (6.67)	7.38 (3.35)	4.35 (1.97)	13
FA3	KR	25.97 (11.78)	14.84 (6.73)	7.38 (3.35)	4.35 (1.97)	14
FA4	KR	25.97 (11.78)	14.77 (6.7)	7.38 (3.35)	4.35 (1.97)	10
FA5	KR	25.97 (11.78)	14.65 (6.65)	7.38 (3.35)	4.35 (1.97)	23
FA2	LBG	25.97 (11.78)	14.02 (6.36)	7.38 (3.35)	4.39 (1.99)	26
FA3	LBG	25.97 (11.78)	14.16 (6.42)	7.38 (3.35)	4.39 (1.99)	16
FA4	LBG	25.97 (11.78)	14.08 (6.39)	7.38 (3.35)	4.39 (1.99)	16
FA5	LBG	25.97 (11.78)	13.96 (6.33)	7.38 (3.35)	4.39 (1.99)	30
FA2	LX	25.8 (11.7)	13.18 (5.98)	7.38 (3.35)	4.67 (2.12)	18
FA3	LX	25.8 (11.7)	13.315 (6.04)	7.38 (3.35)	4.67 (2.12)	4
FA4	LX	25.8 (11.7)	13.24 (6.01)	7.38 (3.35)	4.67 (2.12)	6
FA5	LX	25.8 (11.7)	13.12 (5.95)	7.38 (3.35)	4.67 (2.12)	14
FA2	WOR	26.09 (11.83)	13.12 (5.95)	7.38 (3.35)	4.58 (2.08)	3
FA3	WOR	26.09 (11.83)	13.26 (6.01)	7.38 (3.35)	4.58 (2.08)	8
FA4	WOR2	26.09 (11.83)	13.19 (5.98)	7.38 (3.35)	4.58 (2.08)	5
FA4	WOR	26.12 (11.85)	13.2 (5.99)	7.38 (3.35)	4.55 (2.06)	-
FA5	WOR	26.09 (11.83)	13.07 (5.93)	7.38 (3.35)	4.58 (2.08)	3

Cement Na_2O_{eq} = 1.01 percent, NaOH = 0.023 lb (0.01 kg), Fly ash = 2.46 lb (1.12 kg)

Source: UW Tanner research group.

Table 24. Physical properties for MCPTs.

Fly Ash	Aggregate	Coarse Moisture Content (%)	Fine Moisture Content (%)	Slump in. (mm)	Unit Weight pcf (kg/m^3)
FA2	GP	0.04	0.09	4.5 (114)	148 (2375)
FA3	GP	0.04	0.09	4 (102)	149 (2390)
FA4	GP	0.04	0.09	5 (127)	149 (2381)
FA5	GP	0.04	0.09	3.25 (83)	148 (2378)
FA2	KR	0.18	0.26	1 (25)	150 (2395)
FA3	KR	0.18	0.26	2.25 (57)	148 (2367)
FA4	KR	0.18	0.26	2.25 (57)	150 (2395)
FA5	KR	0.18	0.26	1.75 (44)	150 (2401)
FA2	LBG	0.08	0.29	2.25 (57)	148 (2365)
FA3	LBG	0.08	0.29	2 (51)	148 (2365)
FA4	LBG	0.08	0.29	2 (51)	149 (2386)
FA5	LBG	0.08	0.29	3.25 (83)	148 (2377)
FA2	LX	0.6	0.46	6 (152)	148 (2367)
FA3	LX	0.6	0.46	3.25 (83)	148 (2368)
FA4	LX	0.6	0.46	2.75 (70)	148 (2365)
FA5	LX	0.6	0.46	4.75 (121)	148 (2365)
FA2	WOR	0.37	0.28	1 (25)	146 (2346)
FA3	WOR	0.37	0.28	4.5 (114)	148 (2372)
FA4	WOR	0.46	0.34	-	149 (2390)
FA4	WOR2	0.37	0.28	3.25 (83)	148 (2370)
FA5	WOR	0.37	0.28	2.75 (70)	148 (2368)

Source: UW Tanner research group.

Table 25. Batch quantities for separated CPTs.

Aggregate	Coarse lb (kg)	Fine lb (kg)	Cement lb (kg)	Cement Na_2O_{eq} (%)	Water lb (kg)	NaOH lb (kg)	Superplasticizer (mL)
BF-F	41.7 (18.9)	22.06 (10)	15.42 (7)	0.94	5.8 (2.6)	0.062 (0.028)	10
BR-C	41.3 (18.7)	23.88 (10.8)	15.73 (7.1)	0.94	6.781 (3.1)	0.063 (0.029)	8
BT-Control	42.476 (19.3)	22.12 (10)	15.7 (7.1)	0.94	6.52 (3)	0.063 (0.029)	5
DF-2C	41.43 (18.8)	22.92 (10.4)	15.69 (7.1)	0.94	6.24 (2.8)	0.063 (0.029)	10
DF-2F	42.492 (19.3)	21.22 (9.6)	15.69 (7.1)	0.94	6.52 (3)	0.063 (0.029)	0
DF-C	41.36 (18.8)	24.5 (11.1)	15.73 (7.1)	0.94	4.95 (2.2)	0.063 (0.029)	11
DF-F	42.65 (19.3)	23.87 (10.8)	15.53 (7)	1.01	3.47 (1.6)	0.048 (0.022)	13
GP-C	41.7 (18.9)	23.96 (10.9)	15.73 (7.1)	0.94	6.06 (2.7)	0.063 (0.029)	0
GP-F	42.76 (19.4)	22.04 (10)	15.73 (7.1)	0.94	6.106 (2.8)	0.063 (0.029)	5
HP-2F	42.578 (19.3)	22.02 (10)	15.69 (7.1)	0.94	6.36 (2.9)	0.063 (0.029)	3
HP-C	41.66 (18.9)	23.86 (10.8)	15.73 (7.1)	0.94	6.17 (2.8)	0.063 (0.029)	6
HP-F	41.12 (18.7)	23.42 (10.6)	15.1 (6.8)	0.94	5.191 (2.4)	0.06 (0.027)	0
KR-C	41.73 (18.9)	25.09 (11.4)	15.73 (7.1)	0.94	6.23 (2.8)	0.063 (0.029)	5
KR-F	40.46 (18.4)	21.68 (9.8)	14.92 (6.8)	0.94	5.265 (2.4)	0.06 (0.027)	29
LBG-C	42.52 (19.3)	22.76 (10.3)	15.73 (7.1)	0.94	6.17 (2.8)	0.063 (0.029)	0
LBG-F	42.78 (19.4)	22.17 (10.1)	15.73 (7.1)	0.94	5.791 (2.6)	0.063 (0.029)	8
LX-C	42.28 (19.2)	23.44 (10.6)	15.73 (7.1)	0.94	5.94 (2.7)	0.063 (0.029)	7
LX-F	41.24 (18.7)	22.34 (10.1)	15.13 (6.9)	1.01	4.55 (2.1)	0.047 (0.021)	0
WOR-2F	42.76 (19.4)	21.2 (9.6)	15.73 (7.1)	0.94	5.42 (2.5)	0.063 (0.029)	0
WOR-C	41.77 (18.9)	23.02 (10.4)	15.73 (7.1)	0.94	6.51 (3)	0.063 (0.029)	0
WOR-F	42.98 (19.5)	21.09 (9.6)	15.73 (7.1)	1.01	5.19 (2.4)	0.049 (0.022)	0

Source: UW Tanner research group.

Table 26. Physical properties for separated CPTs.

Aggregate	Coarse Moisture Content (%)	Fine Moisture Content (%)	Slump in. (mm)	Unit Weight pcf (kg/m^3)
BF-F	0.77	6	2 (51)	149 (2386)
BR-C	0.65	2.63	2.25 (57)	149 (2392)
BT-Control	0.89	1.29	1.75 (44)	147 (2358)
DF-2C	2.67	2.03	1.75 (44)	147 (2360)
DF-2F	1.04	3.27	0 (0)	147 (2360)
DF-C	1.91	9.02	1.75 (44)	147 (2356)
DF-F	1.93	15.28	1.75 (44)	146 (2346)
GP-C	1.02	4.03	2.25 (57)	149 (2379)
GP-F	0.86	3.83	2.75 (70)	149 (2383)
HP-2F	1.4	3.34	1 (25)	149 (2384)
HP-C	2.62	1.7	1.75 (44)	149 (2386)
HP-F	1.44	7.46	1.25 (32)	190 (3038)
KR-C	0.62	2.36	2.5 (64)	149 (2388)
KR-F	0.99	5.87	1.25 (32)	148 (2367)
LBG-C	0.81	2.61	1.75 (44)	149 (2380)
LBG-F	1.36	4.16	1.75 (44)	149 (2384)
LX-C	1.69	4.1	1.5 (38)	147 (2359)
LX-F	1.07	11.1	4.5 (114)	148 (2378)
WOR-2F	1.32	7.02	1.5 (38)	149 (2380)
WOR-C	1.59	1.54	3.5 (89)	148 (2363)
WOR-F	1.38	8.24	2.5 (64)	148 (2373)

Source: UW Tanner research group.

Table 27. Batch quantities for ACPTs.

Aggregate	Coarse lb (kg)	Fine lb (kg)	Cement lb (kg)	Cement Na_2O_{eq} (%)	Water lb (kg)	NaOH lb (kg)	Super-plasticizer (mL)
GP-C	41.2 (18.7)	24.01 (10.9)	15.66 (7.1)	0.94	5.94 (2.7)	0.416 (0.189)	17
GP-F	42.552 (19.3)	22.1 (10)	15.73 (7.1)	0.94	6.23 (2.8)	0.418 (0.19)	13
HP-C	41.22 (18.7)	23.74 (10.8)	15.7 (7.1)	0.94	6.36 (2.9)	0.418 (0.19)	25
HP-F	42.69 (19.4)	21.9 (9.9)	15.69 (7.1)	0.94	6.28 (2.8)	0.417 (0.189)	5
KR-C	41.75 (18.9)	24.88 (11.3)	15.69 (7.1)	0.94	6.2 (2.8)	0.417 (0.189)	16
KR-F	40.32 (18.3)	20.74 (9.4)	14.85 (6.7)	0.94	6.03 (2.7)	0.395 (0.179)	40
LBG-C	42.516 (19.3)	22.8 (10.3)	15.66 (7.1)	0.94	5.79 (2.6)	0.417 (0.189)	32
LBG-F	42.64 (19.3)	22.08 (10)	15.69 (7.1)	0.94	6.1 (2.8)	0.417 (0.189)	20
WOR-C	41.56 (18.9)	23.25 (10.5)	15.7 (7.1)	0.94	6.29 (2.9)	0.418 (0.19)	10
WOR-F	42.42 (19.2)	20.35 (9.2)	15.64 (7.1)	0.94	6.21 (2.8)	0.416 (0.189)	11

Source: UW Tanner research group.

Table 28. Physical properties for ACPTs.

Aggregate	Coarse Moisture Content (%)	Fine Moisture Content (%)	Slump in. (mm)	Unit Weight pcf (kg/m^3)
KR-C	1.04	1.96	1.25 (32)	150 (2405)
KR-F	0.74	3.16	1.25 (32)	149 (2379)
GP-C	1.21	2.82	1 (25)	149 (2385)
GP-F	0.871	3.38	1.25 (32)	149 (2384)
LBG-C	1.45	3.62	1 (25)	149 (2389)
LBG-F	1.34	3.39	1 (25)	149 (2383)
HP-C	2.13	2.22	0.75 (19)	148 (2375)
HP-F	1.52	3.43	1.75 (44)	149 (2392)
WOR-C	1.43	3.29	1.75 (44)	148 (2376)
WOR-F	1.16	3.68	2 (51)	148 (2377)

Source: UW Tanner research group.

Appendix B: CPT of Virgin Aggregates

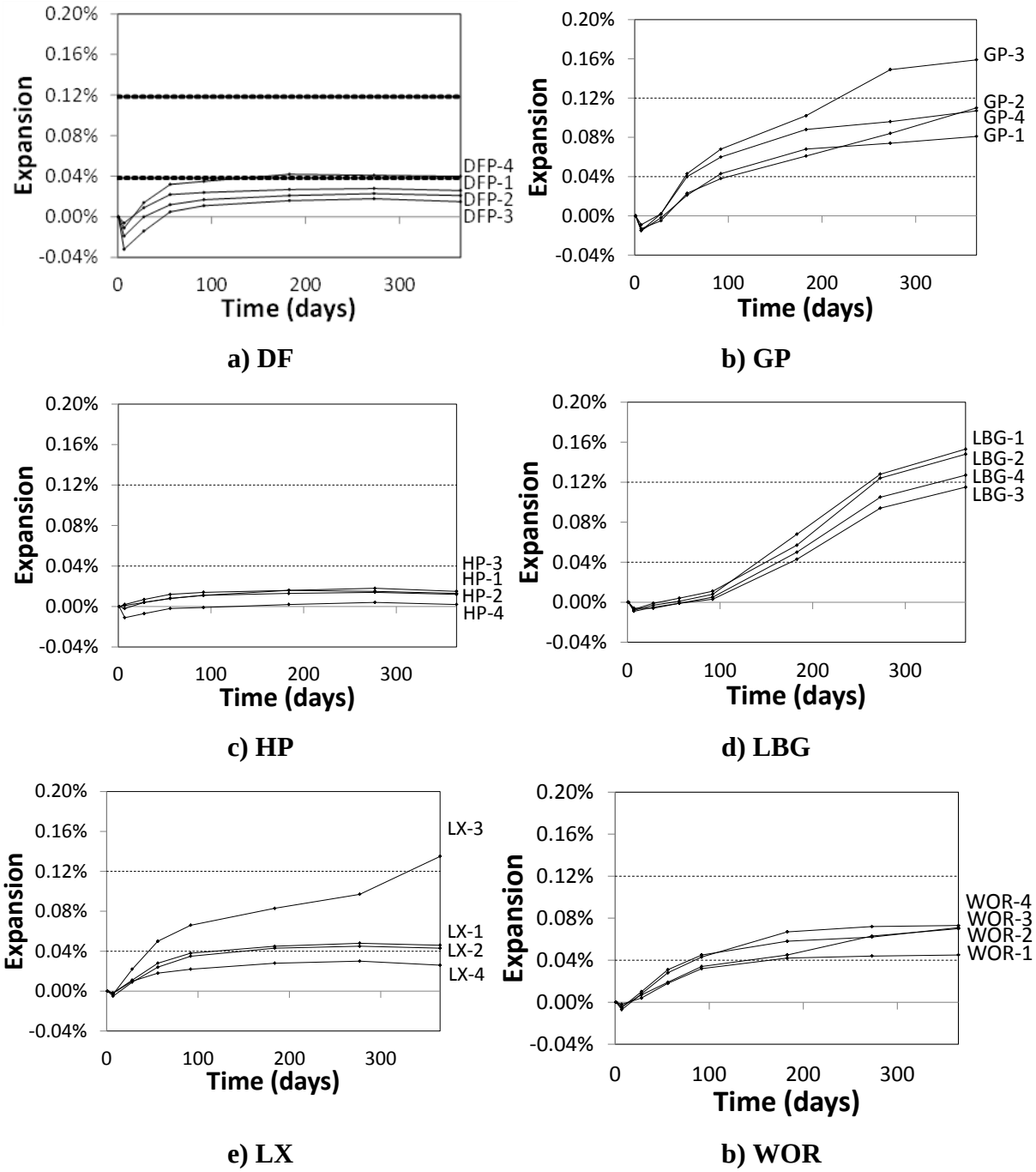

a) DF **b) GP**

c) HP **d) LBG**

e) LX **b) WOR**

Source: UW Tanner research group.

Figure 52. Graph. CPT results for virgin aggregates.

Table 29. CPT results on virgin aggregates.

Source	Average Expansion (%)	CV (%)
BR	0.054	63.3
DF	0.026	41.8
GP	0.114	28.5
HP	0.011	55.3
KR	0.172	7.0
LBG	0.136	13.1
LX	0.063	78.6
WOR	0.065	20.4

Source: UW Tanner research group.

Appendix C: CPT-Separated Coarse and Fine Data

Table 30. Separated coarse and fine CPT expansions.

Aggregate	Reactive Size	Expansions in percent							
		Time (days)							
		1	7	28	56	90	180	290	360
BR	Coarse	0.000	-0.002	0.015	0.037	0.052	0.060	0.0603	0.071
	Fine	0.000	0.000	0.085	0.199	0.275	0.323	0.330	0.337
BT Control	N/A	0.000	0.004	0.008	0.011	0.008	0.015	0.021	0.025
DF	Coarse	0.000	0.012	0.053	0.066	0.070	0.073	0.068	0.074
	Coarse – 2	0.000	0.005	0.024	0.034	0.030	0.035	0.044	0.052
	Fine	0.000	0.005	0.167	0.343	0.421	0.476	0.515	0.523
	Fine – 2	0.000	0.119	0.307	0.405	0.470	0.504	0.513	0.515
GP	Coarse	0.000	-0.008	0.032	0.063	0.099	0.137	0.154	0.174
	Fine	0.000	0.002	0.028	0.116	0.212	0.336	0.389	0.402
HP	Coarse	0.000	-0.001	0.010	0.013	0.017	0.019	0.020	0.021
	Fine	0.000	0.006	0.034	0.127	0.182	0.216	0.235	0.238
	Fine – 2	0.000	0.004	0.017	0.030	0.068	0.094	0.105	0.112
KR	Coarse	0.000	-0.013	0.007	0.009	0.017	0.027	0.043	0.061
	Fine	0.000	0.003	0.011	0.027	0.062	0.153	0.165	0.176
LBG	Coarse	0.000	-0.007	0.004	0.006	0.018	0.086	0.119	0.133
	Fine	0.000	0.000	0.007	0.016	0.024	0.095	0.129	0.141
LX	Coarse	0.000	0.002	0.039	0.063	0.069	0.073	0.066	0.072
	Fine	0.000	0.014	0.230	0.329	0.431	0.527	0.557	0.564
WOR	Coarse	0.000	-0.010	0.023	0.043	0.074	0.108	0.128	0.142
	Fine	0.000	0.004	0.037	0.140	0.236	0.357	0.381	0.394

Source: UW Tanner research group.

CVs:

Table 31. Expansion CVs between unmitigated prisms (3 samples each).

Aggregate	Reactive Size	CV (%)
BR	Coarse	37.99
	Fine	3.59
BT Control	N/A	19.87
DF	Coarse	13.48
	Coarse – 2	4.99
	Fine	4.32
	Fine – 2	7.58
GP	Coarse	17.80
	Fine	2.24
HP	Coarse	25.20
	Fine	1.68
	Fine – 2	6.96
KR	Coarse	11.25
	Fine	17.24
LBG	Coarse	11.85
	Fine	13.09
LX	Coarse	1.48
	Fine	15.77
WOR	Coarse	26.76
	Fine	4.84

Source: UW Tanner research group.

Appendix D: CPT-Fly Ash Data

Table 32. GP CPT expansions by fly ash.

Days	Expansions in percent			
	FA5	FA4	FA2	FA3
1	0.000	0.000	0.000	0.000
7	-0.005	-0.008	-0.018	-0.004
28	-0.003	0.000	0.001	0.000
56	-0.001	0.003	-0.001	0.000
90	-0.004	0.000	0.001	-0.003
180	0.000	0.009	-0.001	0.002
290	0.000	0.012	0.007	0.009
360	0.001	0.014	0.010	0.012
450	0.003	0.019	0.015	0.014
540	0.004	0.022	0.013	0.015
630	0.003	0.031	0.017	0.018
720	0.006	0.035	0.021	0.022

Source: UW Tanner research group.

Table 33. KR CPT expansions by fly ash.

Days	Expansions in percent			
	FA5	FA4	FA2	FA3
1	0.000	0.000	0.000	0.000
7	-0.002	-0.005	-0.001	-0.003
28	0.017	0.015	0.024	0.015
56	0.018	0.018	0.024	0.018
90	0.017	0.017	0.023	0.020
180	0.009	0.009	0.017	0.011
290	0.022	0.015	0.027	0.026
360	0.020	0.018	0.030	0.028
450	0.026	0.021	0.037	0.039
540	0.025	0.016	0.035	0.041
630	0.027	0.020	0.040	0.046
720	0.031	0.023	0.046	0.050

Source: UW Tanner research group.

Table 34. LBG CPT expansions by fly ash.

Days	Expansions in percent			
	FA5	FA4	FA2	FA3
1	0.000	0.000	0.000	0.000
7	-0.011	-0.002	-0.008	-0.007
28	0.013	0.017	0.012	0.015
56	0.013	0.015	0.010	0.015
90	0.012	0.014	0.010	0.013
180	0.003	0.006	0.004	0.010
290	0.010	0.015	0.014	0.018
360	0.009	0.015	0.015	0.019
450	0.017	0.017	0.020	0.030
540	0.013	0.016	0.017	0.027
630	0.014	0.018	0.021	0.028
720	0.018	0.023	0.025	0.035

Source: UW Tanner research group.

Table 35. LX CPT expansions by fly ash.

Days	Expansions in percent			
	FA5	FA4	FA2	FA3
1	0.000	0.000	0.000	0.000
7	-0.004	-0.002	0.010	0.010
28	-0.004	-0.001	0.015	0.017
56	-0.005	-0.002	0.019	0.021
90	-0.006	-0.005	0.018	0.019
180	-0.005	-0.004	0.007	0.012
290	-0.006	-0.004	0.016	0.020
360	-0.006	-0.003	0.018	0.023
450	-0.002	0.000	0.020	0.026
540	-0.003	-0.001	0.018	0.025
630	-0.001	0.002	0.021	0.028
720	0.005	0.006	0.024	0.031

Source: UW Tanner research group.

Table 36. WOR CPT expansions by fly ash.

Days	Expansions in percent				
	FA5	FA4	FA4-2	FA2	FA3
1	0.000	0.000	0.000	0.000	0.000
7	0.000	-0.005	-0.001	0.013	-0.005
28	0.003	0.013	-0.003	0.014	-0.002
56	0.001	0.014	0.005	0.019	0.005
90	-0.001	0.013	0.004	0.020	0.004
180	0.001	0.008	0.009	0.017	0.005
290	0.001	0.008	0.012	0.020	0.010
360	0.001	0.010	0.012	0.021	0.011
450	0.004	0.012	0.020	0.023	0.017
540	0.000	0.011	0.019	0.025	0.019
630	0.000	0.011	0.020	0.023	0.022
720	0.004	0.014	0.023	0.027	0.026

Source: UW Tanner research group.

CVs:

Table 37. Eighteen month between specimen CVs for MCPT.

Aggregate	Fly Ash	CV (%)
GP	FA2	24.7
	FA3	42.7
	FA4	28.9
	FA5	73.3
KR	FA2	1.9
	FA3	16.3
	FA4	12.5
	FA5	1.9
LBG	FA2	21.7
	FA3	10.6
	FA4	10.7
	FA5	21.6
LX	FA2	18.8
	FA3	17.9
	FA4	10.2
	FA5	18.8
WOR	FA2	12.9
	FA3	37.4
	FA4	21.0
	FA4-2	22.1
	FA5	89.2

Source: UW Tanner research group.

Appendix E: ACPT Data

Table 38. CPT and ACPT Compressive strength of concrete cylinders.

	CPT	ACPT-UW	ACPT-UW	ACPT-UA	ACPT-UA
Reactive Aggregate	Compressive Strength	Compressive Strength (ksi)	CV* (%)	Compressive Strength	CV* (%)
BR-C	6.43	N/A	N/A	N/A	N/A
BR-F	6.04	N/A	N/A	N/A	N/A
BT-CONTROL	5.35	N/A	N/A	N/A	N/A
2-DF-C	5.94	N/A	N/A	N/A	N/A
DF-C	6.35	N/A	N/A	N/A	N/A
2-DF-F	3.97	N/A	N/A	N/A	N/A
DF-F	5.72	N/A	N/A	N/A	N/A
GP-C	5.81	4.43	1.6	4.03	0.9
GP-F	5.60	4.03	3.5	4.22	1.6
HP-C	6.39	4.45	1.5	3.72	3.1
2-HP-F	4.15	N/A	N/A	N/A	N/A
HP-F	6.46	4.51	2.1	3.24	15.3
KR-C	6.30	4.39	0.9	N/A	N/A
KR-F	6.30	3.77	2.1	4.25	1.1
LBG-C	6.42	4.02	2.0	4.08	5.4
LBG-F	5.90	4.12	2.3	N/A	N/A
LX-C	7.39	N/A	N/A	N/A	N/A
LX-F	4.09	N/A	N/A	N/A	N/A
WOR2-F	6.35	N/A	N/A	N/A	N/A
WOR-C	6.29	4.40	1.7	3.51	19.0
WOR-F	5.54	4.51	1.5	4.26	7.7

*Three specimens were used in each calculation.

Source: UW Tanner research group.

Appendix F: AMBT Data Virgin Aggregates

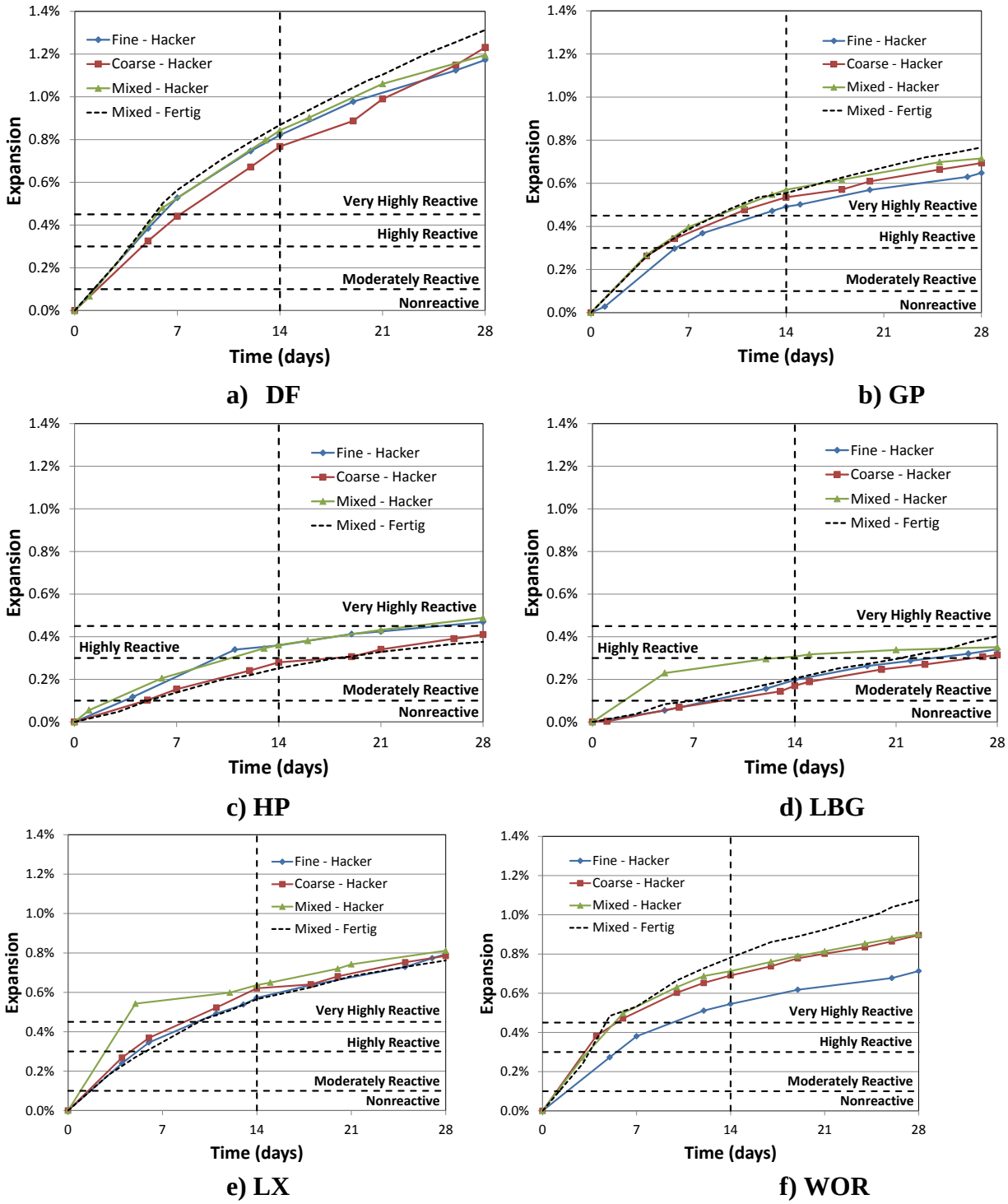

Figure 53. Graph. AMBT results for virgin aggregates.

Table 39. AMBT test results on virgin aggregates.

Source	Average expansion (mixed, coarse and fine) in percent
BR	0.56
DF	0.81
GP	0.53
HP	0.33
KR	0.23
LBG	0.22
LX	0.61
WOR	0.65

Source: UW Tanner research group.

Appendix G: OEB Data

Table 40. Additional materials used in field specimens.

Specimen	Water lb (kg)	NaOH lb (kg)	Air Ent. lb (kg)	Super-plasticizer lb (kg)	Slump in. (mm)	Air Content (%)
BHC-1	57.5 (26.1)	0 (0)	0.2 (0.09)	2.2 (1)	3 (76)	4.5
BHC-2	57.5 (26.1)	0 (0)	0.2 (0.09)	2.32 (1.05)	5.5 (140)	6
BHC-3	53.1 (24.1)	0.68 (0.3)	0.15 (0.07)	2.8 (1.27)	7.5 (191)	4.1
BHP-1	61.25 (27.8)	0 (0)	0.25 (0.11)	0 (0)	5 (127)	7
BHP-2	58 (26.3)	0 (0)	0.25 (0.11)	0 (0)	6 (152)	6
BHP-3	56.5 (25.6)	0.68 (0.3)	0.16 (0.07)	2.18 (0.99)	6.5 (165)	4.2
DF-1	57.5 (26.1)	0 (0)	0.25 (0.11)	0 (0)	3.5 (89)	5
DF-2	58 (26.3)	0 (0)	0.25 (0.11)	0 (0)	4.5 (114)	7
DF-3	57.5 (26.1)	0.68 (0.3)	0.24 (0.11)	2.74 (1.24)	4.5 (114)	5
GP-1	57.5 (26.1)	0 (0)	0.24 (0.11)	2.2 (1)	6.5 (165)	7.5
GP-2	53.4 (24.2)	0 (0)	0.2 (0.09)	2.2 (1)	4.5 (114)	4.5
GP-3	55.2 (25)	0.68 (0.3)	0.19 (0.09)	2.3 (1.04)	7 (178)	5.2
HP-1	57.5 (26.1)	0 (0)	0.25 (0.11)	0 (0)	2.5 (64)	5
HP-2	57.5 (26.1)	0 (0)	0.25 (0.11)	2.3 (1.04)	5.5 (140)	7
HP-3	57.5 (26.1)	0.68 (0.3)	0.24 (0.11)	2.44 (1.11)	3.5 (89)	5
KR-1	57.5 (26.1)	0 (0)	0.2 (0.09)	2.26 (1.03)	7.5 (191)	6.6
KR-2	49 (22.2)	0 (0)	0.2 (0.09)	2.3 (1.04)	5 (127)	4.7
KR-3	55 (24.9)	0 (0)	0.25 (0.11)	2.1 (0.95)	3.5 (89)	5
KR-4	55 (24.9)	0.68 (0.3)	0.25 (0.11)	2.3 (1.04)	4 (102)	8
LBG-1	60.4 (27.4)	0 (0)	0.25 (0.11)	0 (0)	0.5 (13)	4
LBG-2	65 (29.5)	0 (0)	0.25 (0.11)	0 (0)	2 (51)	4
LBG-3	65 (29.5)	0.68 (0.3)	0.25 (0.11)	0 (0)	6 (152)	6
LX-1	57.5 (26.1)	0 (0)	0.25 (0.11)	3 (1.36)	6 (152)	8
LX-2	53.9 (24.4)	0 (0)	0.25 (0.11)	2.4 (1.09)	8.5 (216)	9
LX-3	57.5 (26.1)	0.68 (0.3)	0.24 (0.11)	2.47 (1.12)	7.5 (191)	7.4
WOR-1	63 (28.6)	0 (0)	0.25 (0.11)	0 (0)	5.5 (140)	4.5
WOR-2	60.2 (27.3)	0 (0)	0.25 (0.11)	0 (0)	5 (127)	6
WOR-3	57.5 (26.1)	0.68 (0.3)	0.15 (0.07)	2.3 (1.04)	5.5 (140)	5.8

Source: UW Tanner research group.

BIBLIOGRAPHY

ACI Committee 211. (2008). Report on Alkali-Aggregate Reactivity. *American Concrete Institute*.

Adams, M. P., Fu, T., Cabrera, A. G., Morales, M., Ideker, J. H., & Isgor, O. B. (2016). Cracking Susceptibility of Concrete Made with Coarse Recycled Concrete Aggregates. *Construction and Building Materials, 102*(1), 802-810.

Adams, M. P., Jones, A., Beauchemin, S., Johnson, R., Fournier, B., Shehata, M., . . . Ideker, J. H. (2013). Applicability of the Accelerated Mortar Bar Test for Alkali Silica Reactivity of Recycled Concrete Aggregates. *Advances in Civil Engineering Materials, 2*(1), 78-96.

Alderman, A. R., Gaskin, A. J., Jones, R. H., & Vivian, H. E. (1947). Australian Aggregates and Cements. *Studies in Cement-Aggregate Reaction*(229), 1-46.

ASCE. (2017). Asce's 2017 Infrastructure Report Card | Gpa: D+. Retrieved from http://www.infrastructurereportcard.org

ASTM C39. (2016). Standard Test Method for Compressive Strength of Cylindrical Concrete Specimens. *ASTM International, 04.02*, 1-7.

ASTM C138. (2016). Standard Test Method for Density (Unit Weight), Yield, and Air Content (Gravimetric) of Concrete. *ASTM International, 04.02*(1-6).

ASTM C143. (2015). Standard Test Method for Slump of Hydraulic-Cement Concrete. *ASTM International, 04.02*, 1-4.

ASTM C157. (2014). Standard Test Method for Length Change of Hardened Hydraulic-Cement Mortar and Concrete. *ASTM International, 04.02*, 1-7.

ASTM C192. (2016). Standard Practice for Making and Curing Concrete Test Specimens in the Laboratory. *ASTM International, 04.02*, 1-8.

ASTM C305. (2014). Standard Practice for Mechanical Mixing of Hydraulic Cement Pastes and Mortars of Plastic Consistency. *ASTM International, 04.02*.

ASTM C311. (2013). Standard Test Methods for Sampling and Testing Fly Ash or Natural Pozzolans for Use in Portland-Cement Concrete. *ASTM International, 04.02*.

ASTM C441. (2011). Standard Test Method for Effectiveness of Pozzolans or Ground Blast-Furnace Slag in Preventing Excessive Expansion of Concrete Due to the Alkali-Silica Reaction. *ASTM International, 04.02*.

ASTM C618. (2015). Standard Specification for Coal Fly Ash and Raw or Calcined Natural Pozzolan for Use in Concrete. *ASTM International, 04.02*.

ASTM C670. (2015). Standard Practice for Preparing Precision and Bias Statements for Test Methods for Construction Materials. *ASTM International, 04.02*.

ASTM C802. (2014). Standard Practice for Conducting an Interlaboratory Test Program to Determine the Precision of Test Methods for Construction Materials. *ASTM International, 04.02*.

ASTM C1260. (2014). Standard Test Method for Potential Alkali Reaction of Aggregates (Mortar-Bar Method). *ASTM International, 04.02*.

ASTM C1293. (2014). Standard Test Method for Determination of Length Change of Concrete Due to Alkali-Silica Reaction. *ASTM International, 04.02*.

ASTM E177. (2014). Standard Practice for Use of the Terms Precision and Bias in ASTM Test Methods. *ASTM International, 04.02*.

ASTM E691. (2016). Standard Practice for Conducting an Interlaboratory Study to Determine the Precision of a Test Method. *ASTM International, 04.02*.

ASTM E2586. (2016). Standard Practice for Calculating and Using Basic Statistics. *ASTM International, 04.02*.

Berube, M. A. (1993). Canadian Experience with Testing for Alkali-Aggregate Reactivity in Concrete. *Cement and Concrete composites, 15*, 27-47.

Berube, M. A., Duchesne, J., Dorion, J. F., & Rivest, M. (2002). Laboratory Assessment of Alkali Contributions by Aggregates to Concrete and Application to Concrete Structures Affected by Alkali-Silica Reactivity. *Cement and concrete Research, 32*, 1215-1227.

Blackwell, B. Q., & K., P. (1992). Alkali-Reactivity of Grewacke Aggregates in the Maentwrog Dam (North Wales). *Magazine of Concrete Research, 44*(11), 255-264.

Buck, A. D., Houston, B. J., & Pepper, L. (1953). Effectiveness of Mineral Admixtures in Preventing Excessive Expansion of Concrete Due to Alkali-Aggregate Reaction. *Journal of the American Concrete Institute, 30*(10), 1160.

C1260, A. (2013). Standard Test Method for Determining the Potential Alkali-Silica Reaction of Combinations of Cementitious Materials and Aggregate (Accelerated Mortar-Bar Method) *ASTM International* (Vol. 04.02). West Conshohocken, PA.

Cox, H. P., Colemen, R. B., & White, L. (1950). Effect of Blast Furnace-Slag Cement on Alkali-Aggregate Reaction in Concrete. *Pit and Quarry, 45*(5), 95-96.

Crow, J. M. (2008). The Concrete Conundrum. *Royal Society of Chemistry*, 62-66. CSA A3000-13, A. (2013). Cementitious Materials Compendium.

Detwiler, R. J. (2002). Substitution of Fly Ash for Cement or Aggregate in Concrete: Strength Development and Suppression of ASR. 1-28.

Diamond, S. (1976). A Review of Alkali-Silica Reaction and Expansion Mechanism, Part 2: Reactive Aggregates. *Cement and concrete Research, 6*, 549-560.

Duchene, J., & Bérubé, M. A. (1992). An Autoclave Mortar Bar Test for Assessing the Effectiveness of Mineral Admixtures in Suppressing Expansion Due to AAR. *Proceedings of the 12th International Conference on Alkali Aggregate Reaction in Concrete*, 279-285.

Farny, J. A., & Kerkhoff, B. (2007). Diagnosis and Control of Alkali-Aggregate Reactions in Concrete. *Portland cement Association*.

Fertig, R. J. (2010). Evaluation of ASR Potential in Wyoming Aggregates.

Fournier, B., & Berube, M. A. (2000). Alkali-Aggregate Reaction in Concrete: A Review of Basic Concepts and Engineering Implications. *Canadian Journal of Civil Engineers, 27*, 167-191.

Fournier, B., Bérubé, M. A., & Bergeron, G. (1991). A Rapid Autoclave Mortar Bar Method to Determine the Potential Alkali-Silica Reactivity of St. Lawrence Lowlands Carbonate Aggregates (Quebec, Canada). *Cement Concrete and Aggregates, 13*(1), 58-71.

Fournier, B., Nkinamubanzi, P. C., & Chevrier, R. (2004). Comparative Field and Laboratory Investigations on the Use of Supplementary Cementing Materials to Control Alkali-Silica Reaction in Concrete. *Proceedings of the 12th International conference on Alkali-Aggregate Reaction in Concrete*, 528-537.

Gao, X. X., Cyr, M., Multon, S., & Sellier, A. (2013). A Comparison of Methods for Chemical Assessment of Reactive Silica in Concrete Aggregates by Selective Dissolution. *Cement and Concrete composites, 37*, 82-94.

Giannini, E. (2012). Evaluation of Concrete Structures Affected by Alkali-Silica Reaction and Delayed Ettringite Formation.

Giannini, E., & Folliard, K. (2013). Determining Alkali-Silica Reactivity of Aggregates Using a Rapid Autoclaved Concrete Prism Test. *Portland cement Association*, 1-21.

Glasser, L. S., & Kataoka, N. (1981). The Chemistry of 'Alkali-Aggregate' Reaction. *Cement and concrete Research, 11*, 1-9.

Goonan, T. G. (2000). Usgs Fact Sheet Fs-181-99: Recycled Aggregates - Profitable Resource Conservation. https://pubs.usgs.gov/fs/fs-0181-99/fs-0181-99po.pdf. Retrieved from https://pubs.usgs.gov/fs/fs-0181-99/fs-0181-99po.pdf

Grattan-Bellew, P. (1997). A Critical Review of Ultra-Accelerated Tests for Alkali-Silica Reactivity. *Cement and Concrete composites, 19*(5-6), 403-414.

Hacker, D. P. (2014). Evaluation of ASR Potential in Wyoming Aggregates and the Stiffness Damage Test as a Method for Assessing Expansion in ASR Affected Concrete.

Hanna, W. C. (1947). Unfavorable Chemical Reactions of Aggregate in Concrete and a Suggested Corrective. *ASTM Proceedings, 47*, 986-1009.
Hooton, R. D., & Bickley, J. A. (2014). Design for Durability: The Key to Improving Concrete Sustainability. *Construction and Building Materials, 67*, 422-430.
Hooton, R. D., & Rogers, C. A. (1993). Development of the Nbri Rapid Mortar Bar Test Leading to Its Use in North America. *Construction and Building Materials, 7*(3), 145-148.
Ichikawa, T. (2009). Alkali-Silica Reaction, Pessimum Effects and Pozzolanic Effect. *Cement and concrete Research, 39*, 716-726.
Ideker, J. H., Adams, M. P., Tanner, J. E., & Jones, A. (2014). Durability Assessment of Recycled Concrete Aggregates for Use in New Concrete-Phase Ii. *Oregon Transportation Research and Education Consortium*, 1-110.
Ideker, J. H., Bentivegna, A. F., Folliard, K. J., & Juenger, M. C. G. (2012). Do Current Laboratory Test Methods Accurately Predict Alkali-Silica Reactivity? *ACI Materials Journal, 109*(4), 395-402.
Ideker, J. H., Folliard, K. J., Juenger, M. G., & Thomas, M. D. (2004). Laboratory and Field Experience with ASR in Texas, USA. *Proceedings of the 12th International conference on Alkali-Aggregate Reaction in Concrete*, 1062-1070.
IEA, & WBCSD. (2009). *Carbon Emissions Reductions up to 2050* (W. B. C. f. S. Development Ed.). Paris, France: International Energy Agency [IEA].
Jin, R., & Chen, Q. (2015). Investigation of Concrete Recycling in the U.S. Construction Industry. *Procedia Engineering, 118*, 894-901.
Johnson, R., & Shehata, M. H. (2016). The Efficacy of Accelerated Test Methods to Evaluate Alkali Silica Reactivity of Recycled Concrete Aggregates. *Construction and Building Materials, 112*, 518-528.
Jones, A. (2011). Evaluation of ASR Potential in Wyoming Aggregates and Recycled Concrete Aggregate.
Kawabata, Y., Hamada, H., Sagawa, Y., Miyake, J., & Ikeda, T. (2008). Fly Ash Characterization Related to Mitigation of Expansion Due to Asr. *Proceedings of the 13th International Conference on Alkali-Aggregate Reaction*.
Kawano, H. (2003). The State of Using by-Products in Concrete in Japan and Outline of Jis/Tr on Recycled Concrete Using Recycled Aggregate. *Proceedings of the 1st FIB Congress on Recycling*, 245-253.
Kimble, M. L. (2015). Evaluation of ASR Potential in Wyoming Aggregates and Development of Mitigation Protocals.
Kosmatka, S. H., Kerkhoff, B., & Panarese, W. C. (2003). Design and Control of Concrete Mixtures. *Portland cement Association*.
Kou, S. C., Poon, C. S., & Etxeberria, M. (2011). Influence of Recycled Aggregates on Long Term Mechanical Properties and Pore Size Distribution of Concrete. *Cement and Concrete composites, 22*, 286–291.
Lau, A. (2009). What Are Repeatability and Reproducibility? Part 1: A D02 Viewpoint for Laboratories. *ASTM Standardization News*.
Leeman, A., Lothenbach, B., & Thalman, C. (2010). Influence of Superplasticizers on Pore Solution Composition and on Expansion of Concrete Due to Alkali-Silica Reaction. *Construction and Building Materials*, 1-7.
Levy, S. M., & Helene, P. (2004). Durability of Recycled Aggregates Concrete: A Safe Way to Sustainable Development. *Cement and Concrete Research, 34*, 1975-1980.
Li, X., & Gress, D. L. (2006). Mitigating Alkali-Silica Reaction in Concrete Containing Recycled Concrete Aggregate. *Transportation Research Record*, 30–35.
Lindgard, J., Andic-Cakir, O., Borchers, I., Broekmans, M., Brouard, E., Fernandes, I., . . . Wigum, B. J. (2011). Literature Survey on Performance Testing. *SINTEF Building and Infrastructure*.
Liu, C. C., Lee, C., & Wang, W. C. (2011). Study of Autoclave Methods for Evaluating the Alkali-Silica Reactivity of Aggregates. *Journal of the Chinese institute of engineers, 34*(5), 663-670.

Lu, D. Y., Fournier, B., & Grattan-Bellew, P. E. (2004). A Comparative Study on Accelerated Test Methods for Determining Alkali-Silica Reactivity of Concrete Aggregates. *Proceedings of the 12th International conference on Alkali-Aggregate Reaction in Concrete*, 377-385.

Malhotra, V. M. (1978). Recycled Concrete – a New Aggregate. *Canadian Journal of Civil Engineering, 5*(1), 42-52.

Malvar, L. J., & Lenke, L. R. (2006). Efficiency of Fly Ash in Mitigating Alkali-Silica Reaction Based on Chemical Composition. *ACI Materials Journal, 103*(5), 319-326.

Marie, I., & Quiasrawi, H. (2012). Close-Loop Recycling of Recycled Concrete Aggregates. *Journal of Cleaner Production, 37*, 243-248.

McCoy, W. J., & Caldwell, A. G. (1951). New Approach to Inhibiting Alkali-Aggregate Expansion. *Journal of the American Concrete Institute, 22*(9), 693-706.

Mehta, P. K. (1997). Durability - Critical Issues for the Future. *Concrete International, 19*(7), 27-33.

Mehta, P. K. (2001). Reducing the Environmental Impact of Concrete. *Concrete International, 23*(10), 61-66.

Mehta, P. K. (2002). Greening of the Concrete Industry for Sustainable Development. *Concrete International, 24*(7), 23-38.

Meissner, H. S. (1941). Cracking in Concrete Due to Expansive Reaction between Aggregate and High-Alkali Cement as Evidenced in Parker Dam. *Journal of the American Concrete Institute Proceedings, 37*, 549-568.

Meyer, C. (2007). *The Economics of Recycling in the Us Construction Industry* (Y. M. Chun Ed.). Coventry, UK: Taylor & Francis.

Meyer, C. (2009). The Greening of the Concrete Industry. *Cement and Concrete Composites, 31*, 601-605.

Miller, I., & Miller, M. (2014). *John E. Freund's 'Mathematical Statistics with Applications'* (8th ed.): Pearson Education.

Mukhopadhyay, A. K. (2013). An Effective Approach to Utilize Recycled Aggregates (RAs) from Alkali-Silica Reaction (ASR) Affected Portland Cement Concrete. *Woodhead Publishing Series in Civil and Structural Engineering*, 555-568.

Multon, S., M., C., A., S., P., D., & L., P. (2010). Effects of Aggregate Size and Alkali Content on ASR Expansion. *Cement and concrete Research, 40*, 508-516.

Multon, S., Sellier, A., & Cyr, M. (2009). Chemo-Mechanical Modeling for Prediction of Alkali Silica Reaction (Asr) Expansion. *Cement and concrete Research, 39*, 490-500.

Nishibayahsi, S., Kuroda, T., & Inoue, S. (1996). Expansion Characteristics of AAR in Concrete by Autoclave Method. *Proceedings of the 10th International Conference on Alkali-Aggregate Reactions in Concrete*, 370-376.

Oberholster, R. E., & Davies, G. (1986). An Accelerated Method for Testing the Potential Alkali Reactivity of Siliceous Aggregates. *Cement and concrete Research, 16*, 181-189.

Osmani, M. (2012). Construction Waste Minimization in the Uk: Current Pressures for Change and Approaches. *Procedia - Social and Behavioral Sciences, 40*, 37-40.

Poole, A. B. (1992). Introduction to Alkali-Aggregate Reaction in Concrete. *The Alkali-Silica Reaction in Concrete*, 1-29.

Poon, C. S., Shui, Z. H., Lam, L., Fok, H., & Kou, S. C. (2004). Influence of Moisture States of Natural and Recycled Aggregates on the Slump and Compressive Strength of Concrete. *Cement and concrete Research, 34*, 31-36.

Powers, T. C., & Steinour, H. H. (1955). An Interpretation of Published Researches on the Alkali-Aggregate Reaction. *Journal of the American Concrete Institute, 51*, 497-516 and 785-812.

Rajabipour, F., Giannini, E., Dunant, C., Ideker, J., & Thomas, M. (2015). Alkali-Silica Reaction: Current Understanding of the Reaction Mechanisms and the Knowledge Gaps. *Cement and concrete Research, 76*, 130-146.

Rao, A., KumaJha, K. N., & Misra, S. (2007). Use of Aggregates from Recycled Construction and Demolition Waste in Concrete. *Resources, Conservation and Recycling, 50*, 71-81.

RILEM 121-DRG. (1994). Specifications for Concrete with Recycled Aggregates. *Materials and Structures, 27*(173), 557-559.
Rogers, C., & Lane, B. (2000). Outdoor Exposure for Validating the Effectiveness of Preventative Measures for Alkali-Silica Reaction. *Proceedings of the 11th International Conference on Alkali-Aggregate Reaction*, 743-752.
Rogers, C. A. (1999). Multi-Laboratory Study of the Accelerated Mortar Bar Test (ASTM C1260) for Alkali Silica Reaction. *Cement and Concrete Research, Aggregates, 21*(2), 185–194.
Rogers, C. A., & Hooton, R. D. (1991). Reduction in Mortar and Concrete Expansion with Aggregates Due to Alkali Leaching. *Cement Concrete and Aggregates, 13*(1), 42-49.
Sagoe-Crentsil, K. K., Brown, T., & Taylor, A. H. (2001). Performance of Concrete Made with Comnmercially Produced Coarse Recycled Concrete Aggregate. *Cement and concrete Research, 31*, 707-712.
Schumacher, K., & Ideker, J. (2014). New Considerations in Predicting Mitigation of Alkali-Silica Reaction Based on Fly Ash Chemistry. *Journal of Materials in Civil Engineering, 27*(4).
Scott, H. C. I., & Gress, D. L. (2004). Mitigating Alkali Silica Reaction in Recycled Concrete. *Recycling Concrete and Other Materials for Sustainable Development, American Concrete Institute, 219*, 61-76.
Sellier, A., Saouma, V., Multon, S., Pape, Y. L., & Orbovic, N. (2016). Benchmark/Round Robin Analyses. *Rilem Technical Committe 259-ISR, 1*, 1-31.
Shafaatian, S. M. H., Akhavan, A., Maraghechi, H., & Rajabipour, F. (2013). How Does Fly Ash Mitigate Alkali-Silica Reaction (ASR) in Accelerated Mortar Bar Test (ASTM C1567? *Cement and Concrete composites, 37*, 143-153.
Shehata, M. H., Christidis, C., Mikhaiel, W., Rogers, C., & Lachemi, M. (2010). Reactivity of Reclaimed Concrete Aggregate Produced from Concrete Affected by Alkali-Silica Reaction. *Cement and Concrete Research, 40*(4), 575–582.
Shehata, M. H., & Thomas, M. D. (2000). The Effect of Fly Ash Composition on the Expansion of Concrete Due to Alkali-Silica Reaction. *Cement and Concrete Research, 30*, 1063-1072.
Smaoui, N., Berube, M. A., Fournier, B., Bissonnette, B., & Durand, B. (2005). Effects of Alkali Addition on the Mechanical Properties and Durability of Concrete. *Cement and concrete Research, 35*(2), 203-212.
Stanton, T. E. (1940). Expansion of Concrete through Reaction between Cement and Aggregate. *Proceedings of the American Society of Civil Engineers, 66(10)*, 1781-1810.
Stanton, T. E. (1940). Expansion of Concrete through Reaction between Cement and Aggregate. *Proceedings of the American Society of Civil Engineers, 66*(10), 1781-1810, with permission from ASCE.
Stanton, T. E. (1950). Studies of Use of Pozzolans for Counteracting Excessive Concrete Expansion Resulting from Reaction between Aggregates and the Alkalies in Cement. *Pozzolanic Materials in Mortars and Concretes*, 178-203.
Stark, D., Morgan, B., Okamoto, P., & Diamond, S. (1993). Eliminating or Minimizing Alkali-Silica Reactivity. *Strategic Highway Research Program*.
Sutter, L., Hooton, R. D., & Schlorholtz, S. (2013). Methods for Evaluating Fly Ash for Use in Highway Concrete. *Transportaton Research Board of the National Academies*.
Suwito, A., Jin, W., Xi, Y., & Meyer, C. (2002). A Mathematical Model for the Pessimum Size Effect of ASR in Concrete. *Concrete Science and Engineering, 4*(13), 23-34.
Swenson, E. G., & Gillott, J. E. (1964). Alkali-Carbonate Rock Reaction. *Highway Research Record, 45*, 21-40.
Tabsh, S. W., & Abdelfatah, A. S. (2009). Influence of Recycled Concrete Aggregates on Strength Properties of Concrete. *Construction and Building Materials, 23*, 1163-1167.
Tam, V. (2008). Economic Comparison of Concrete Recycling: A Case Study Approach. *Resources, Conservation and Recycling, 52*, 821-828.

Tam, V. (2009). Comparing the Implementation of Cocnrete Recycling in the Australian and Japanese Construction Industries. *Journal of Cleaner Production, 17*, 688-702.
Tang, M. S., & Fen, S. H. (1980). Effect of Ca(Oh)2 on Alkali-Silica Reaction. *Proceedings of the Eighth International Congress of Cement Chemistry, 2*, 94-99.
Tang, M. S., Han, S. F., & Zhen, S. H. (1983). A Rapid Method for Identification of Alkali Reactivity of Aggregate. *Cement and concrete Research, 13*, 417-422.
Taylor, H. F. W., Famy, C., & Scrivener, K. L. (2001). Delayed Ettringite Formation. *Cement and concrete Research, 31*, 683-693.
Thomas, M., Fournier, B., Folliard, K., Ideker, J., & Shehata, M. (2006a). Test Methods for Evaluating Preventative Measures for Controlling Expansion Due to Alkali-Silica Reaction in Concrete. *Cement and Concrete Research, 36*(10), 1842-1856.
Thomas, M., Fournier, B., Folliard, K., Ideker, J., & Shehata, M. (2006b). Test Methods for Evaluating Preventive Measures for Controlling Expansion Due to Alkali-Silica Reaction in Concrete. *International Center for Aggregates Research*.
Thomas, M. D., Folliard, K., Fournier, B., Drimalas, T., & Garber, S. (2013). Methods for Preventing Asr in New Construction, Results of Field Exposure Sites. *U.S Department of Transportation Federal Highway Administration*.
Thomas, M. D., Fournier, B., & Folliard, K. J. (2012). Selecting Measures to Prevent Deleterious Alkali-Silica Reaction in Concrete: Rationale for the AASHTO Pp65 Prescriptive Approach. *U.S. Department of Transportation Federal Highway Administration*.
Thomas, M. D., & Innis, F. A. (1999). Use of the Accelerated Mortar Bar Test for Evaluating the Efficacy of Mineral Admixtures for Controlling Expansion Due to Alkali-Silica Reaction. *Cement Concrete and Aggregates, 21*(2), 157-164.
Thomas, M. D., Shehata, M. H., & Shashiprakash, S. G. (1999). The Use of Fly Ash in Concrete: Classification by Composition. *Cement Concrete and Aggregates, 21*(2), 105-110.
Touma, W. E., Fowler, D. W., Carrasquillo, R. L., Folliard, K. J., & Nelson, N. R. (2001). Characterizing Alkali-Silica Reactivity of Aggregates Using Astm C 1293, Astm C 1260, and Their Modifications. *Transportation Research Record*(1757), 157-165.
Ullman, N. (2009). What Are Repeatability and Reproducibility? Part 2: The E11 Viewpoint. *ASTM Standardization News*.
Vayghan, A. G., Wright, J. R., & Rajabipour, F. (2016). An Extended Chemical Index Model to Predict the Fly Ash Dosage Necessary for Mitigating Alkali-Silica Reaction in Concrete. *Cement and concrete Research, 82*, 1-10.
Wright, J. R., Shafaatian, S., & Rajabipour, F. (2014). Reliability of Chemical Index Model in Determining Fly Ash Effectiveness against Alkali-Silica Reaction Induced by Highly Reactive Glass Aggregates. *Construction and Building Materials, 64*, 166-171.
Zhang, C., Wang, A., Tang, M., Wu, B., & Zhang, N. (1999). Influence of Aggregate Size and Aggregate Size Grading on ASR Expansion. *Cement and concrete Research, 29*, 1393-1396.